Credit: Rick Peterson, W.M. Keck Observatory

Star-formation history and chemical enrichment in the early Universe

clues from the rest-UV and rest-optical spectra of z~2-3 galaxies

Allison Strom (Caltech)
Chuck Steidel (Caltech)
Gwen Rudie (Carnegie)
Ryan Trainor (UC Berkeley)
Max Pettini (IoA Cambridge)
Naveen Reddy (UC Riverside)

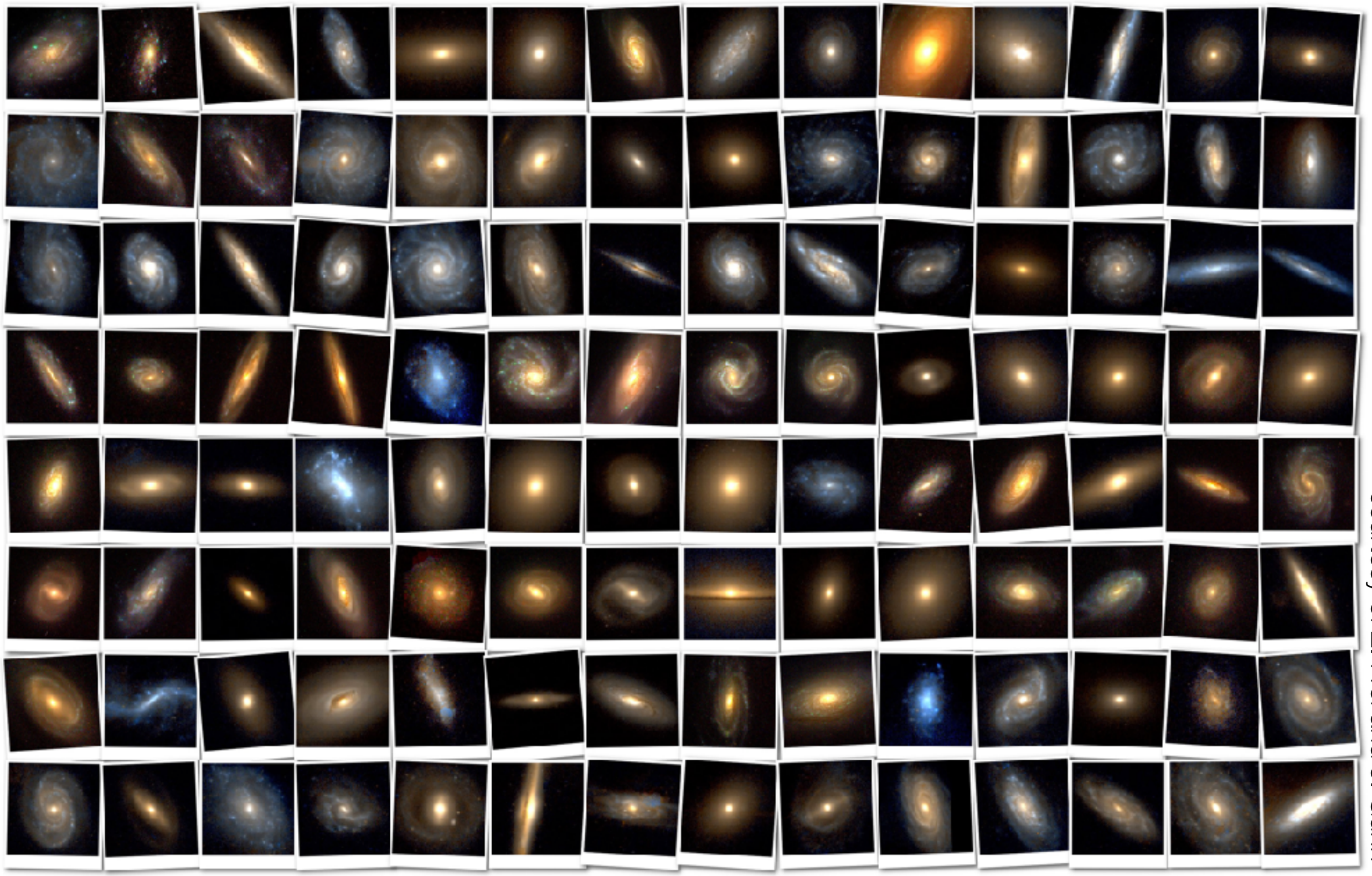

courtesy of Z. Frei and J. Gunn

Explaining the diversity of observed galaxy properties remains a challenge

The Universe was more active 10 Gyr ago

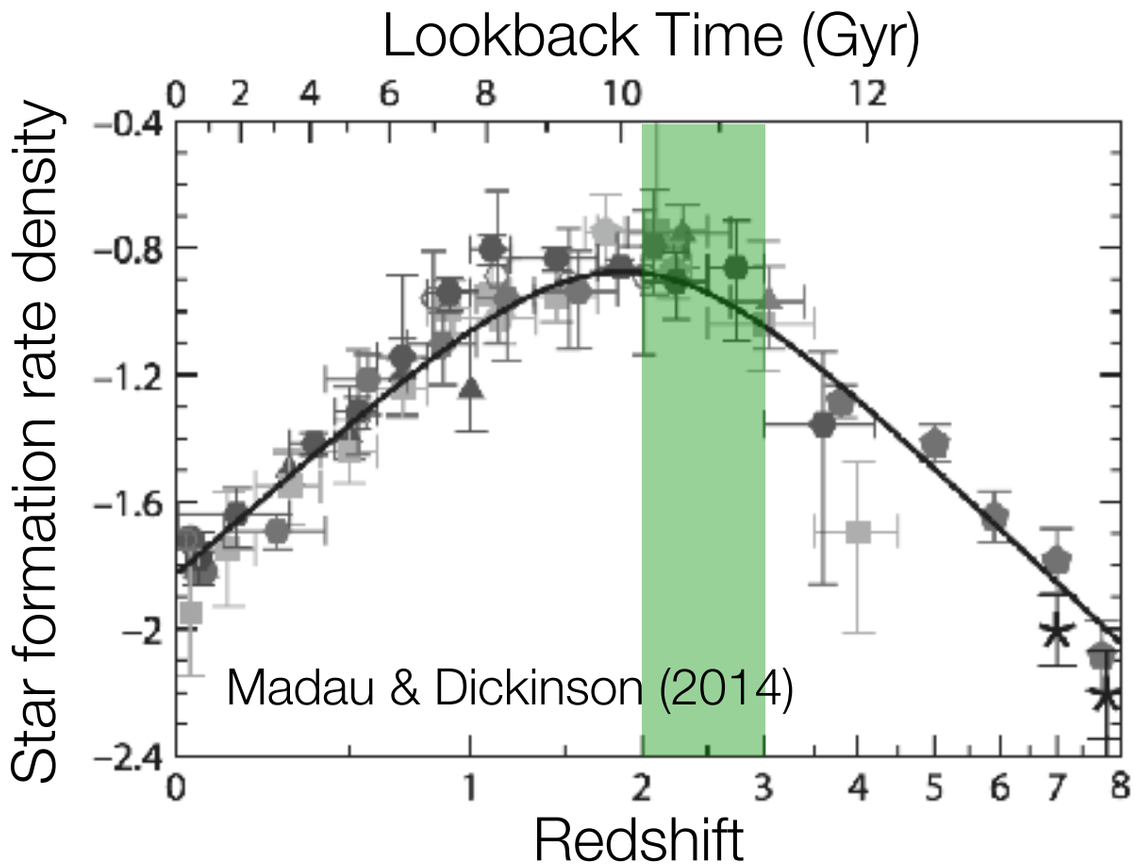

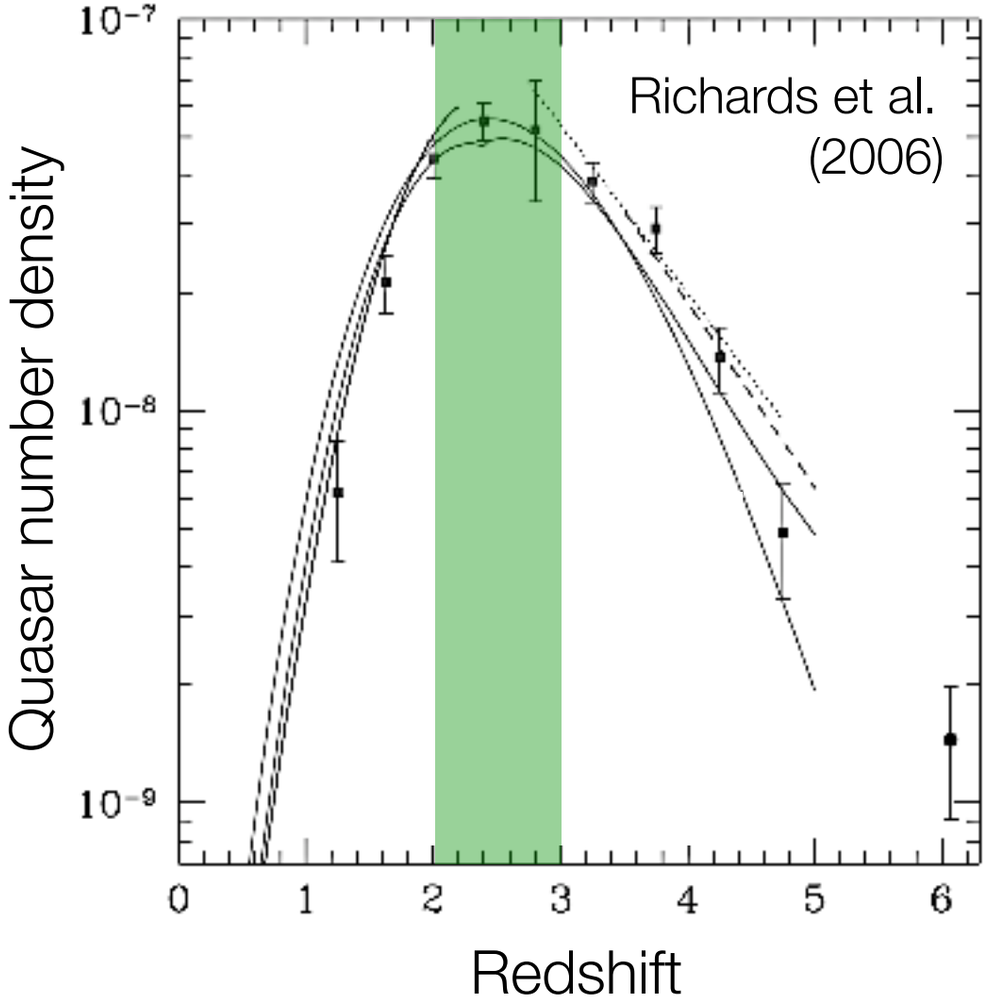

Properties of HII regions provide clues about galaxy assembly

massive stars

Properties of HII regions provide clues about galaxy assembly

ionized gas

massive stars

ionized gas

ionized gas

Properties of HII regions provide clues about galaxy assembly

Recombination lines:

- Balmer series (Hα, Hβ, HɣΥ…)
- modulated primarily by the number of ionizing photons

ionized gas

massive stars

ionized gas

ionized gas

Properties of HII regions provide clues about galaxy assembly

Recombination lines:

- Balmer series (Hα, Hβ, HɣŸ…)
- modulated primarily by the number of ionizing photons

Collisionally-excited forbidden lines of metallic species:

- [O III], [O II], [N II], [S II], [Ne IIII]
- sensitive to abundance of elements, ionization equilibrium, and gas temperature

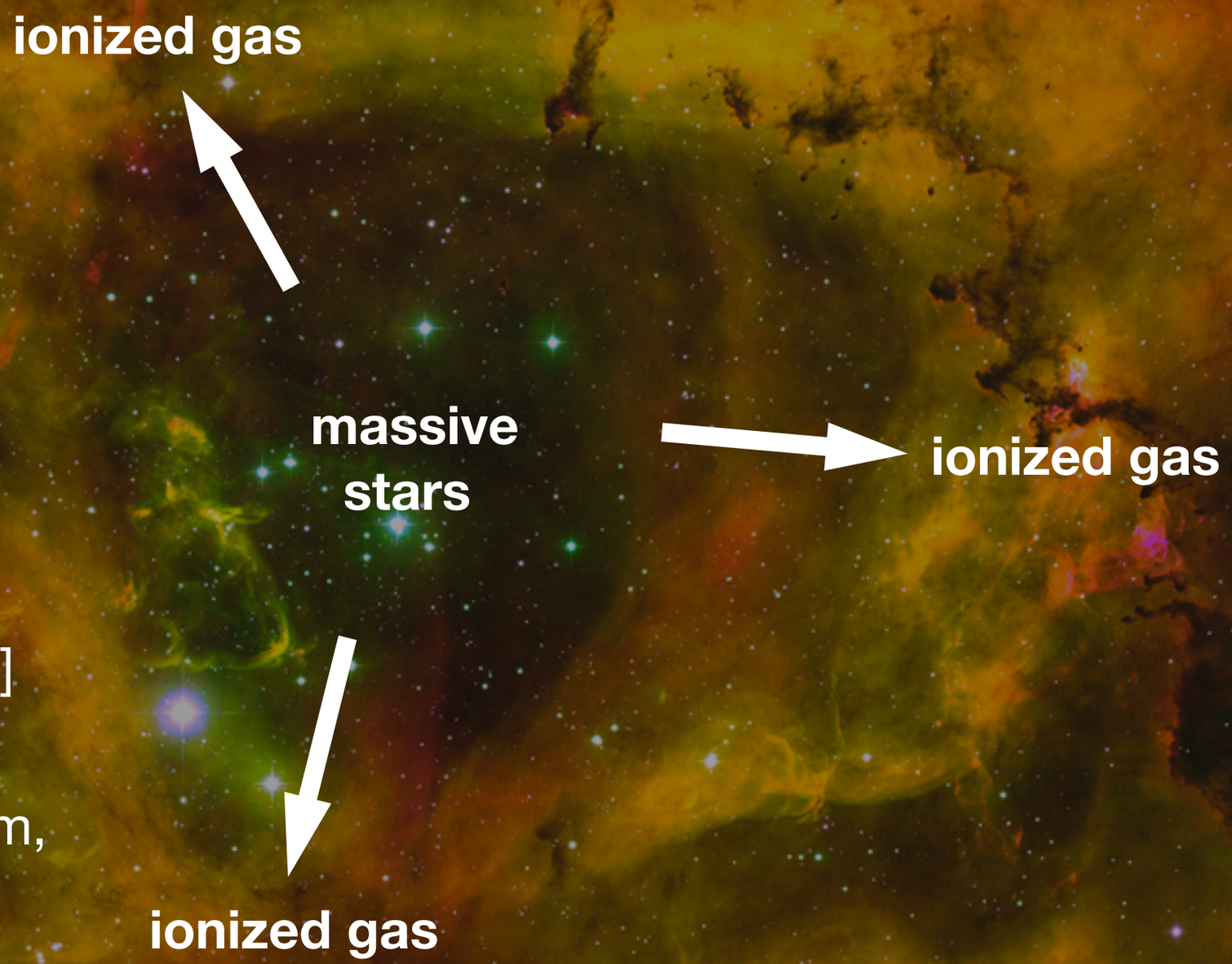

HII region spectra reveal detailed astrophysics

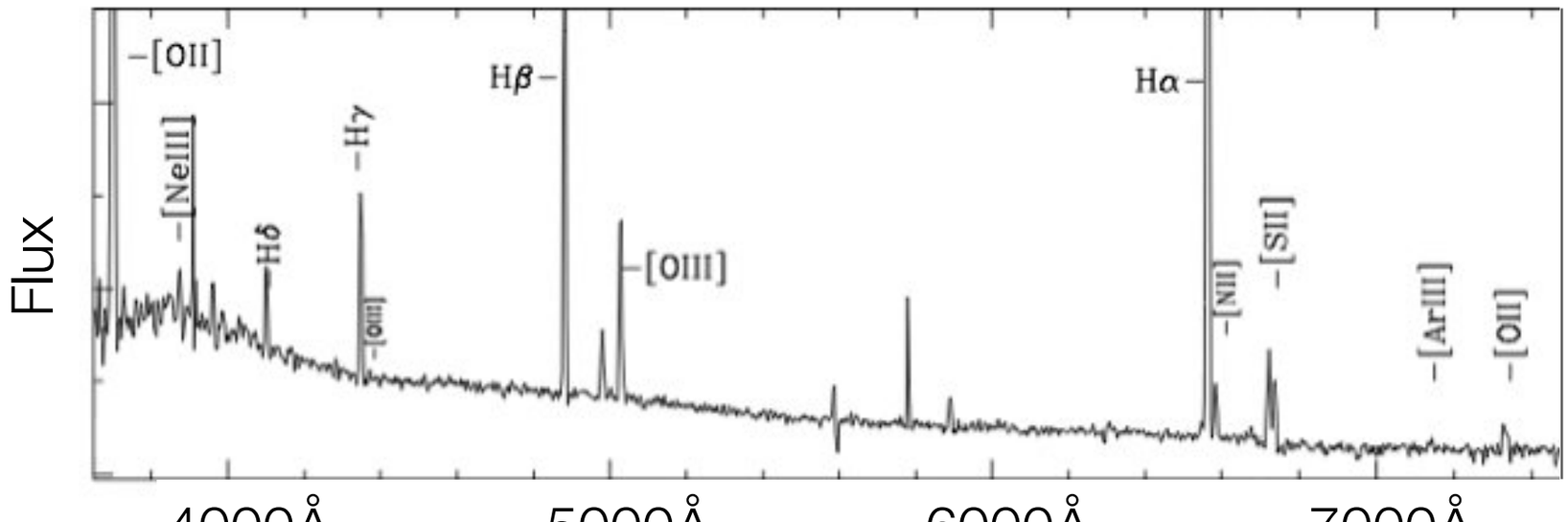

HII region spectra reveal detailed astrophysics

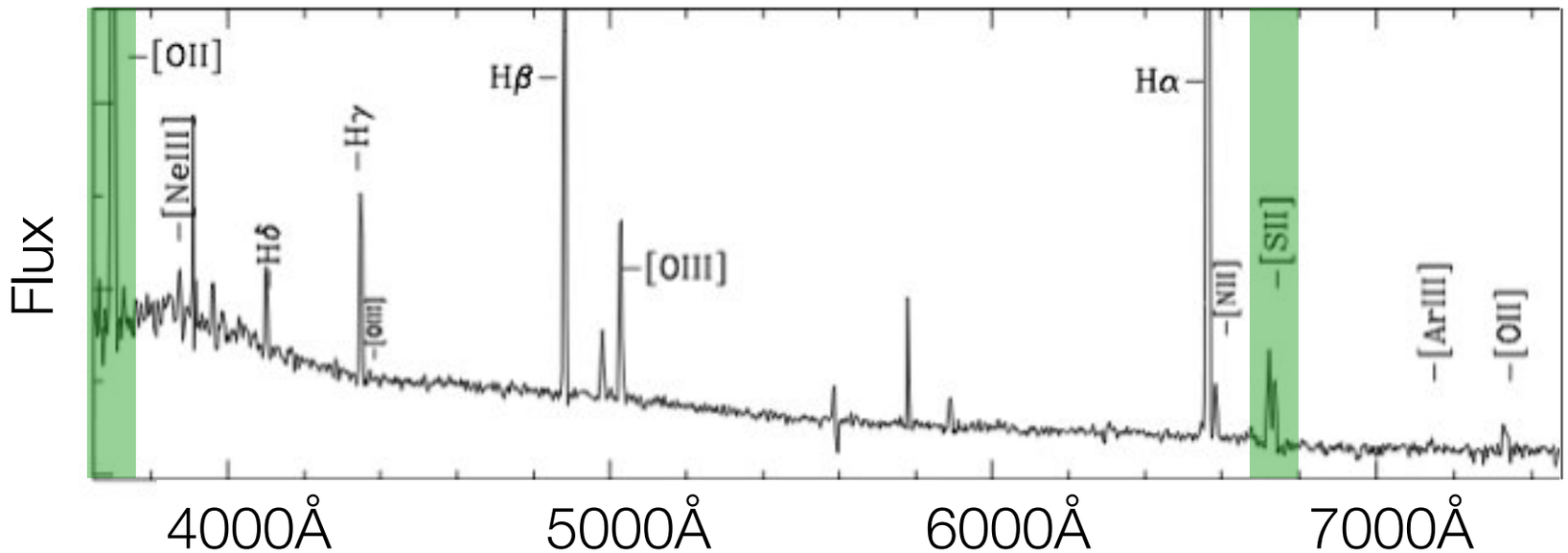

1. **Electron density:** lines with similar excitation energies, but different critical densities, including [OII]λλ3727,3729, [SII]λλ6717,6731

HII region spectra reveal detailed astrophysics

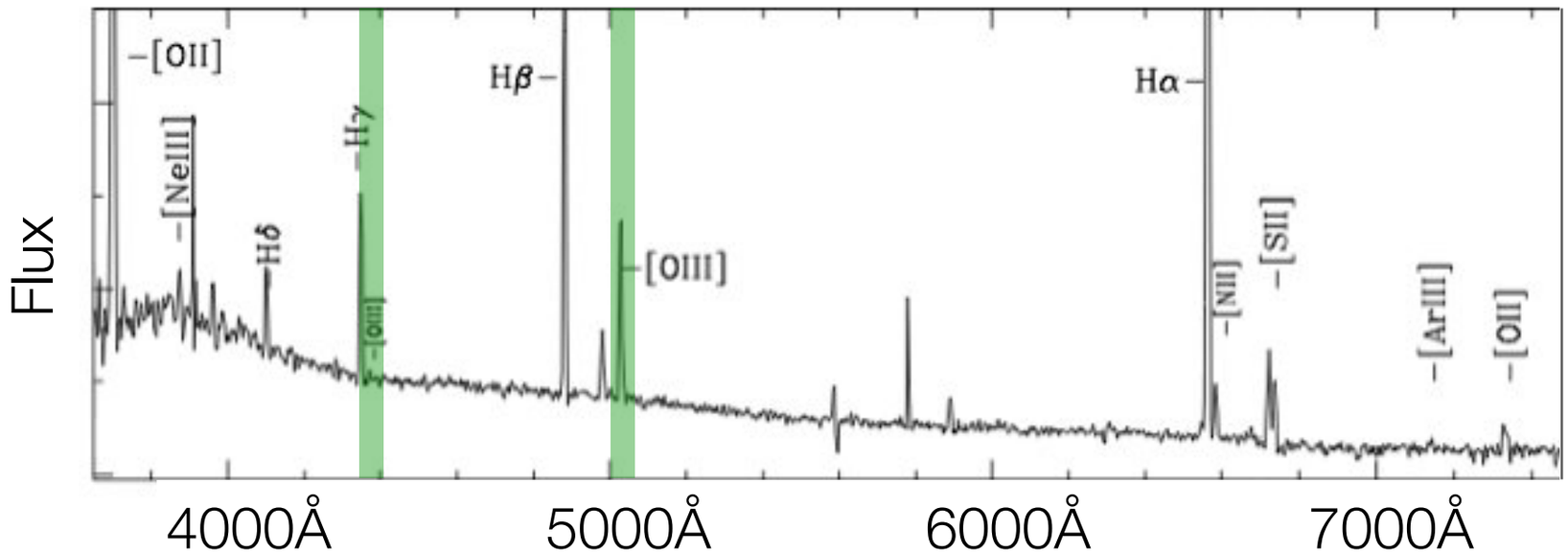

1. **Electron density:** lines with similar excitation energies, but different critical densities, including [OII]λλ3727,3729, [SII]λλ6717,6731
2. **Electron temperature:** lines from same ion with different excitation energies, including [OIII]λ4363/[OIII]λ5007, but also need low-ionization zone temperature

HII region spectra reveal detailed astrophysics

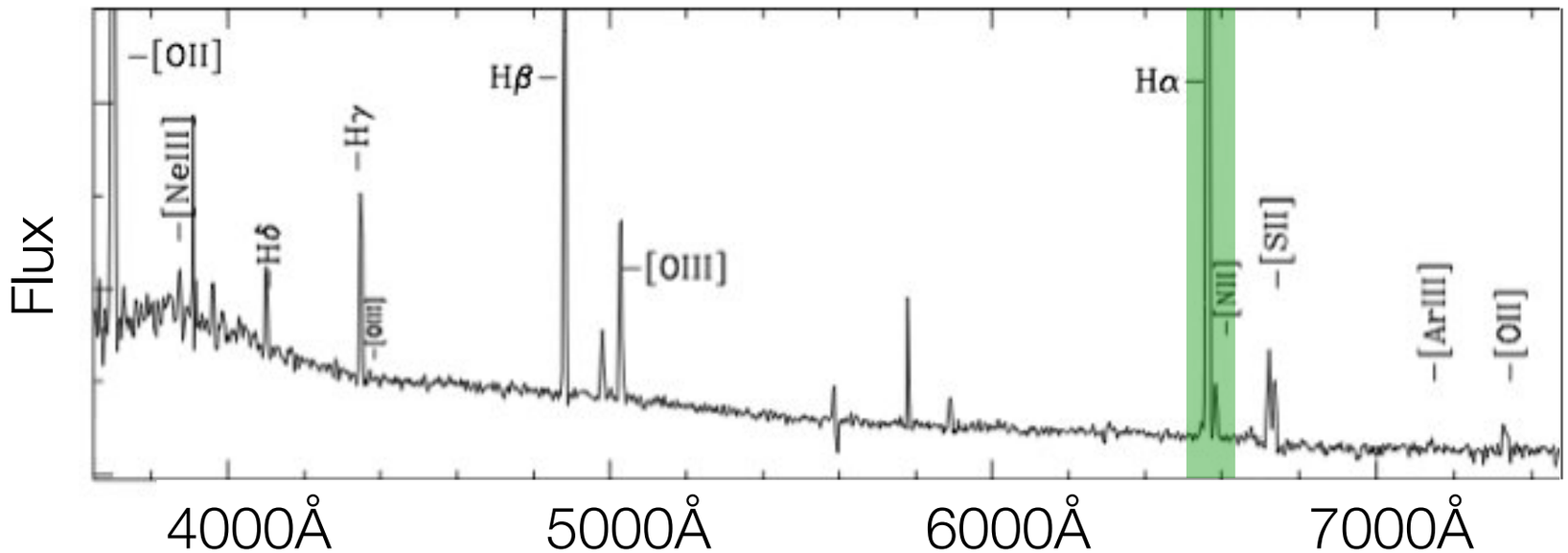

1. **Electron density:** lines with similar excitation energies, but different critical densities, including [OII]λλ3727,3729, [SII]λλ6717,6731
2. **Electron temperature:** lines from same ion with different excitation energies, including [OIII]λ4363/[OIII]λ5007, but also need low-ionization zone temperature
3. **“Metallicity” (oxygen abundance):** N2=[NII]λ6584/Hα, O3N2=([OIII]λ5007/Hβ)/N2

HII region spectra reveal detailed astrophysics

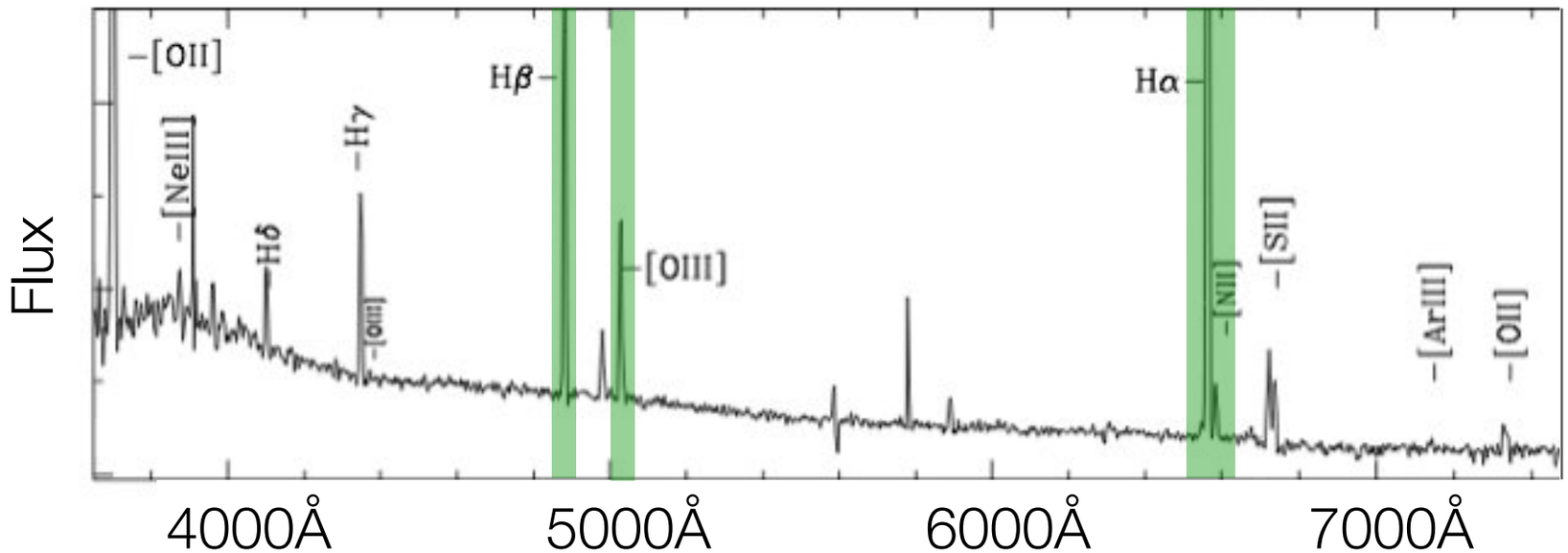

1. **Electron density:** lines with similar excitation energies, but different critical densities, including [OII]λλ3727,3729, [SII]λλ6717,6731
2. **Electron temperature:** lines from same ion with different excitation energies, including [OIII]λ4363/[OIII]λ5007, but also need low-ionization zone temperature
3. **“Metallicity” (oxygen abundance):** N2=[NII]λ6584/Hα, O3N2=([OIII]λ5007/Hβ)/N2

HII region spectra reveal detailed astrophysics

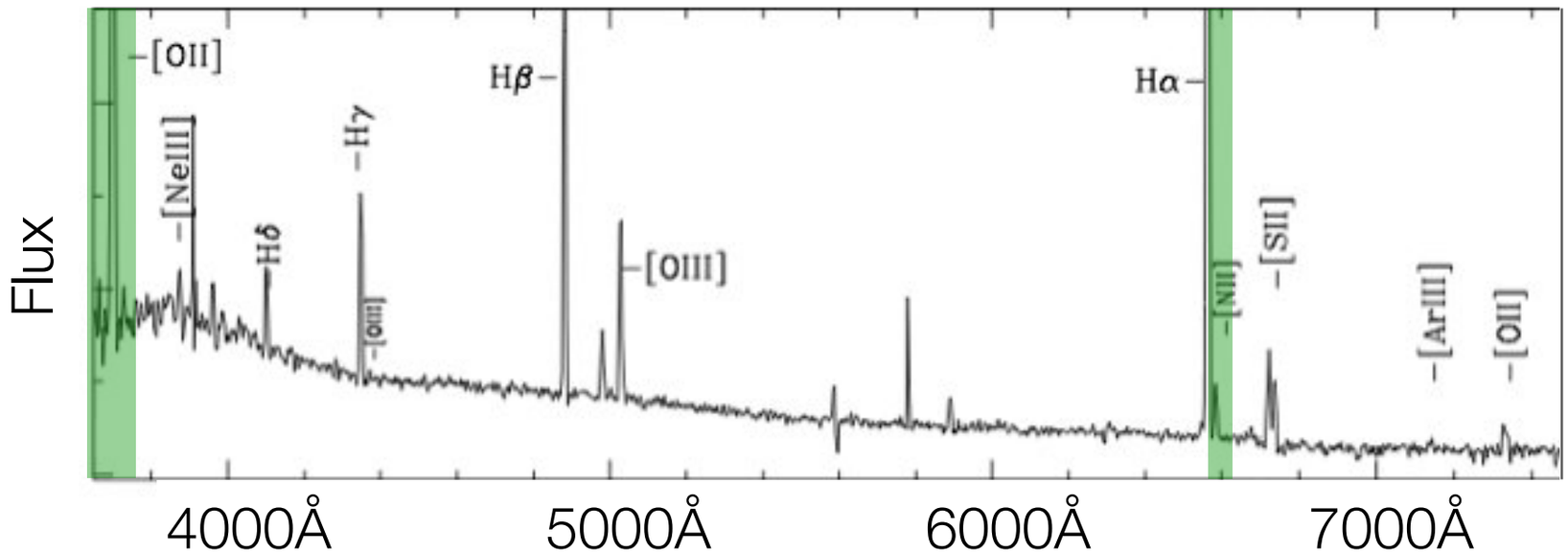

1. **Electron density:** lines with similar excitation energies, but different critical densities, including [OII]λλ3727,3729, [SII]λλ6717,6731
2. **Electron temperature:** lines from same ion with different excitation energies, including [OIII]λ4363/[OIII]λ5007, but also need low-ionization zone temperature
3. **"Metallicity" (oxygen abundance):** N2=[NII]λ6584/Hα, O3N2=([OIII]λ5007/Hβ)/N2
4. **Abundance ratios:** N2O2=[NII]λ6584/[OII]λλ3727,3729 assuming $N/O=N^+/O^+$

HII region spectra reveal detailed astrophysics

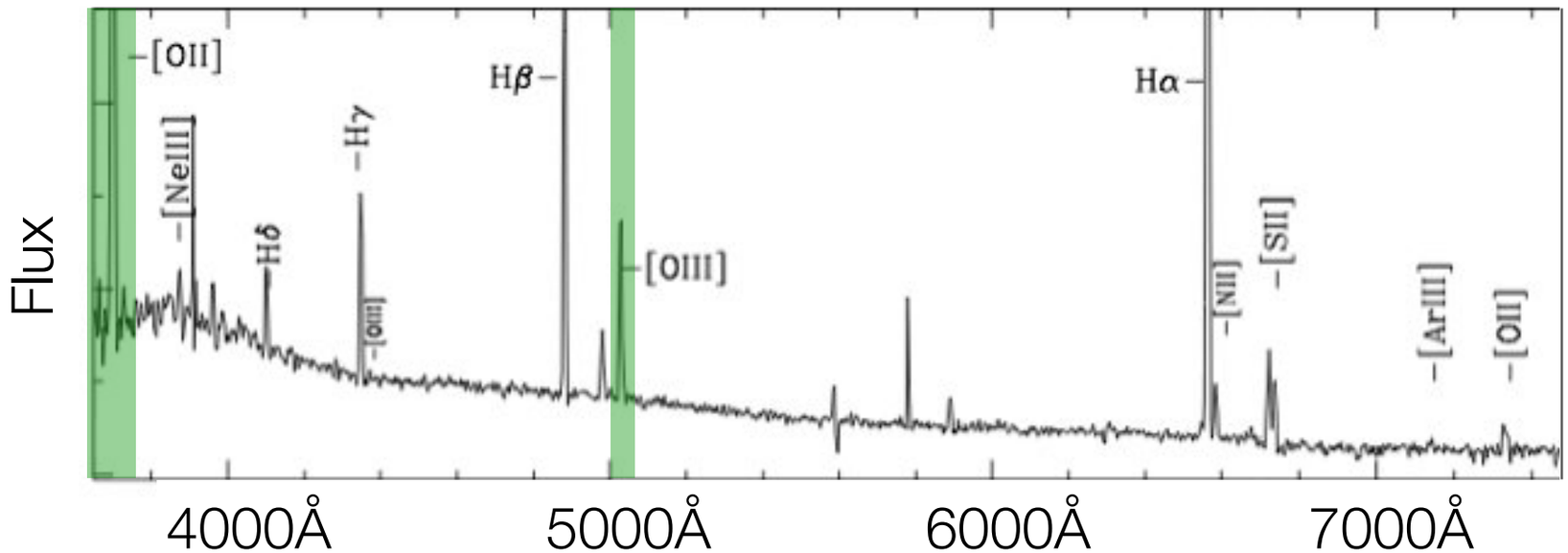

1. **Electron density:** lines with similar excitation energies, but different critical densities, including [OII]λλ3727,3729, [SII]λλ6717,6731
2. **Electron temperature:** lines from same ion with different excitation energies, including [OIII]λ4363/[OIII]λ5007, but also need low-ionization zone temperature
3. **"Metallicity" (oxygen abundance):** N2=[NII]λ6584/Hα, O3N2=([OIII]λ5007/Hβ)/N2
4. **Abundance ratios:** N2O2=[NII]λ6584/[OII]λλ3727,3729 assuming $N/O=N^+/O^+$
5. **Ionization parameter:** emission from different ions of the same element, including [OIII]λ4959,5007/[OII]λλ3727,3729

HII region spectra reveal detailed astrophysics

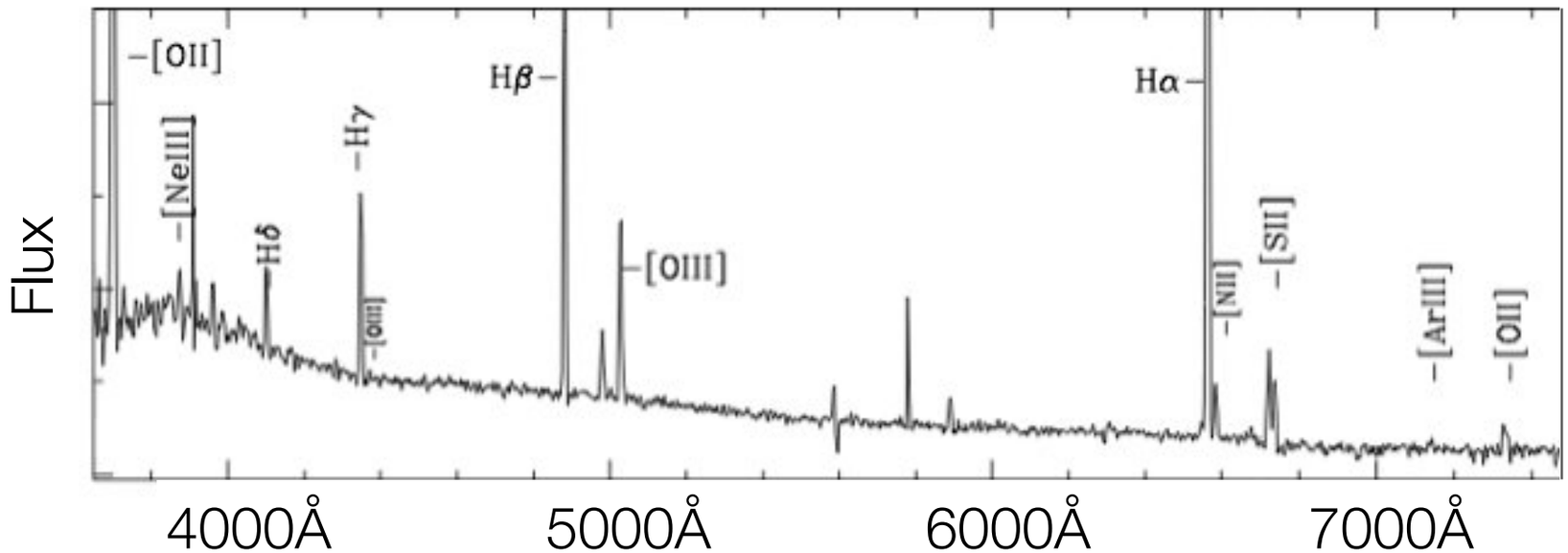

1. **Electron density:** lines with similar excitation energies, but different critical densities, including [OII]λλ3727,3729, [SII]λλ6717,6731
2. **Electron temperature:** lines from same ion with different excitation energies, including [OIII]λ4363/[OIII]λ5007, but also need low-ionization zone temperature
3. **"Metallicity" (oxygen abundance):** N2=[NII]λ6584/Hα, O3N2=([OIII]λ5007/Hβ)/N2
4. **Abundance ratios:** N2O2=[NII]λ6584/[OII]λλ3727,3729 assuming $N/O=N^+/O^+$
5. **Ionization parameter:** emission from different ions of the same element, including [OIII]λ4959,5007/[OII]λλ3727,3729

HII region spectra reveal detailed astrophysics

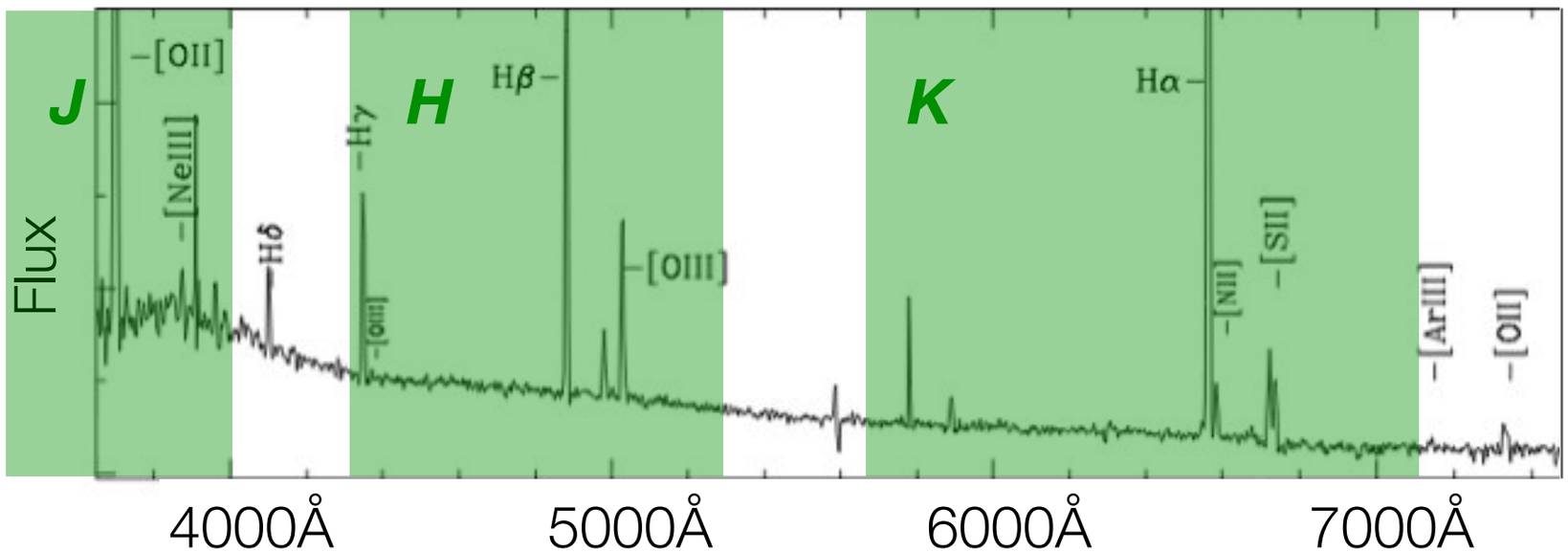

NIR bands for galaxy at z=2.4

1. **Electron density:** lines with similar excitation energies, but different critical densities, including [OII]λλ3727,3729, [SII]λλ6717,6731
2. **Electron temperature:** lines from same ion with different excitation energies, including [OIII]λ4363/[OIII]λ5007, but also need low-ionization zone temperature
3. **"Metallicity" (oxygen abundance):** N2=[NII]λ6584/Hα, O3N2=([OIII]λ5007/Hβ)/N2
4. **Abundance ratios:** N2O2=[NII]λ6584/[OII]λλ3727,3729 assuming $N/O=N^+/O^+$
5. **Ionization parameter:** emission from different ions of the same element, including [OIII]λ4959,5007/[OII]λλ3727,3729

Correlations between astrophysical parameters will manifest as correlated changes in galaxies' spectra.

The N2-BPT diagnostic diagram

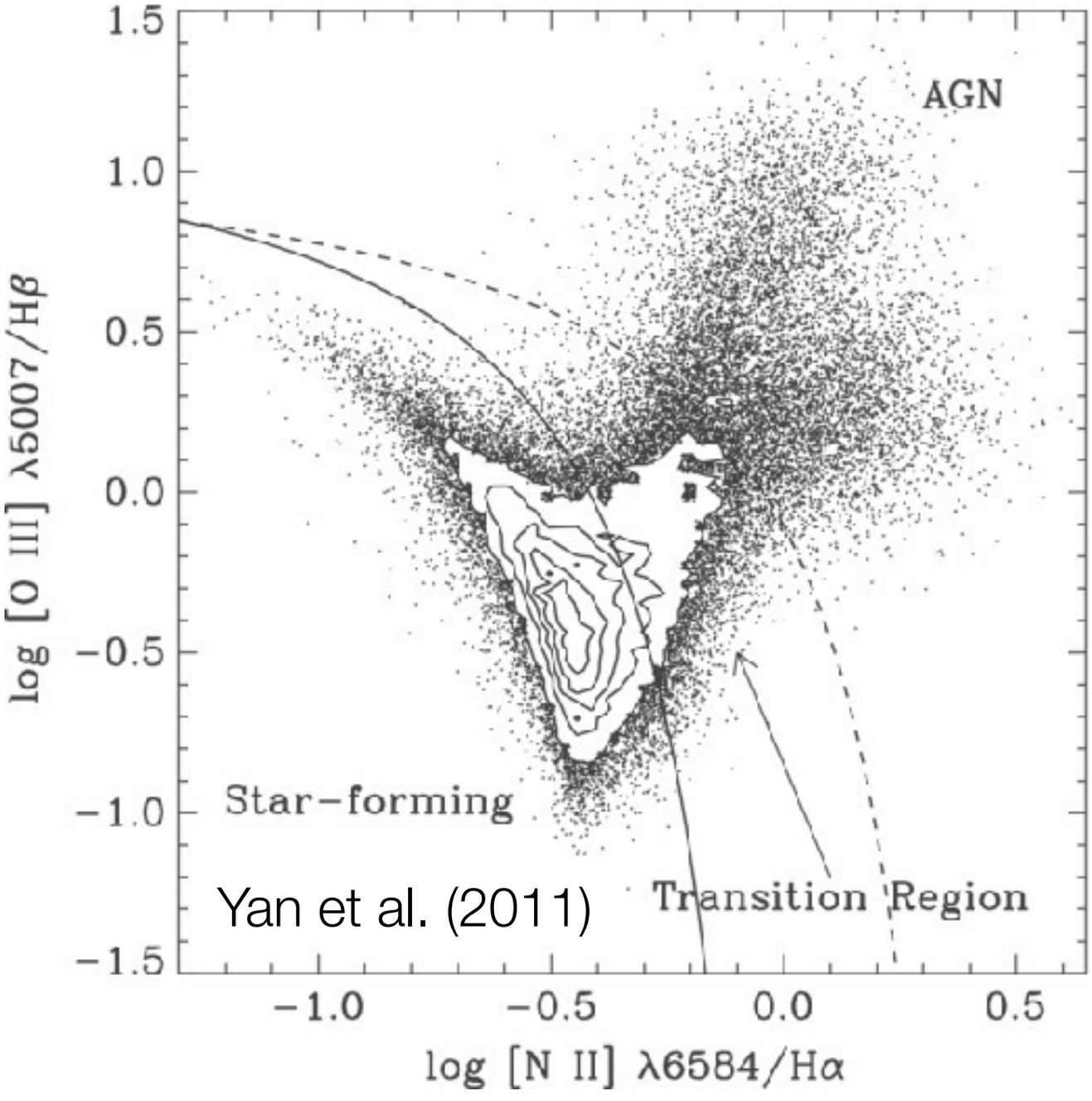

Baldwin, Phillips,
and Terlevich et al. (1981)

Veilleux & Osterbrock (1987)

The N2-BPT diagnostic diagram

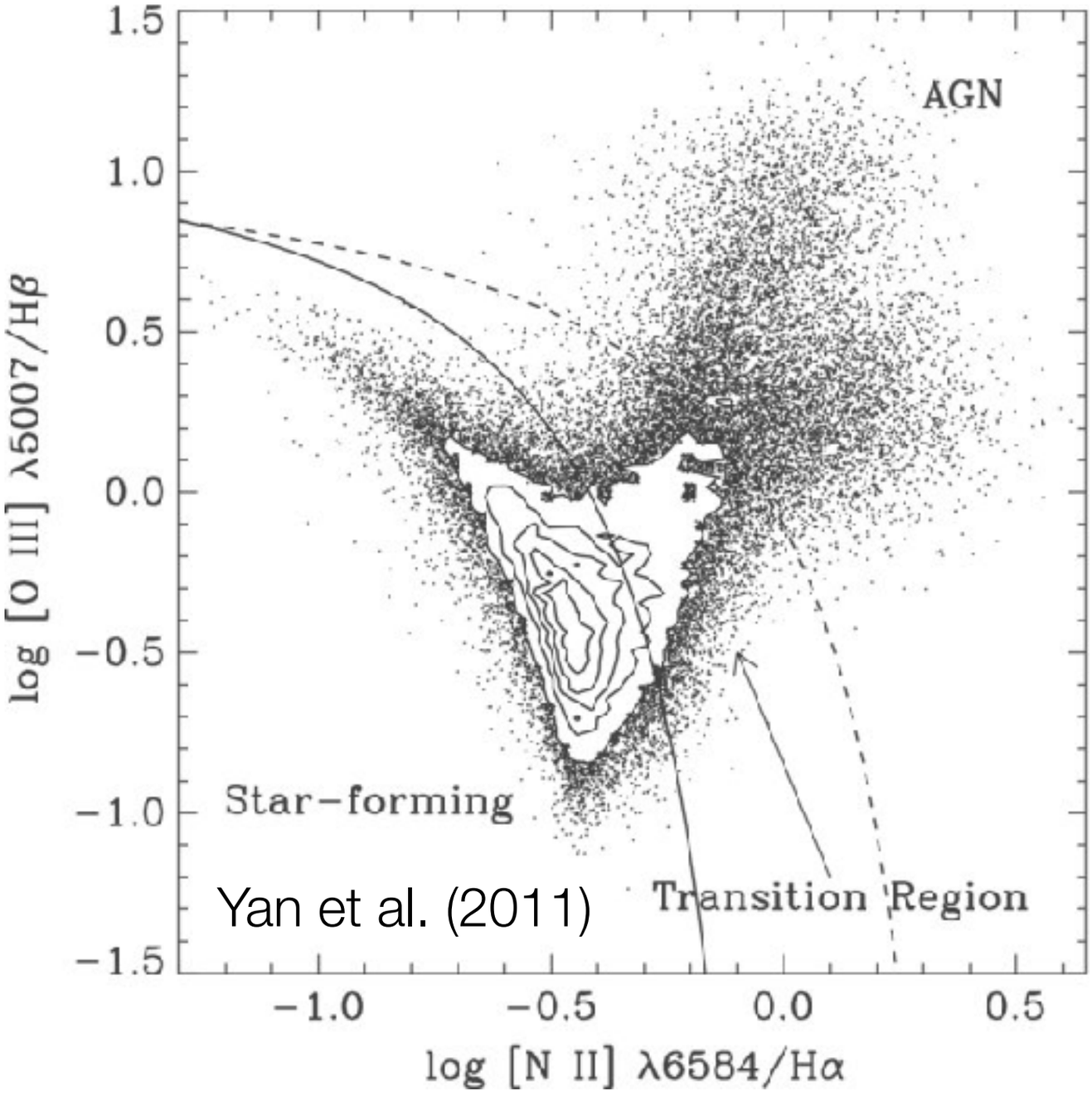

Yan et al. (2011)

Baldwin, Phillips,
and Terlevich et al. (1981)

Veilleux & Osterbrock (1987)

Selected references:
Maiolino et al. (2008)
Brinchmann et al. (2008)
Masters et al. (2016)

The N2-BPT diagnostic diagram

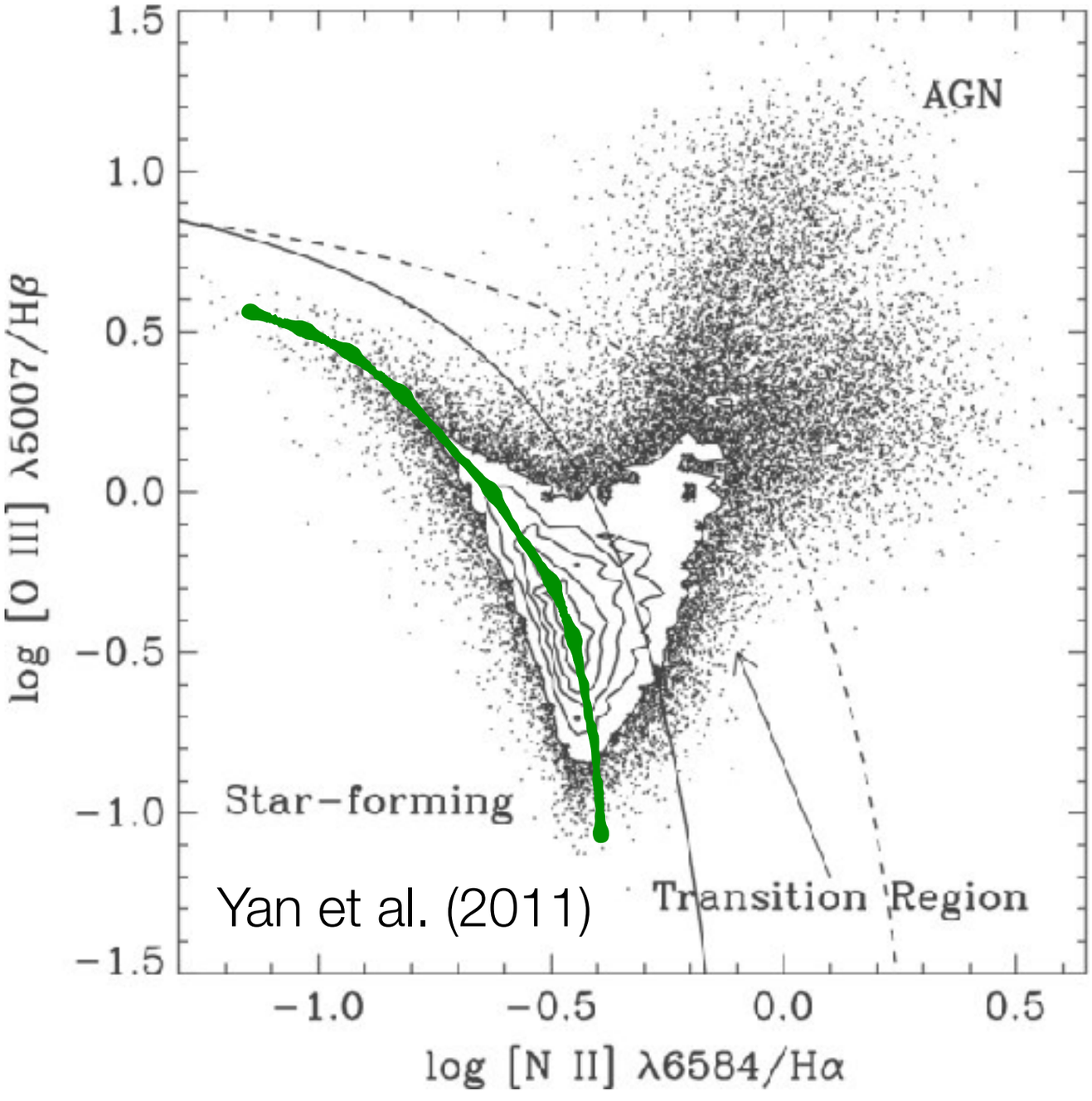

Baldwin, Phillips,
and Terlevich et al. (1981)

Veilleux & Osterbrock (1987)

Selected references:
Maiolino et al. (2008)
Brinchmann et al. (2008)
Masters et al. (2016)

The N2-BPT diagnostic diagram

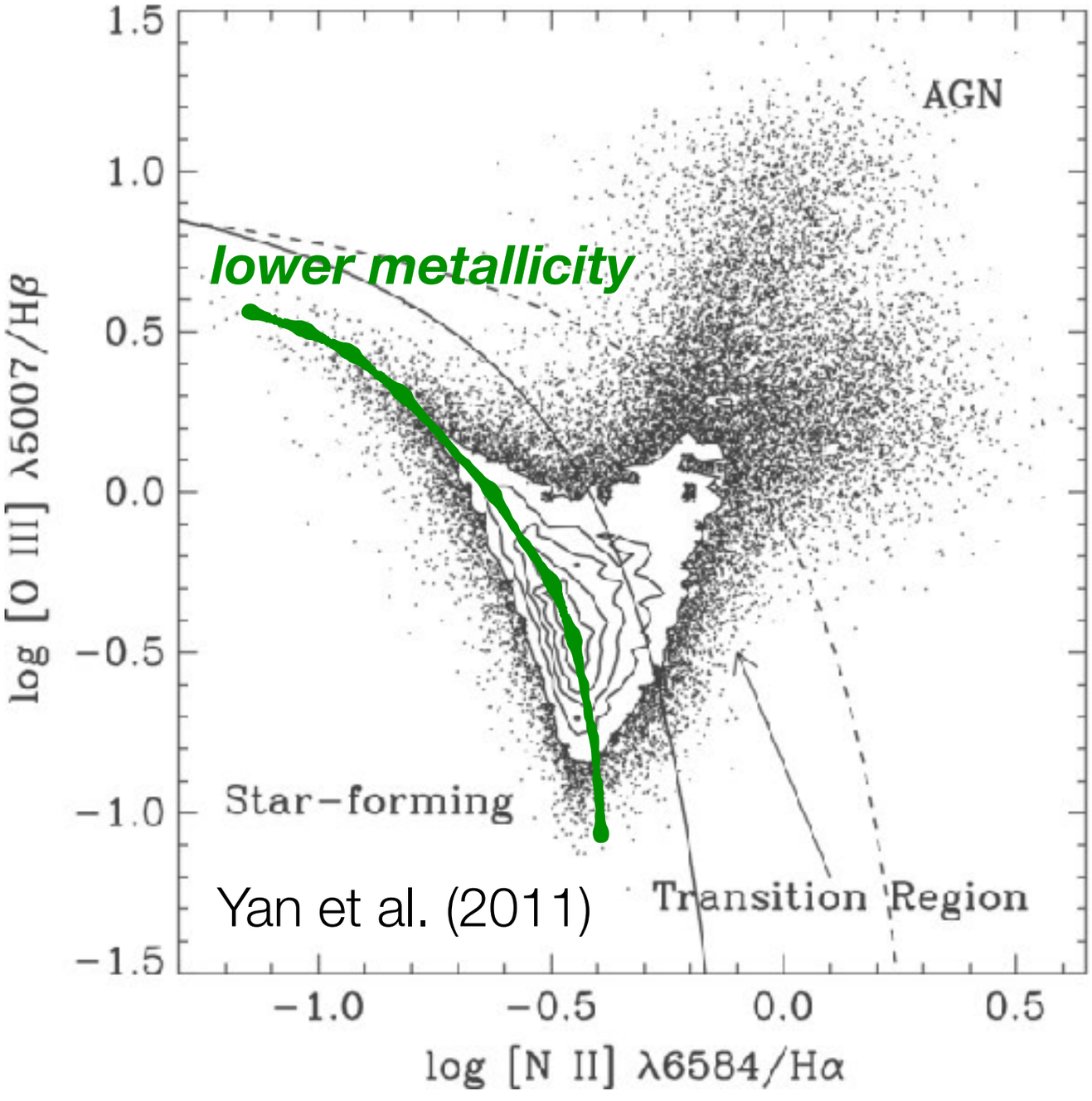

Baldwin, Phillips,
and Terlevich et al. (1981)

Veilleux & Osterbrock (1987)

Selected references:
Maiolino et al. (2008)
Brinchmann et al. (2008)
Masters et al. (2016)

The N2-BPT diagnostic diagram

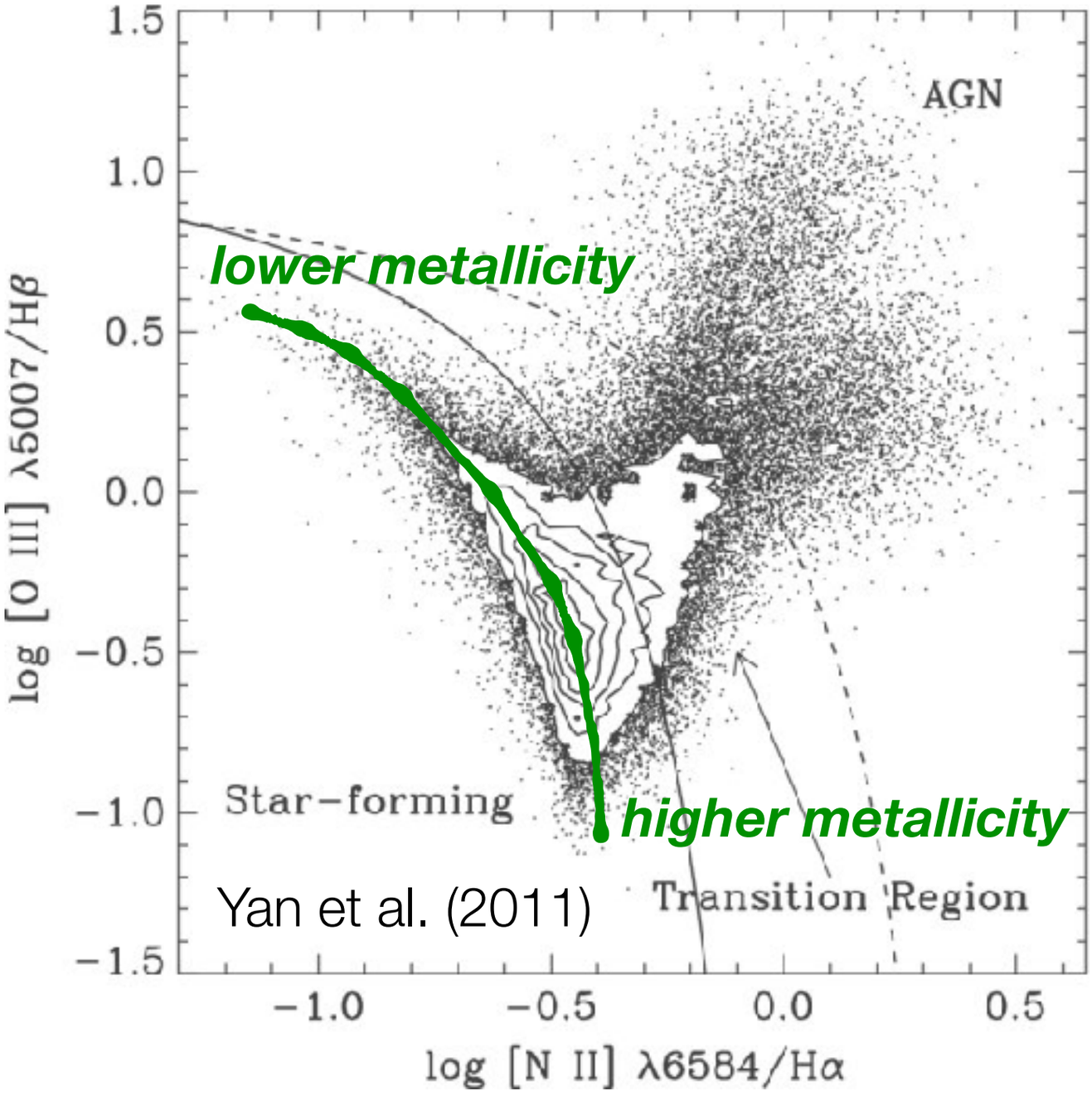

Yan et al. (2011)

Baldwin, Phillips,
and Terlevich et al. (1981)

Veilleux & Osterbrock (1987)

Selected references:
Maiolino et al. (2008)
Brinchmann et al. (2008)
Masters et al. (2016)

The N2-BPT diagnostic diagram

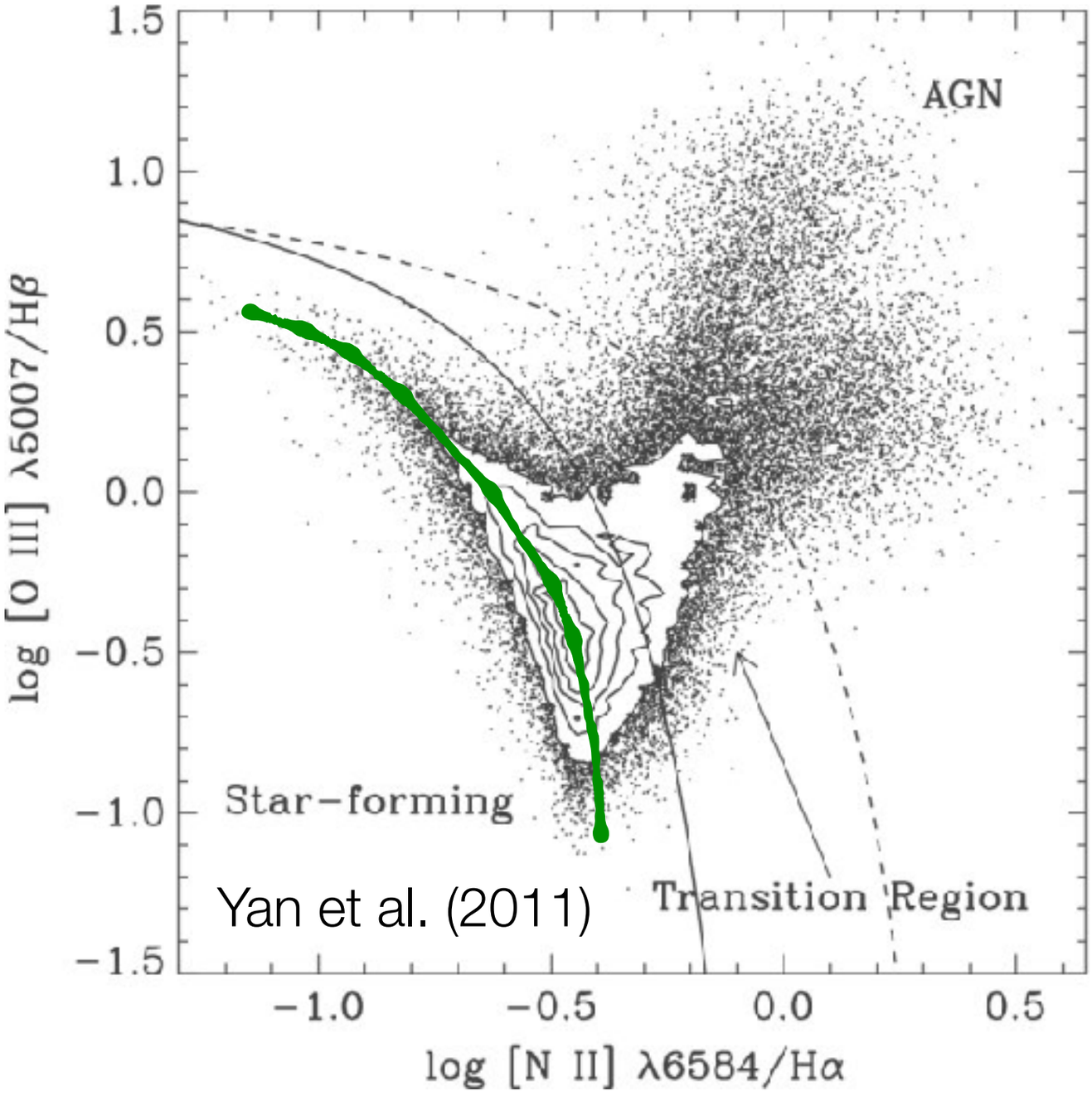

Baldwin, Phillips,
and Terlevich et al. (1981)

Veilleux & Osterbrock (1987)

Selected references:
Maiolino et al. (2008)
Brinchmann et al. (2008)
Masters et al. (2016)

The N2-BPT diagnostic diagram

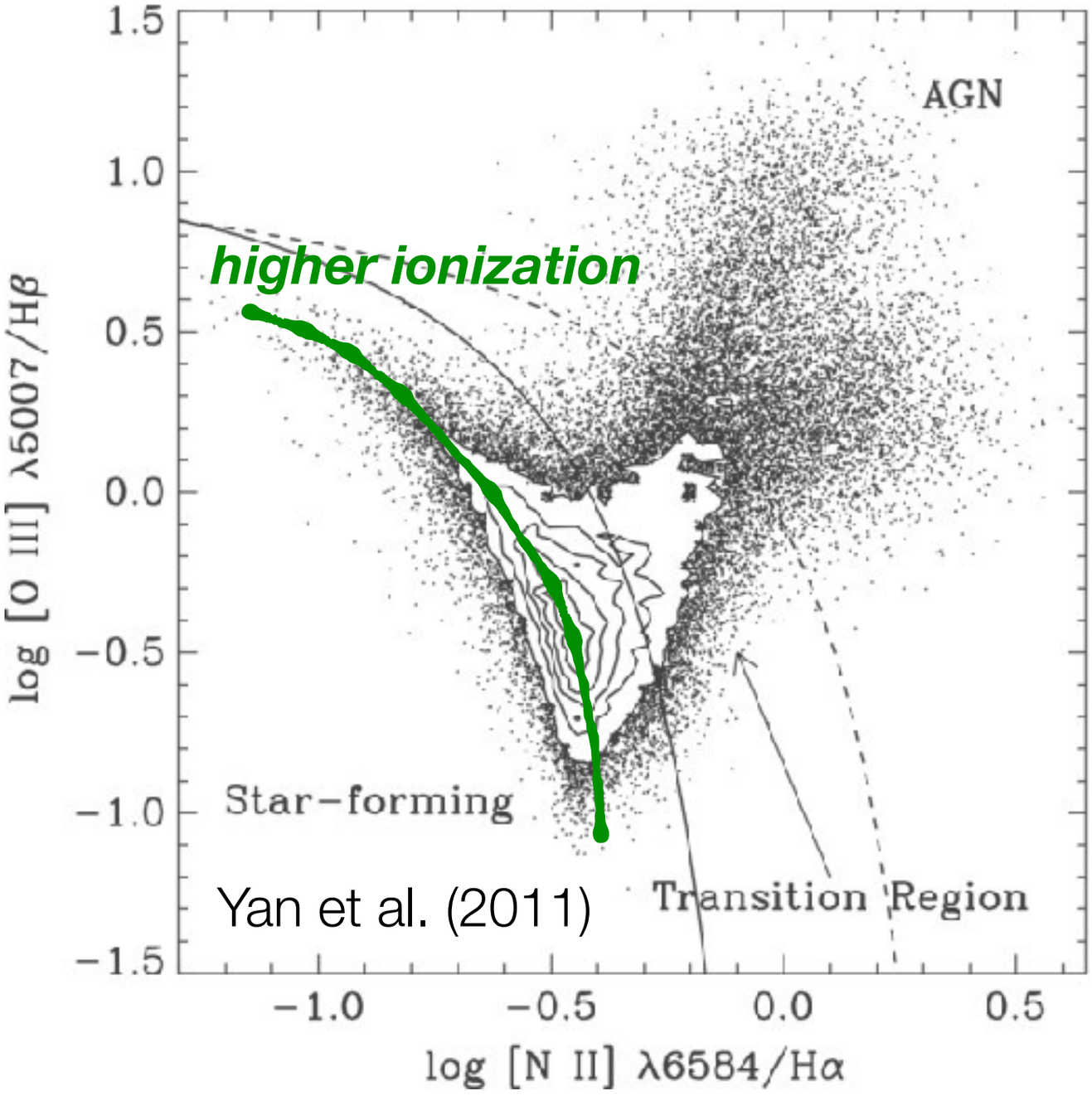

Baldwin, Phillips,
and Terlevich et al. (1981)

Veilleux & Osterbrock (1987)

Selected references:
Maiolino et al. (2008)
Brinchmann et al. (2008)
Masters et al. (2016)

The N2-BPT diagnostic diagram

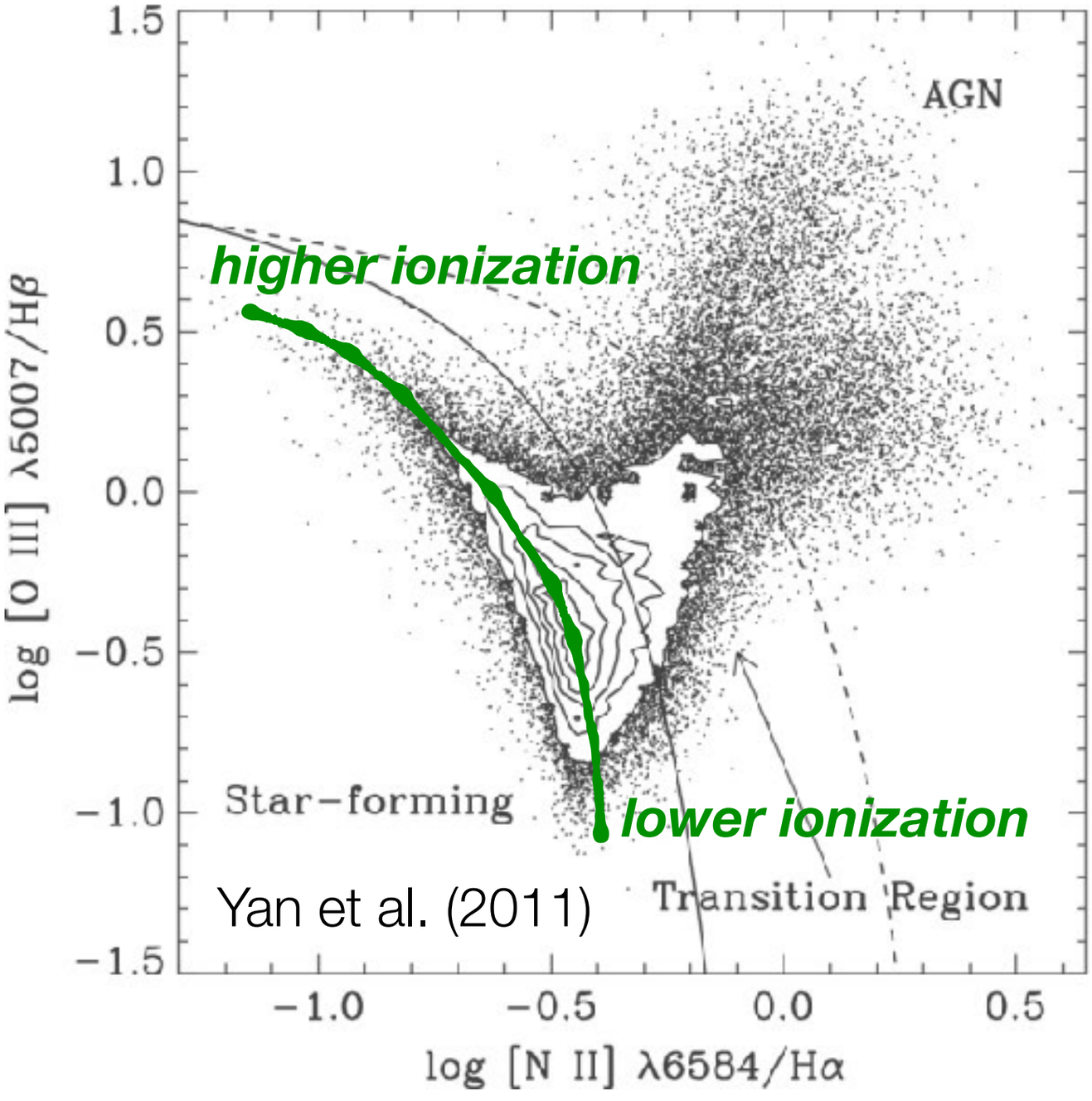

Baldwin, Phillips,
and Terlevich et al. (1981)

Veilleux & Osterbrock (1987)

Selected references:
Maiolino et al. (2008)
Brinchmann et al. (2008)
Masters et al. (2016)

The N2-BPT diagnostic diagram

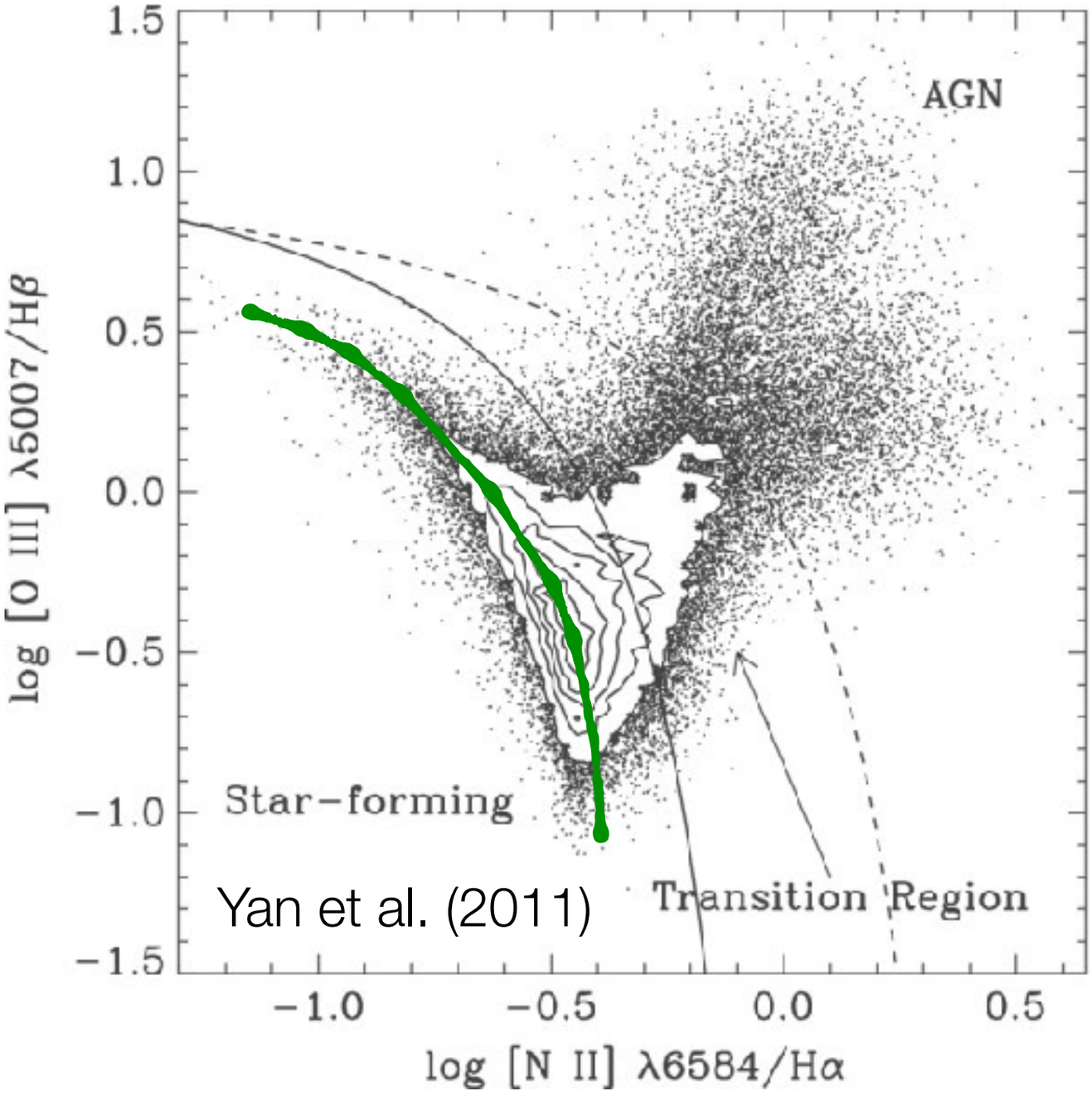

Baldwin, Phillips,
and Terlevich et al. (1981)

Veilleux & Osterbrock (1987)

Selected references:
Maiolino et al. (2008)
Brinchmann et al. (2008)
Masters et al. (2016)

The N2-BPT diagnostic diagram

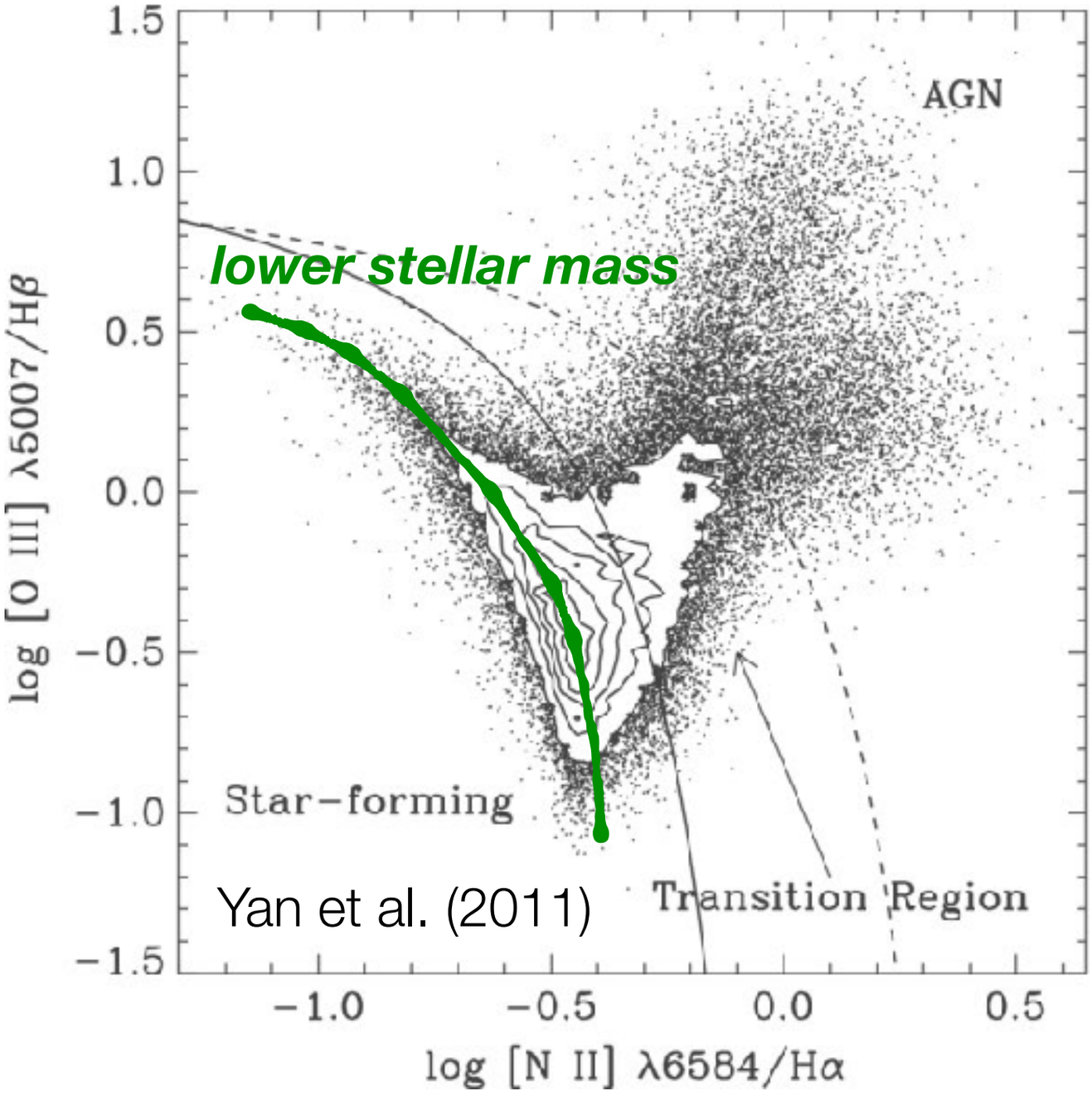

Baldwin, Phillips,
and Terlevich et al. (1981)

Veilleux & Osterbrock (1987)

Selected references:
Maiolino et al. (2008)
Brinchmann et al. (2008)
Masters et al. (2016)

The N2-BPT diagnostic diagram

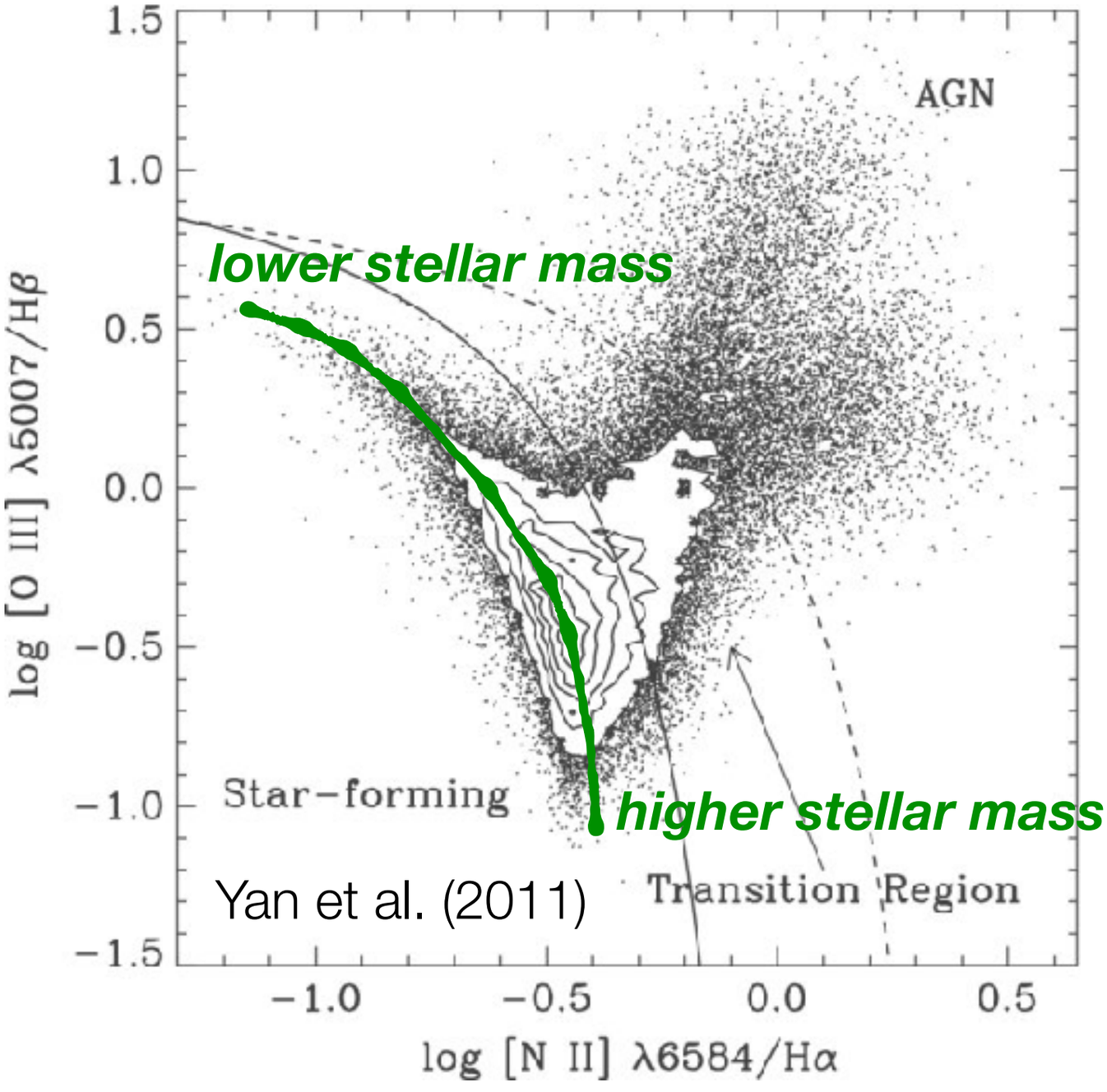

Yan et al. (2011)

Baldwin, Phillips,
and Terlevich et al. (1981)

Veilleux & Osterbrock (1987)

Selected references:
Maiolino et al. (2008)
Brinchmann et al. (2008)
Masters et al. (2016)

The N2-BPT diagnostic diagram

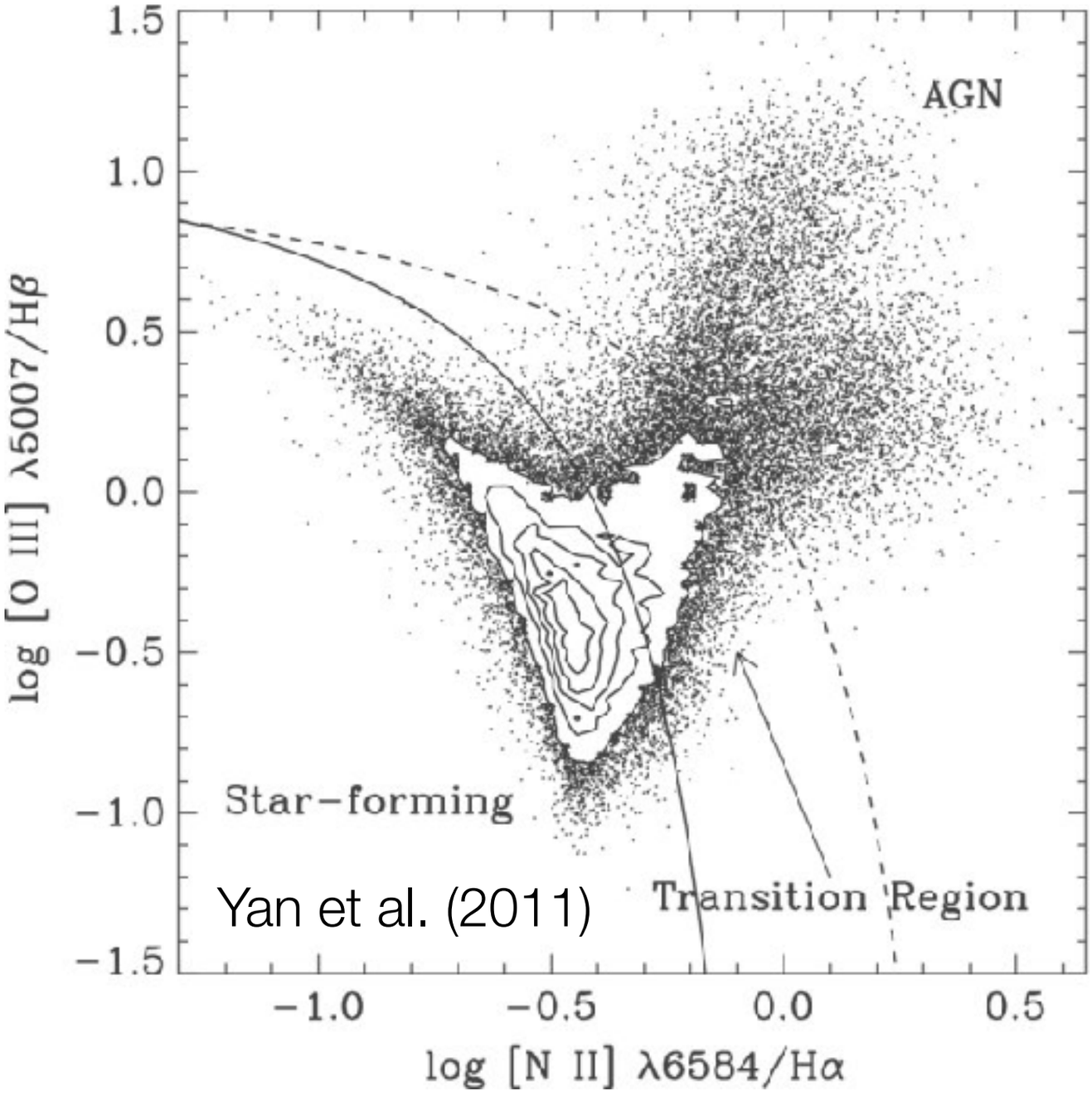

Yan et al. (2011)

Baldwin, Phillips,
and Terlevich et al. (1981)

Veilleux & Osterbrock (1987)

Selected references:
Maiolino et al. (2008)
Brinchmann et al. (2008)
Masters et al. (2016)

The N2-BPT diagnostic diagram

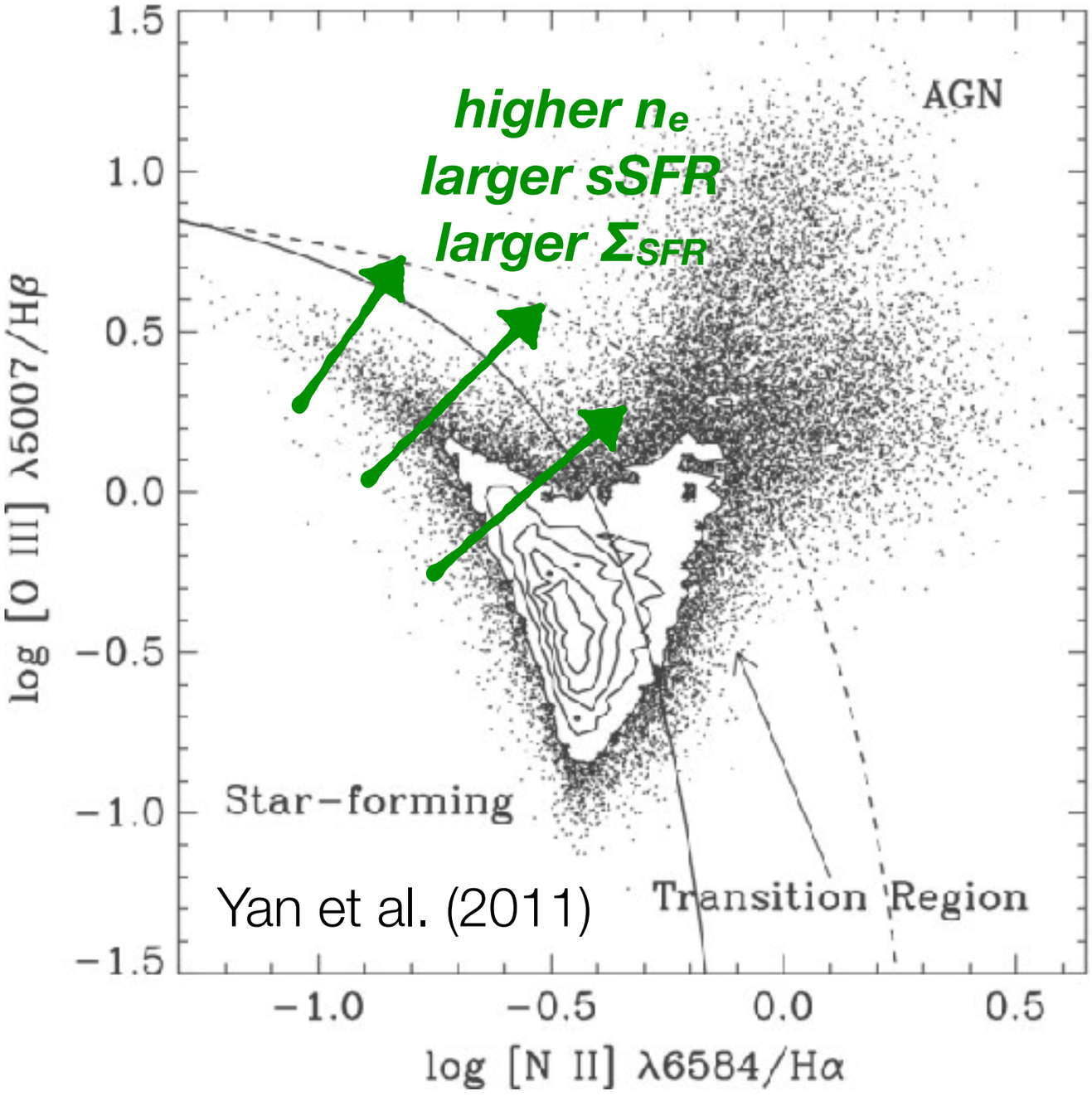

Baldwin, Phillips,
and Terlevich et al. (1981)

Veilleux & Osterbrock (1987)

Selected references:
Maiolino et al. (2008)
Brinchmann et al. (2008)
Masters et al. (2016)

The N2-BPT diagnostic diagram

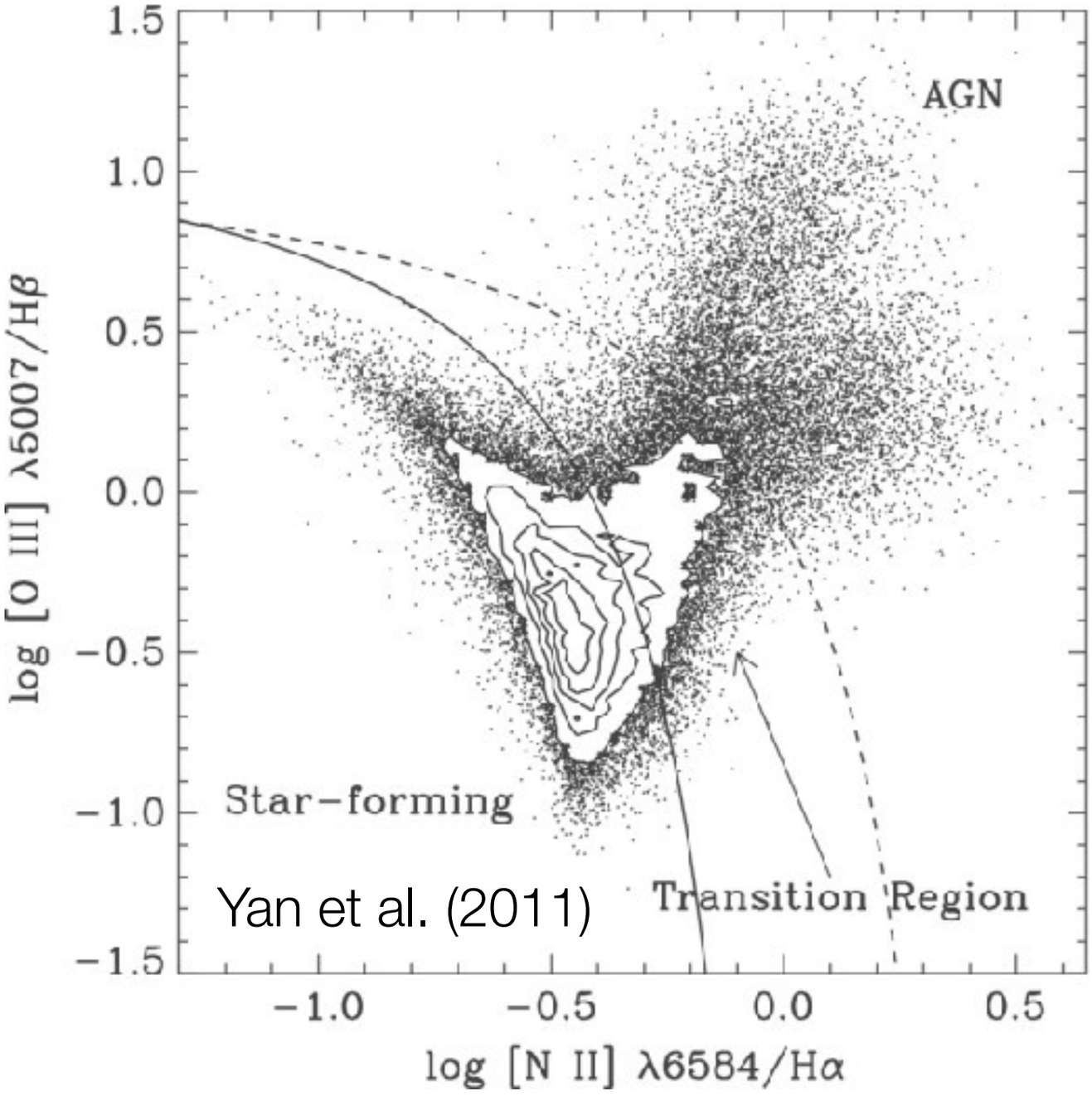

Yan et al. (2011)

Baldwin, Phillips,
and Terlevich et al. (1981)

Veilleux & Osterbrock (1987)

Selected references:
Maiolino et al. (2008)
Brinchmann et al. (2008)
Masters et al. (2016)

The N2-BPT diagnostic diagram

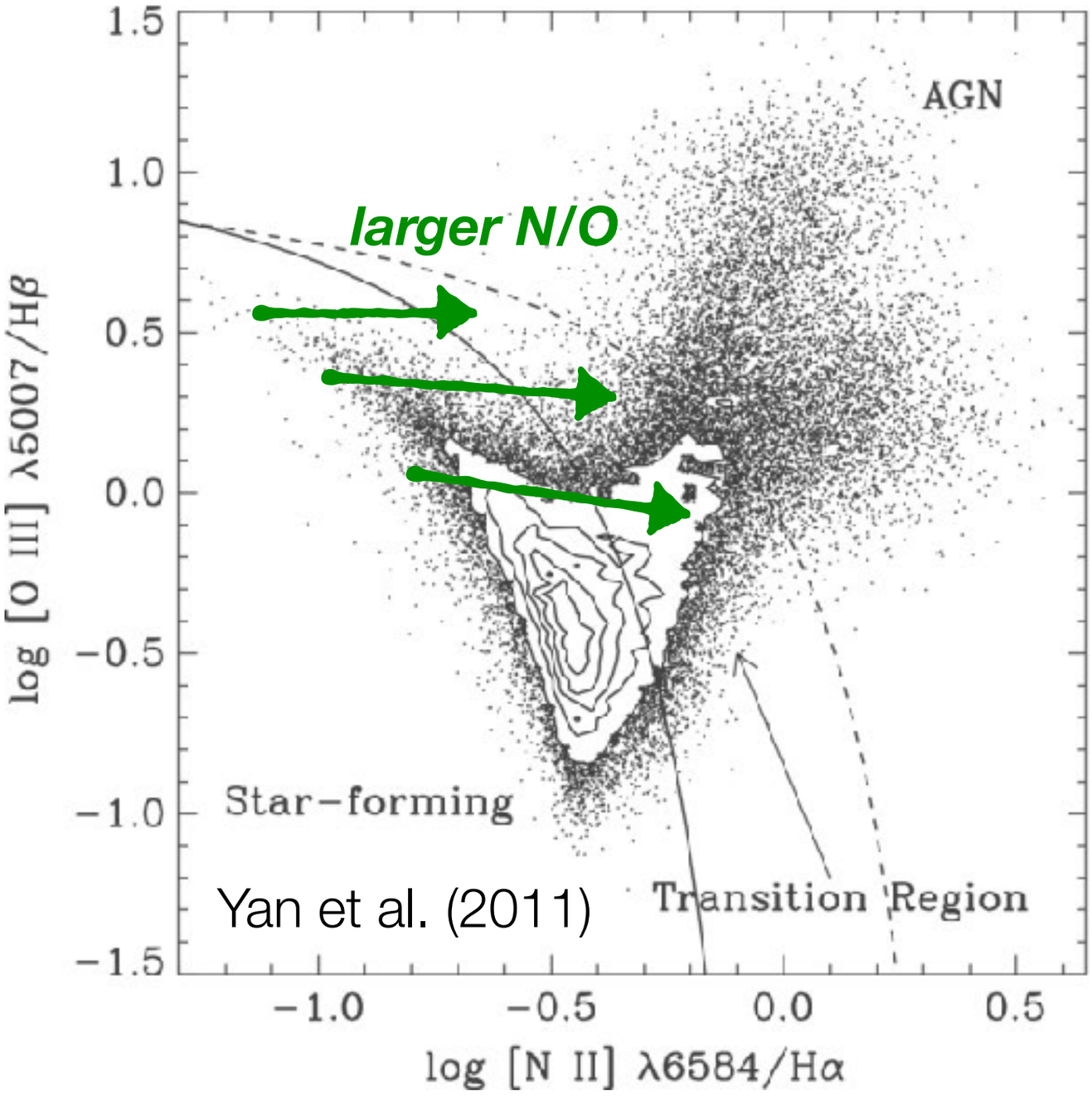

Baldwin, Phillips, and Terlevich et al. (1981)

Veilleux & Osterbrock (1987)

Selected references:
Maiolino et al. (2008)
Brinchmann et al. (2008)
Masters et al. (2016)

The N2-BPT diagnostic diagram

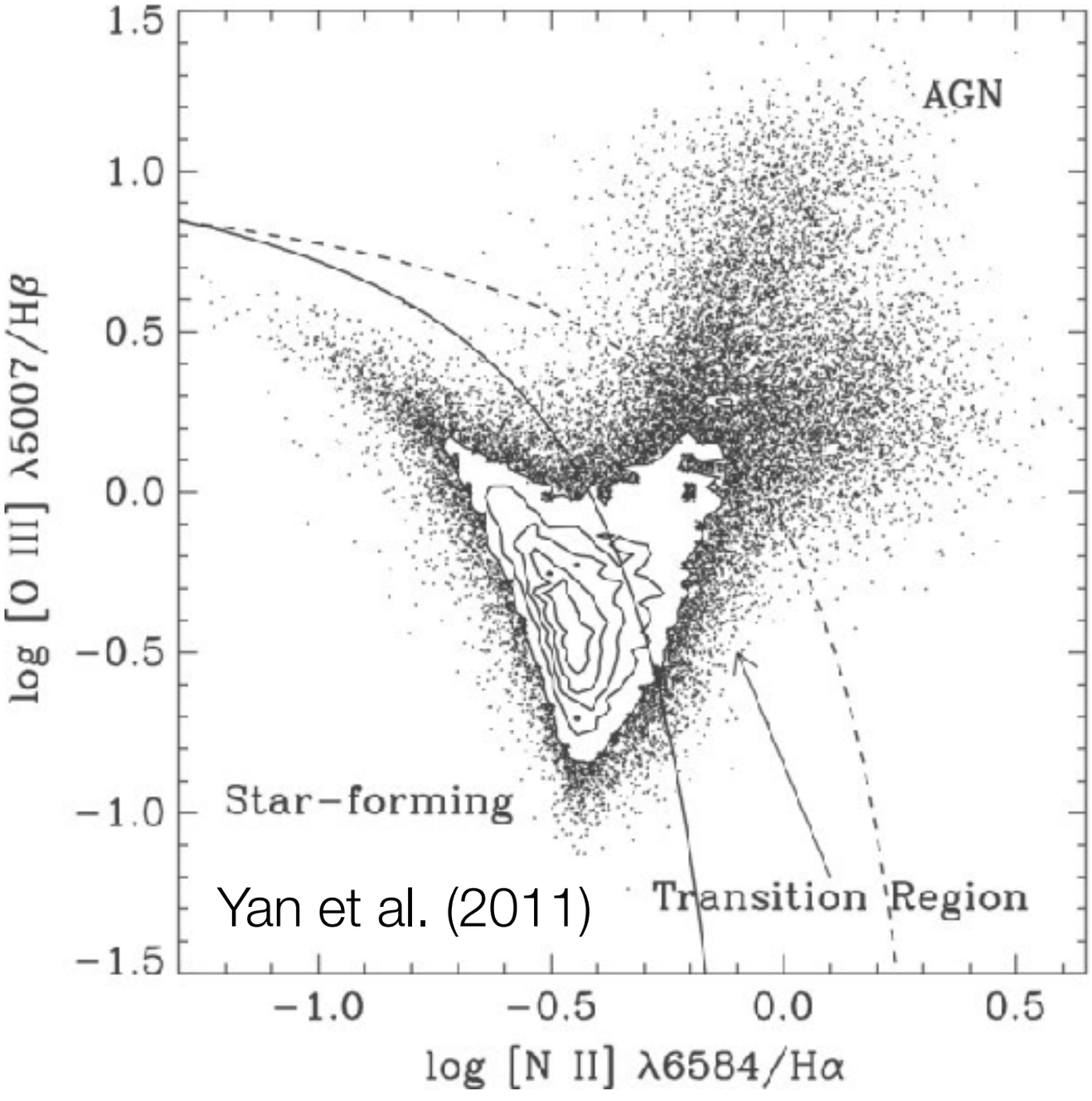

Yan et al. (2011)

Baldwin, Phillips,
and Terlevich et al. (1981)

Veilleux & Osterbrock (1987)

Selected references:
Maiolino et al. (2008)
Brinchmann et al. (2008)
Masters et al. (2016)

The N2-BPT diagnostic diagram

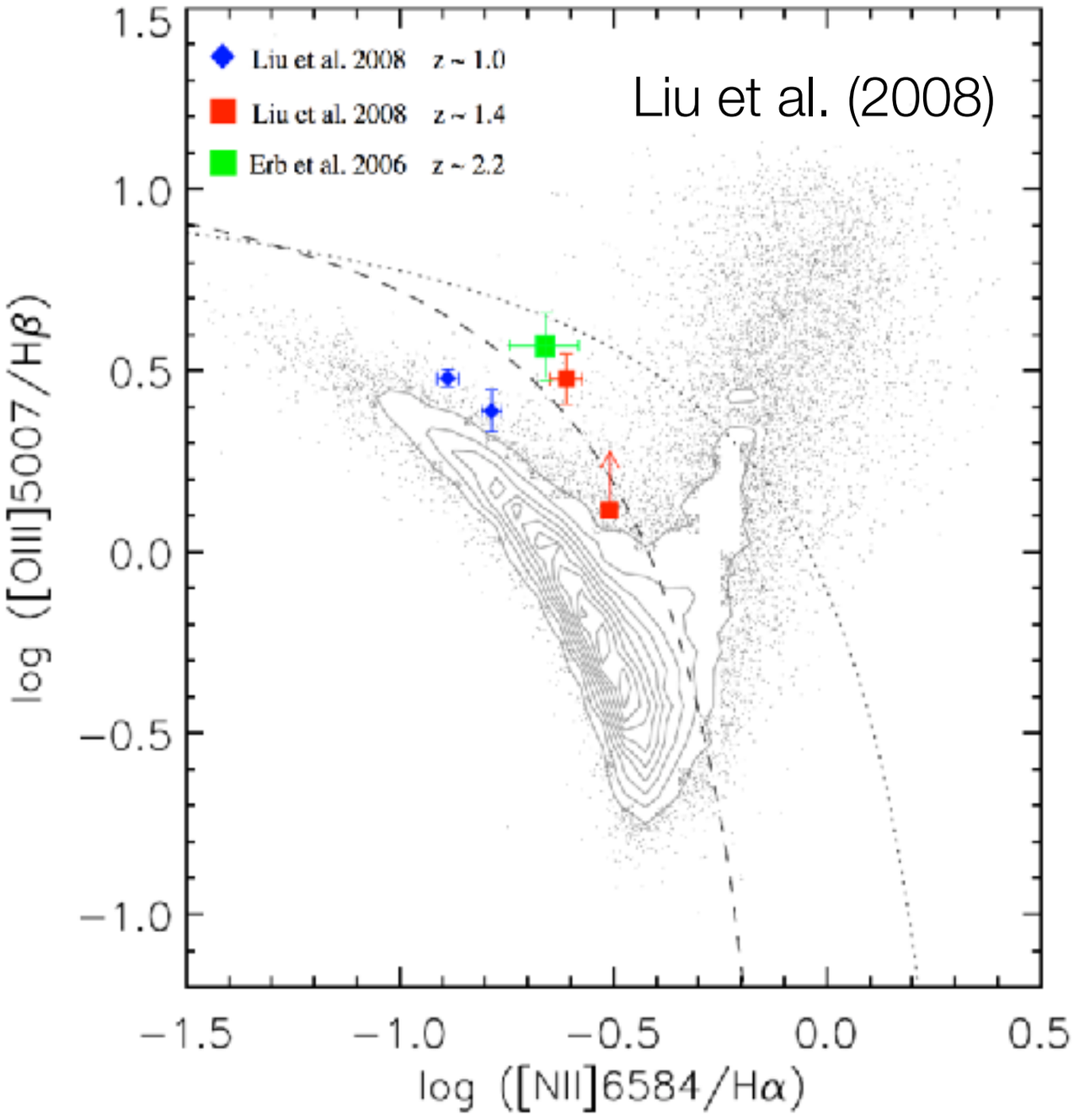

The N2-BPT diagnostic diagram

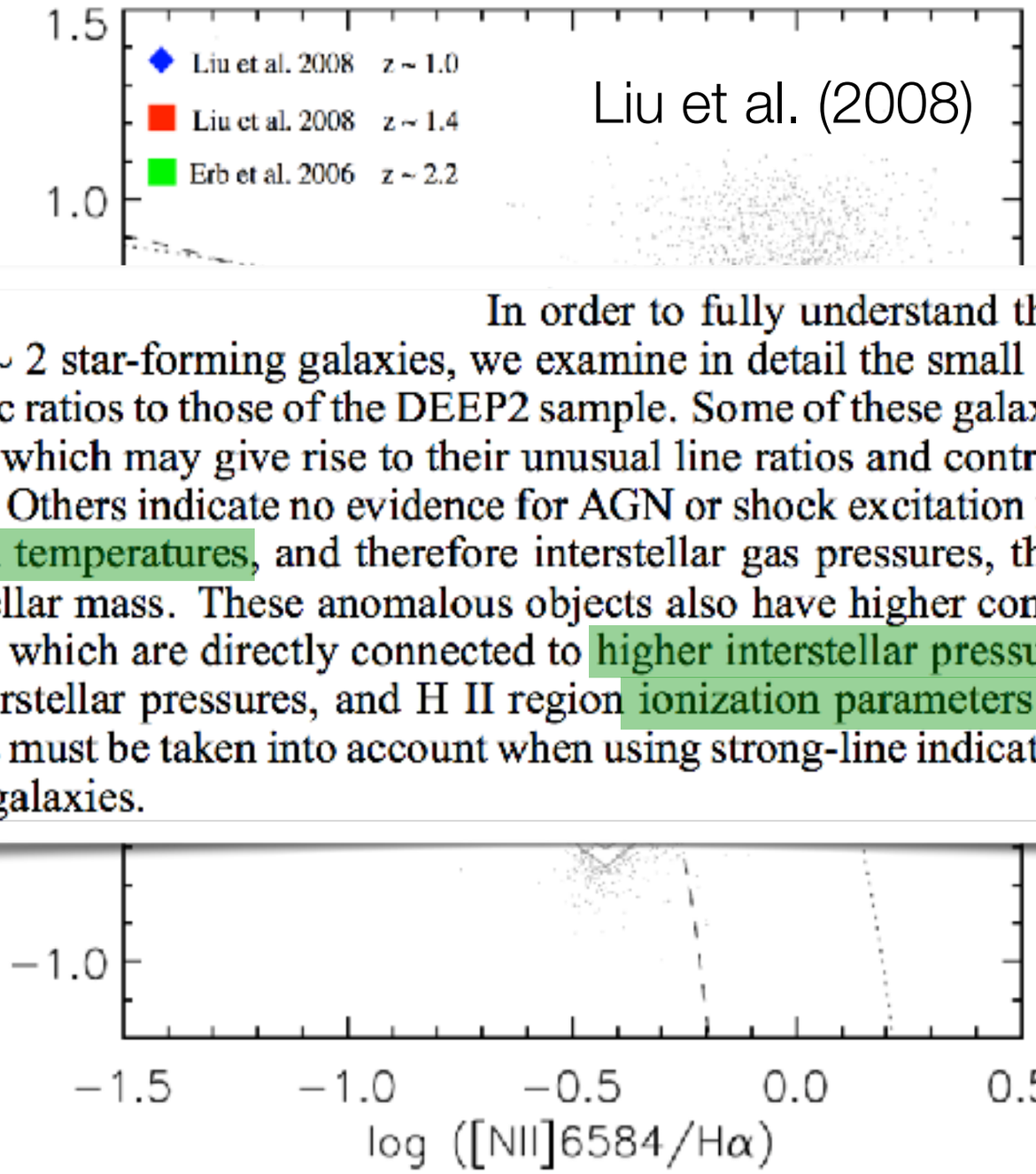

In order to fully understand the causes of this offset, which is also observed in $z \sim 2$ star-forming galaxies, we examine in detail the small fraction of SDSS galaxies that have similar diagnostic ratios to those of the DEEP2 sample. Some of these galaxies indicate evidence for AGN and/or shock activity, which may give rise to their unusual line ratios and contribute to Balmer emission lines at the level of $\sim 20\%$. Others indicate no evidence for AGN or shock excitation yet are characterized by higher electron densities and temperatures, and therefore interstellar gas pressures, than typical SDSS star-forming galaxies of similar stellar mass. These anomalous objects also have higher concentrations and star formation rate surface densities, which are directly connected to higher interstellar pressure. Higher star formation rate surface densities, interstellar pressures, and H II region ionization parameters may also be common at high redshift. These effects must be taken into account when using strong-line indicators to understand the evolution of heavy elements in galaxies.

Can we apply the paradigm developed for understanding present-day galaxies to galaxies ~2-3 Gyr after the Big Bang?

Early high-z observations were challenging

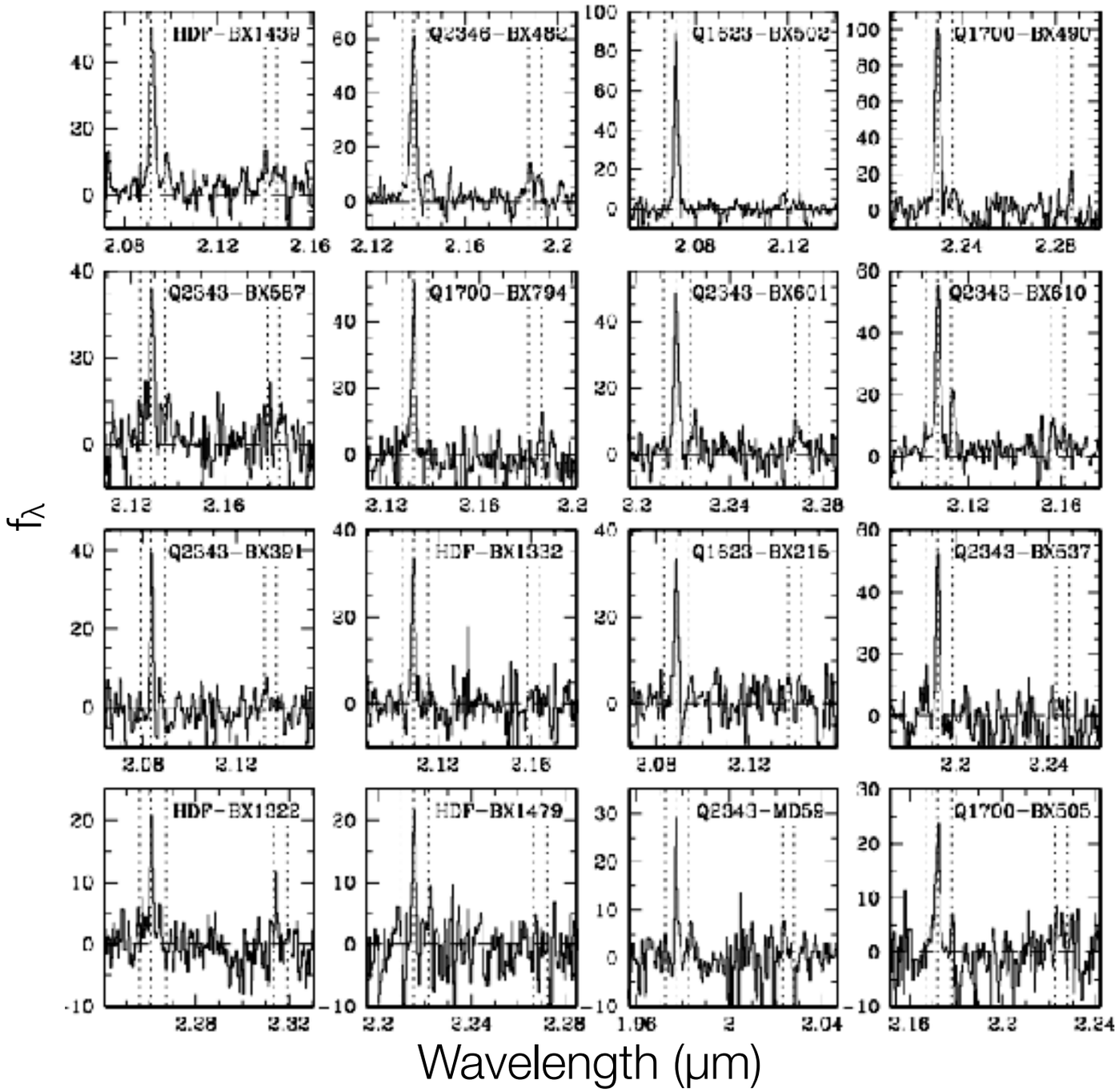

Erb et al. (2006)
114 galaxies with NIRSPEC

Needed to stack galaxies to measure multiple emission lines

Keck/MOSFIRE

Co-PIs:
Chuck Steidel (Caltech)
Ian McLean (UCLA)

6.14’ × 6.14’ field-of-view

Spectroscopy and imaging
in Y, J, H, K bands

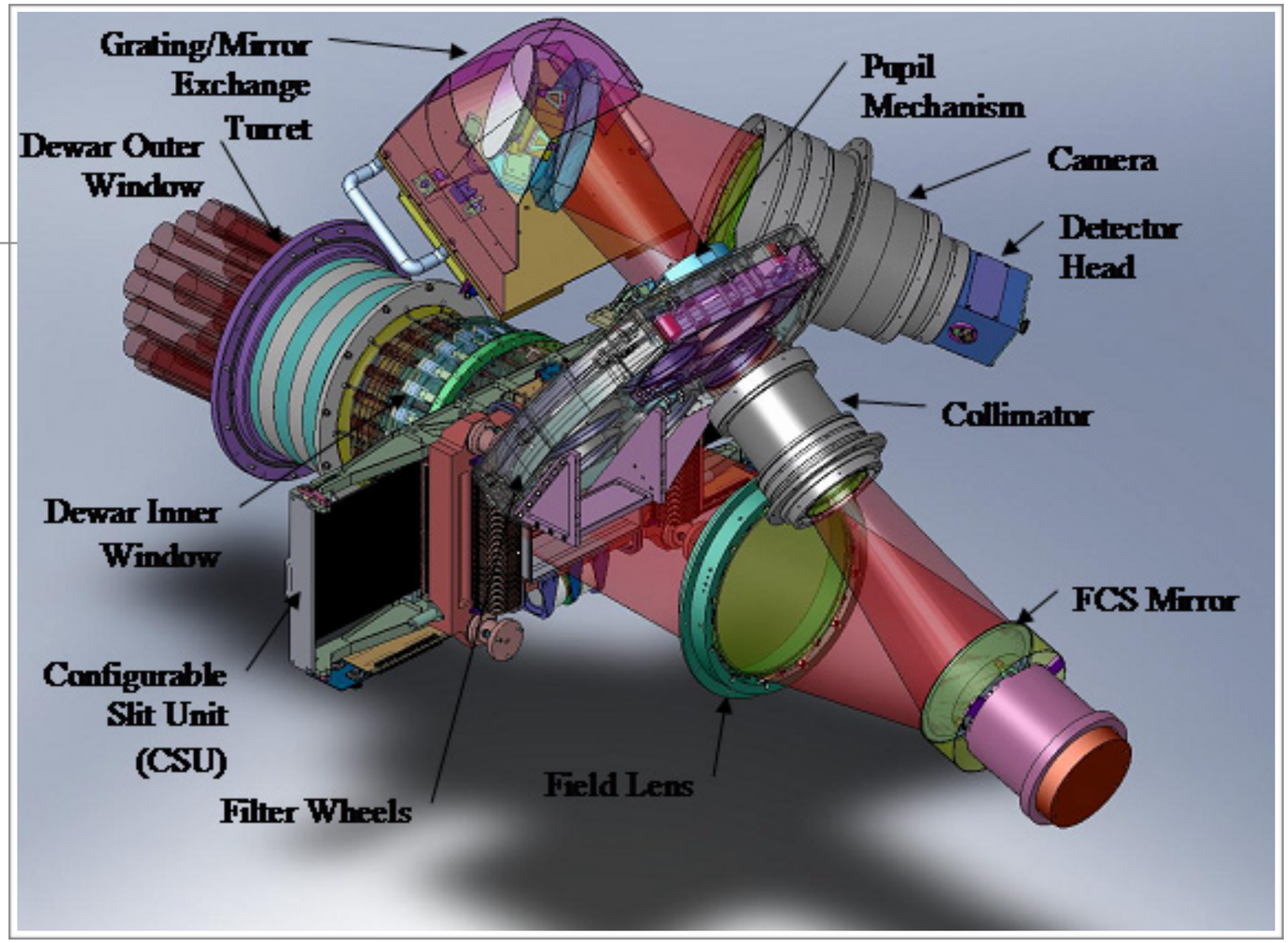

Configurable slit unit (CSU):
46 re-positionable slits maximizes flexibility and efficiency

Keck/MOSFIRE is **5× more efficient for single objects** than Keck/NIRSPEC and is **~200× more efficient when multiplexing**

Keck Baryonic Structure Survey (KBSS)

15 separate survey fields, with a total area = 0.24 deg^2

Spectroscopic observations:

- **2354 with rest-UV spectra (LRIS)**
- **1097 with rest-optical spectra**
  61 nights with MOSFIRE since commissioning in June 2012

>700 galaxies with z≈2-2.7 have at least one MOSFIRE spectrum

283 galaxies with good detections of many of the strong diagnostic emission lines in J, H, and K

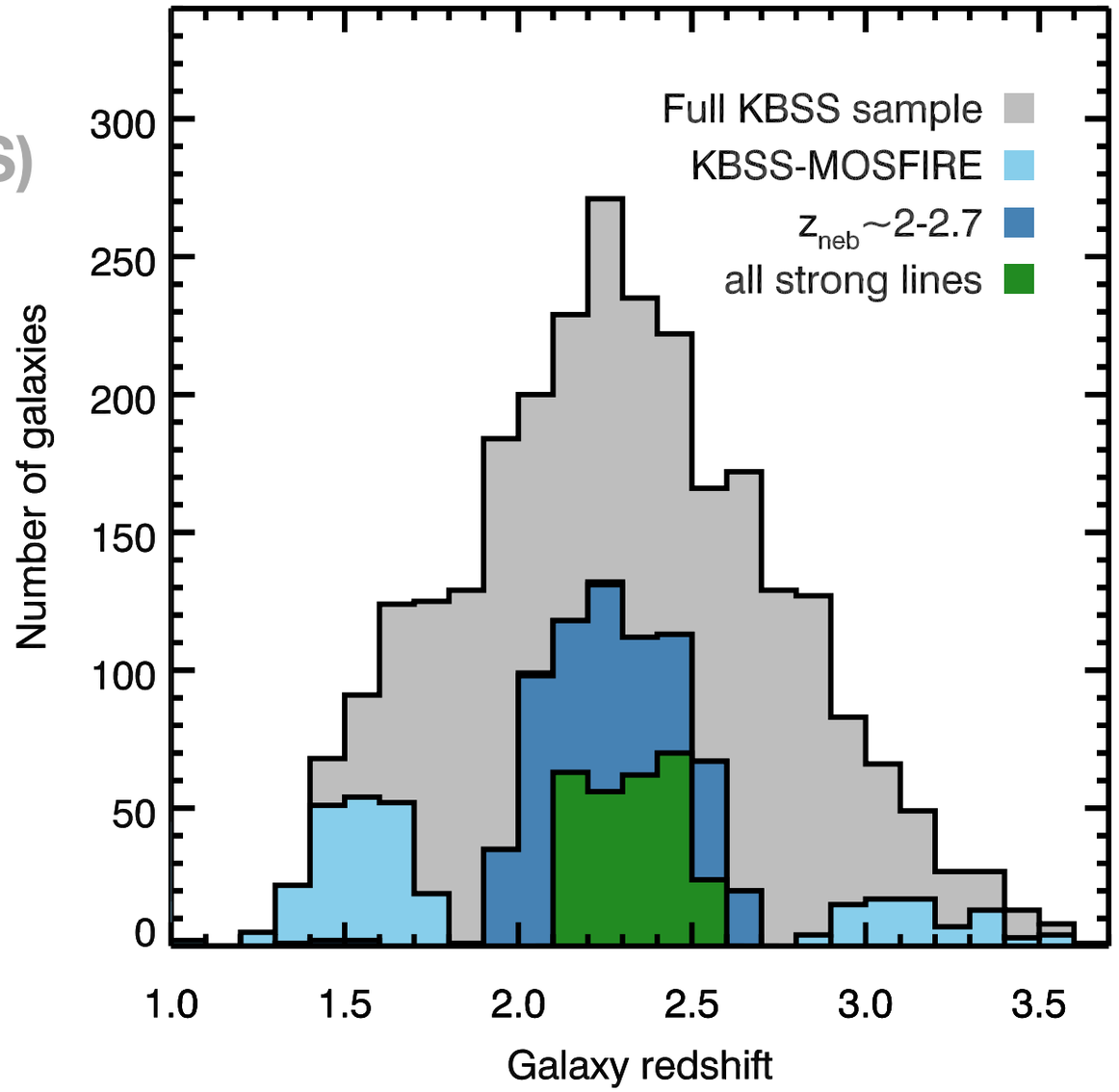

KBSS-MOSFIRE allows us to study individual galaxies in detail

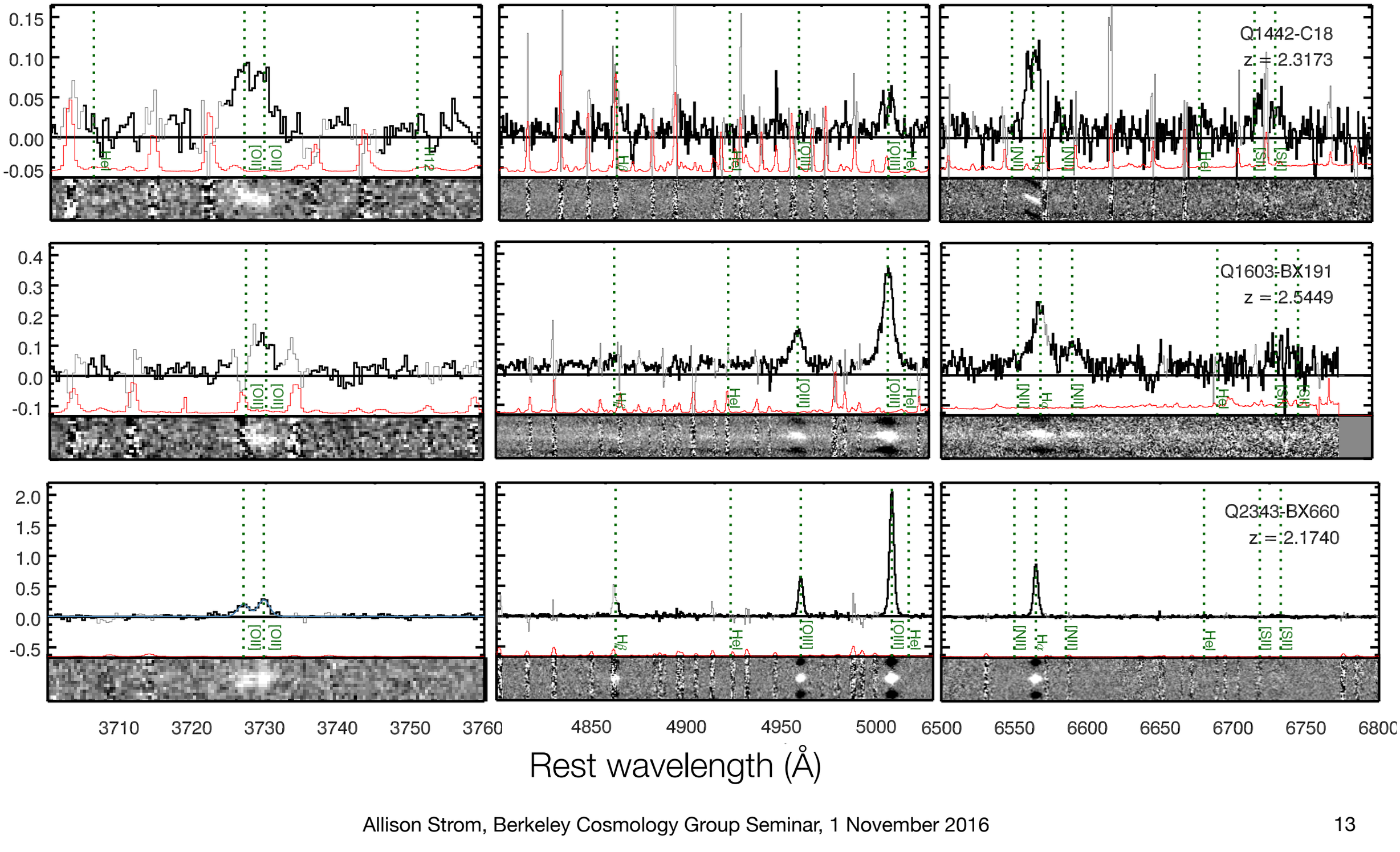

KBSS-MOSFIRE allows us to study individual galaxies in detail

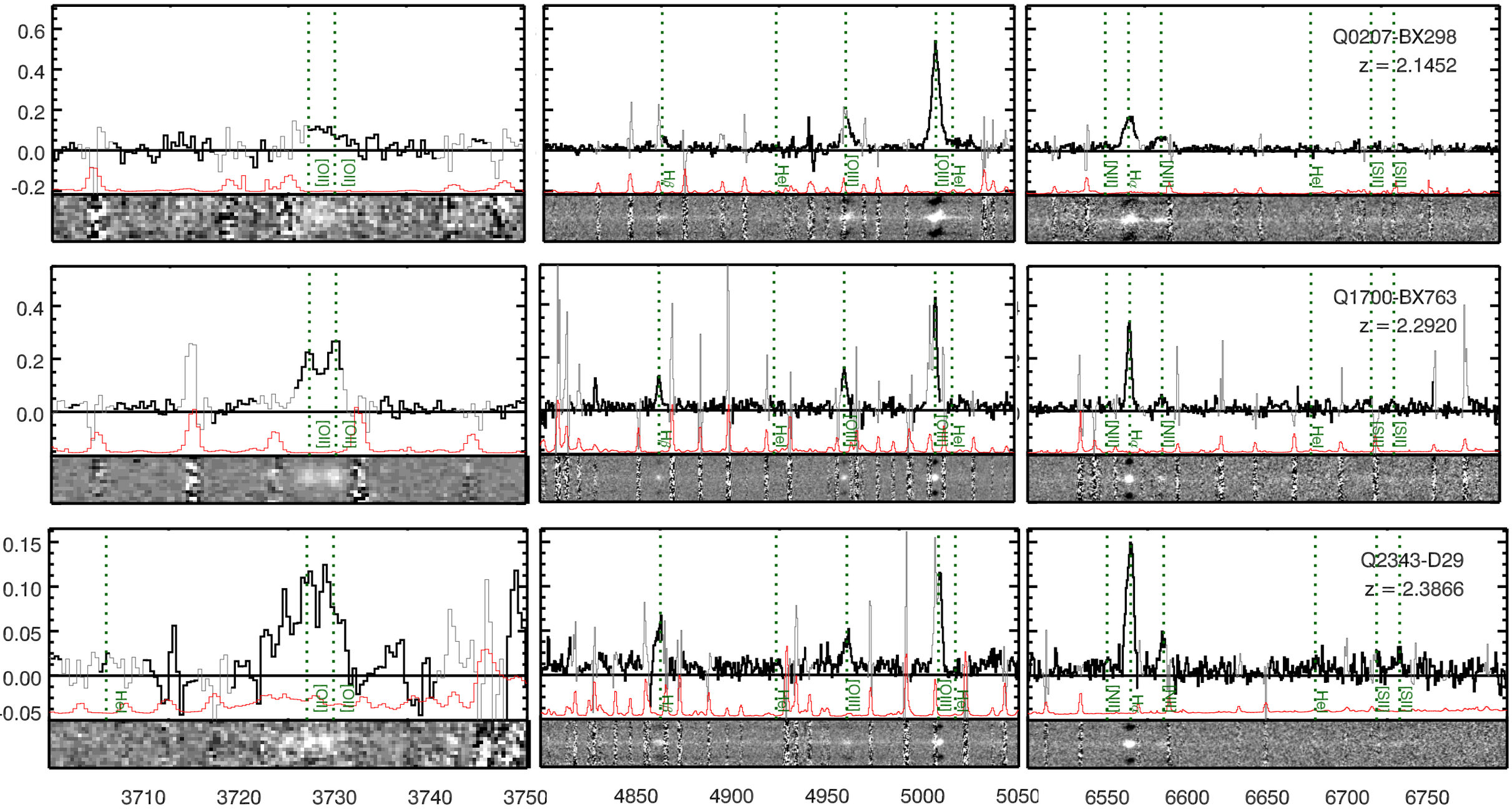

BPT diagrams for z~2-3 star-forming galaxies

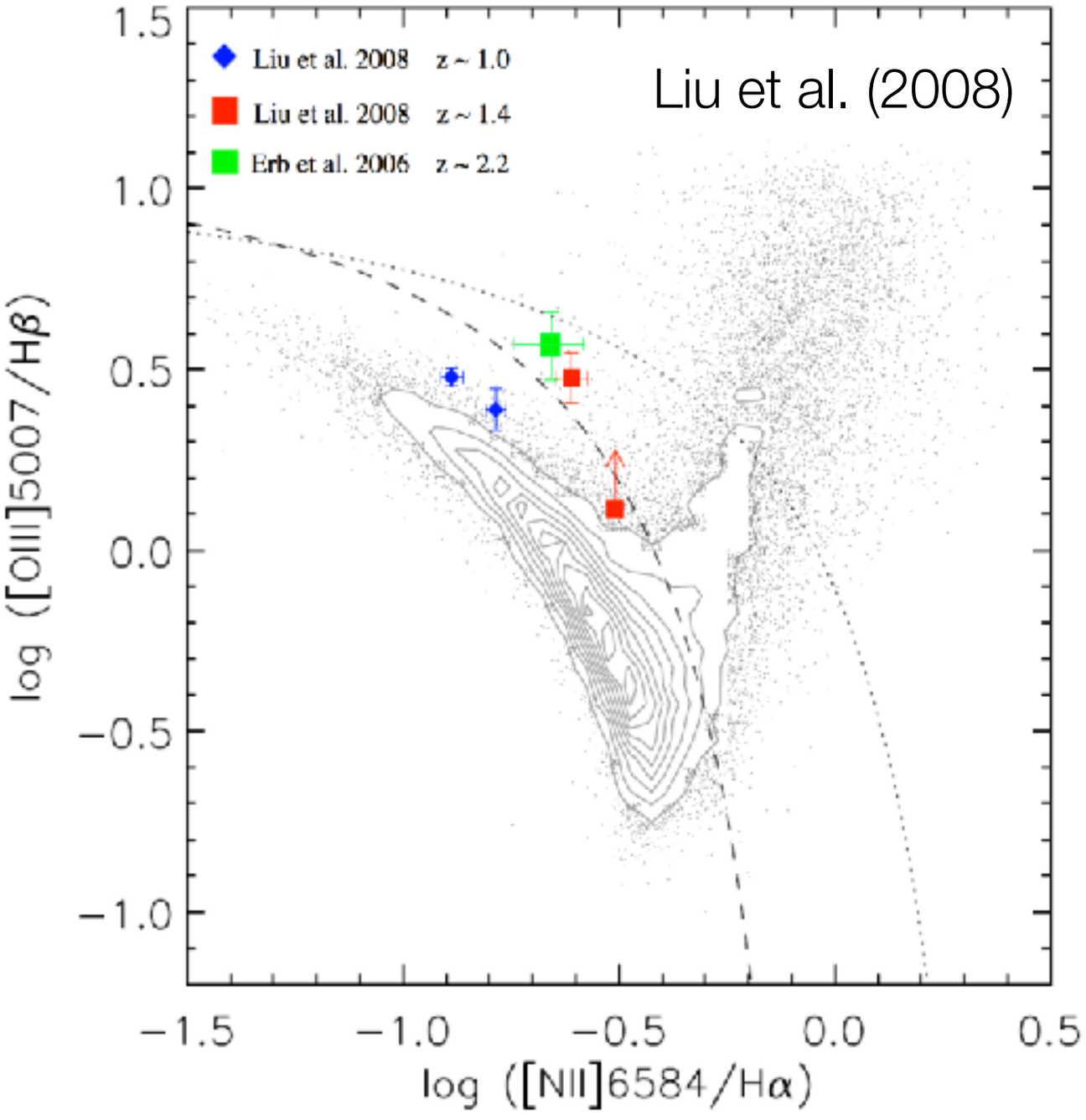

BPT diagrams for z~2-3 star-forming galaxies

Strom et al. (2016), arXiv:1608.02587

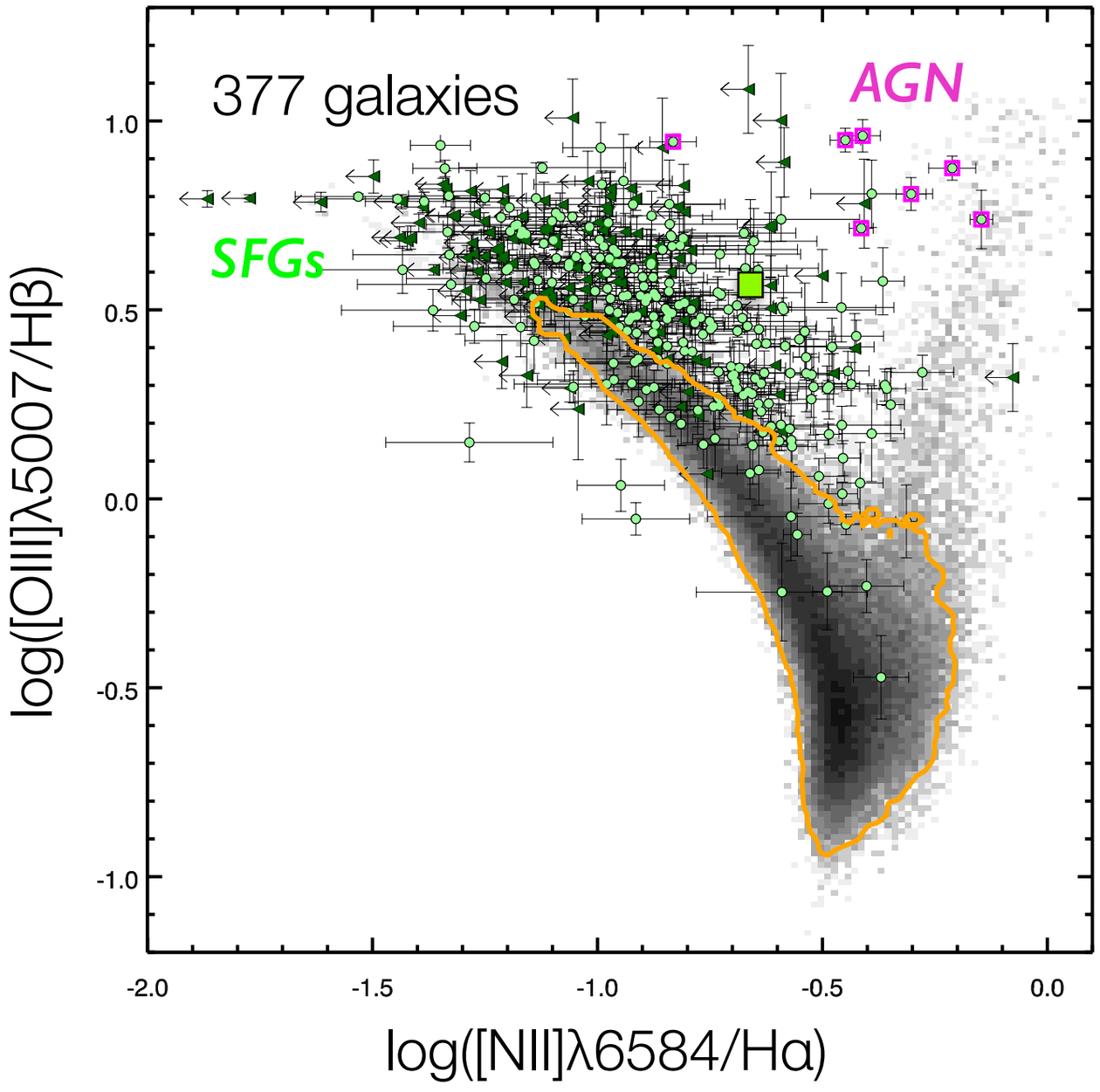

BPT diagrams for z~2-3 star-forming galaxies

Strom et al. (2016), arXiv:1608.02587

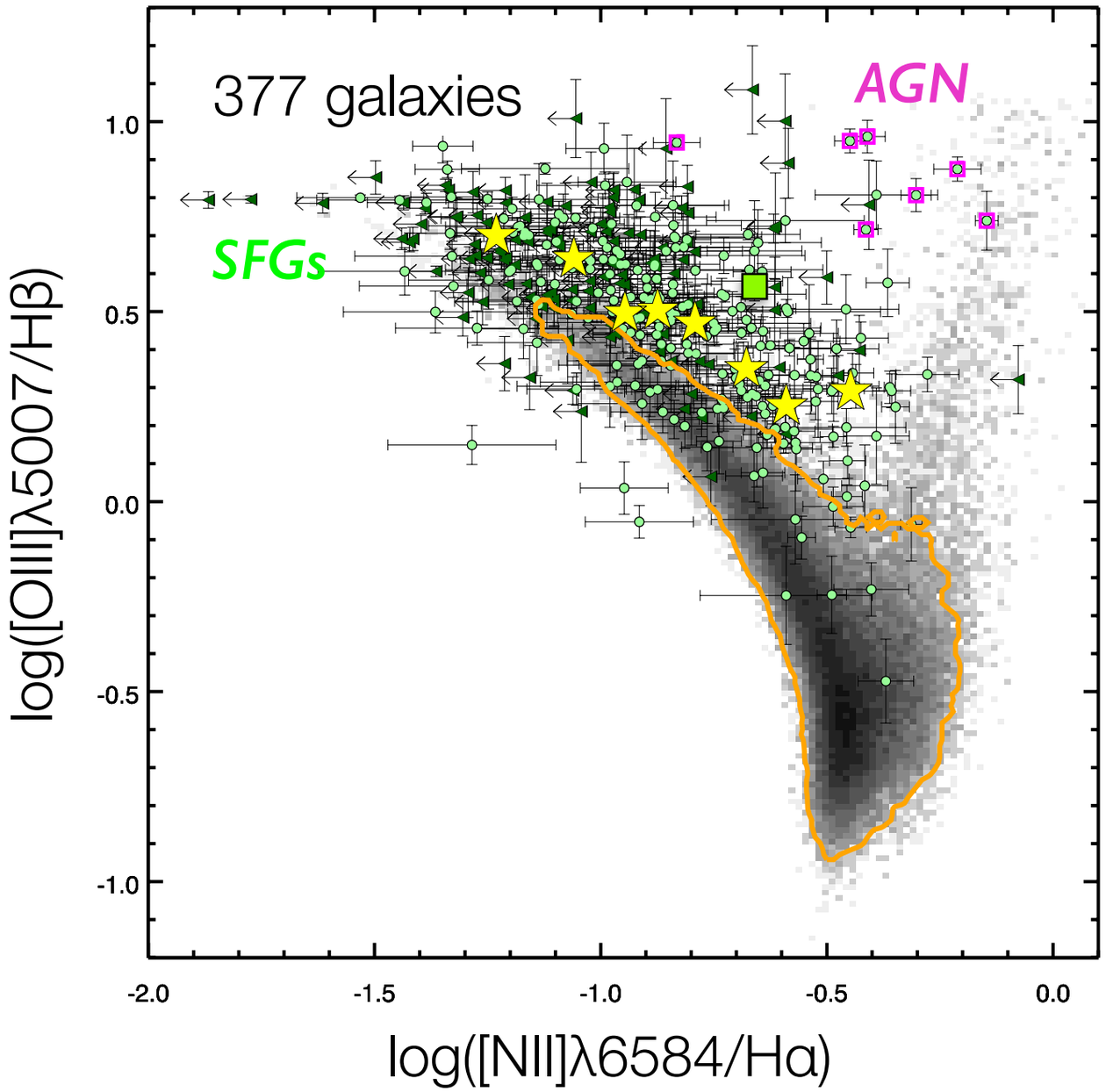

BPT diagrams for z~2-3 star-forming galaxies

Strom et al. (2016), arXiv:1608.02587

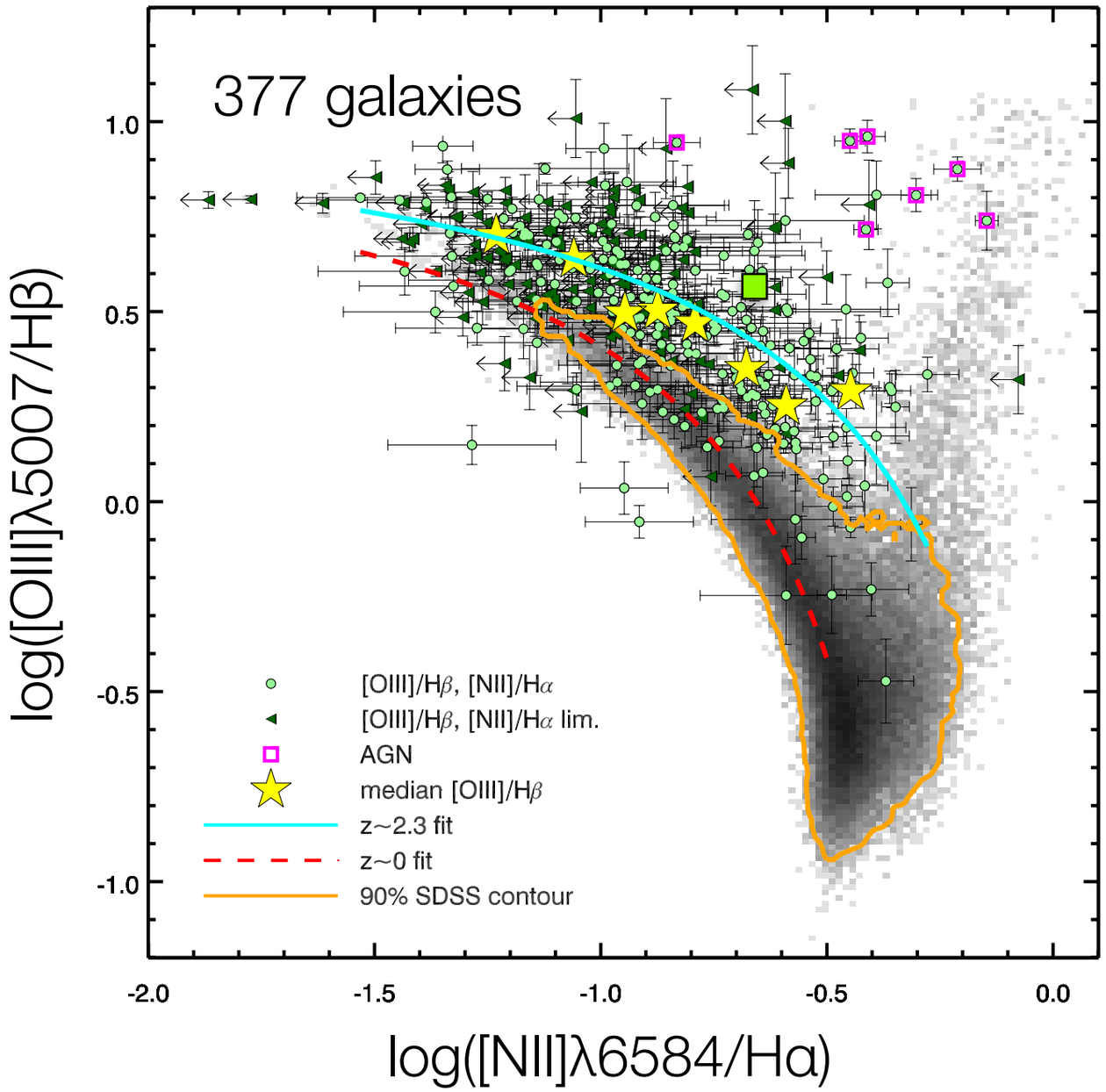

What is different about z~2-3 galaxies?

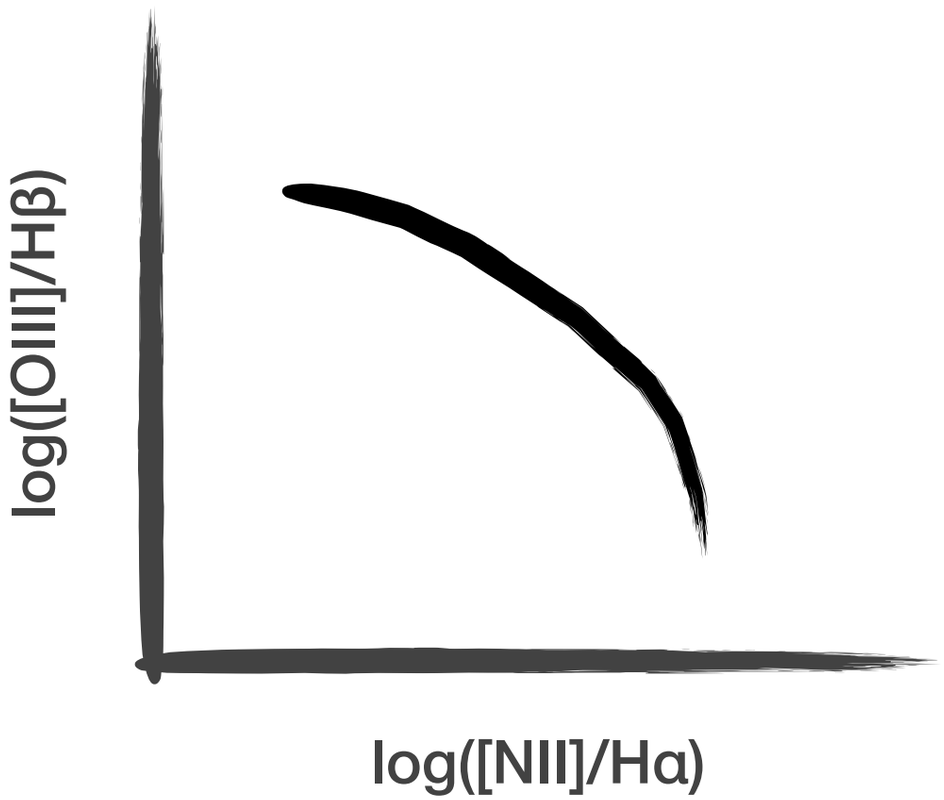

What is different about z~2-3 galaxies?

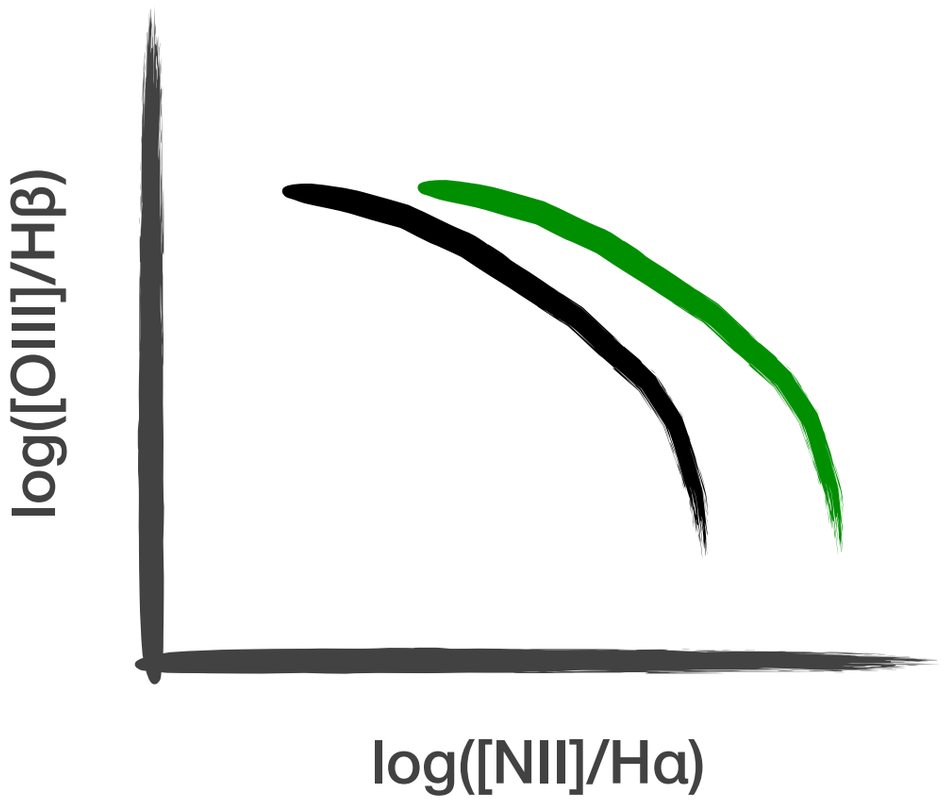

enhanced N/O at fixed O/H

(e.g., Masters+14, Shapley+15, Sanders+16, Masters+16)

What is different about z~2-3 galaxies?

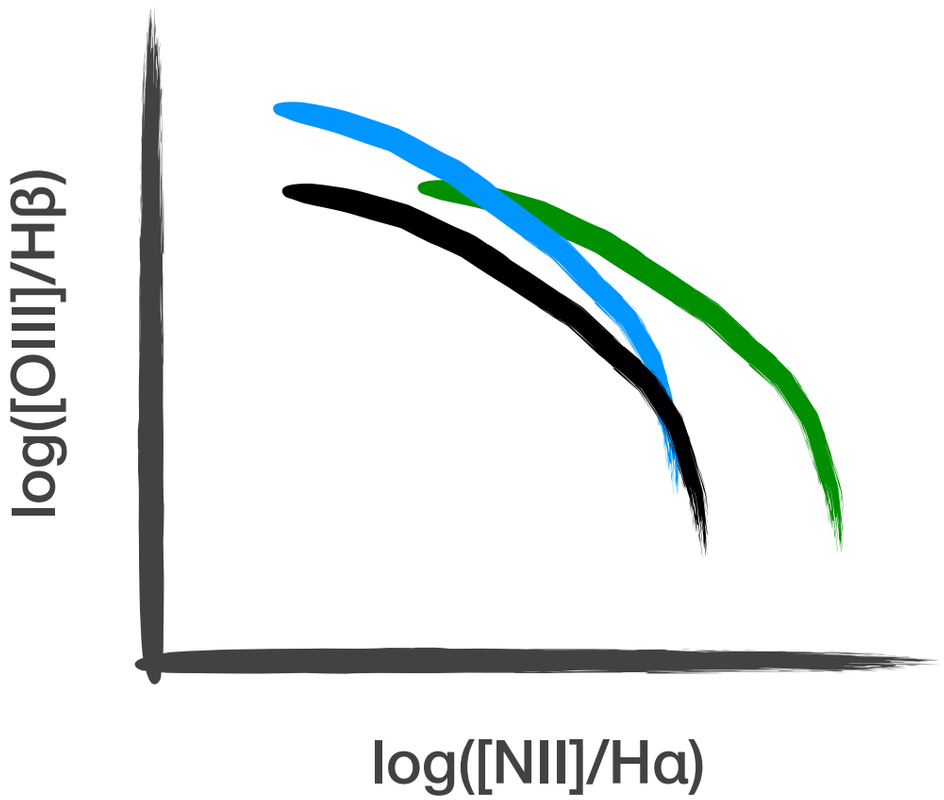

enhanced N/O at fixed O/H

(e.g., Masters+14, Shapley+15, Sanders+16, Masters+16)

more ionizing photons

(e.g., Kewley+15)

What is different about z~2-3 galaxies?

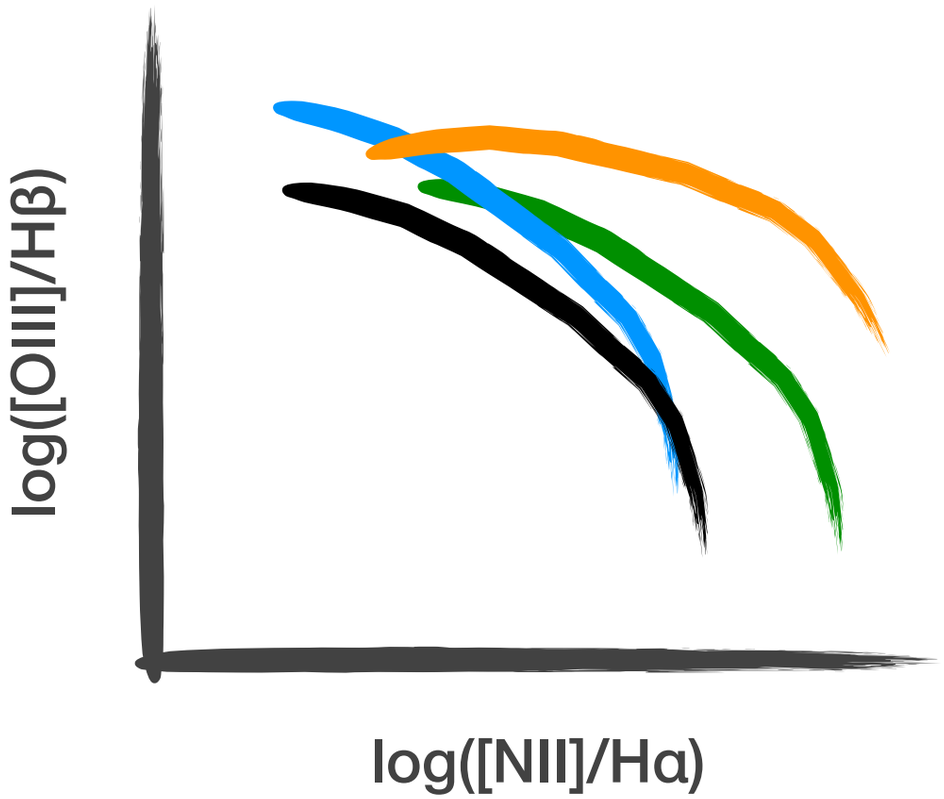

enhanced N/O at fixed O/H

(e.g., Masters+14, Shapley+15, Sanders+16, Masters+16)

more ionizing photons

(e.g., Kewley+15)

harder ionizing radiation

(e.g., Steidel+14, Steidel+16, Strom+16)

Absence of offset in S2-BPT suggested that N was anomalous

Masters et al. (2014)

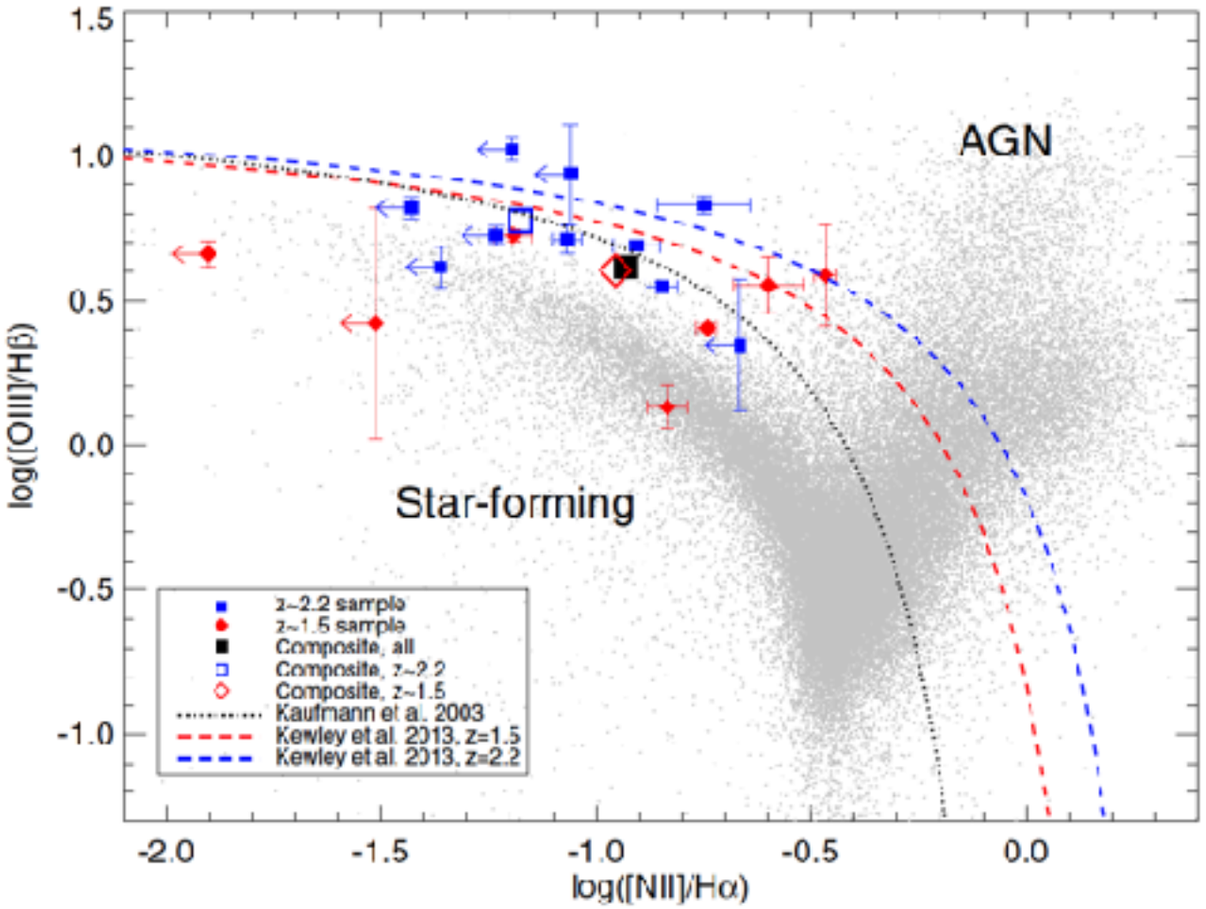

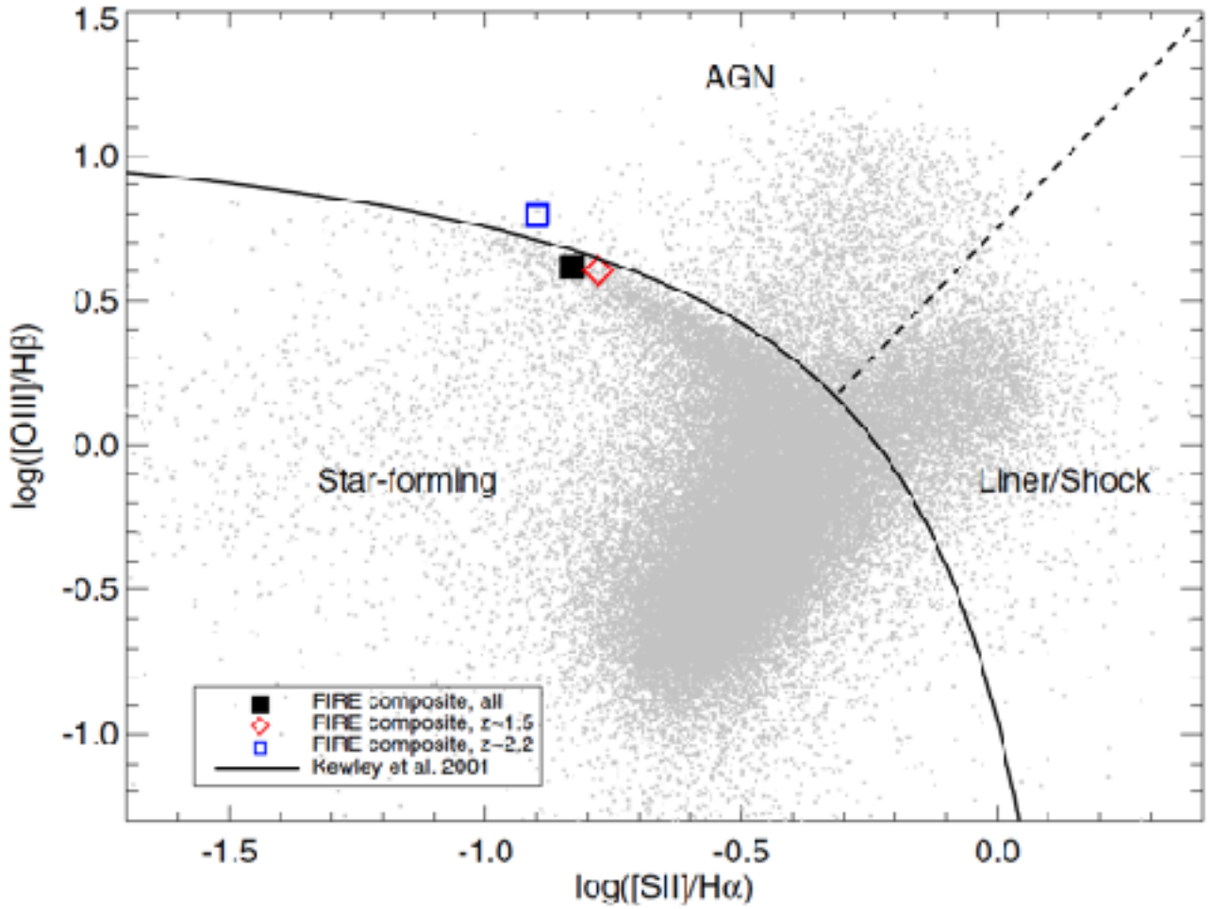

Absence of offset in S2-BPT suggested that N was anomalous

Strom et al. (2016), arXiv:1608.02587

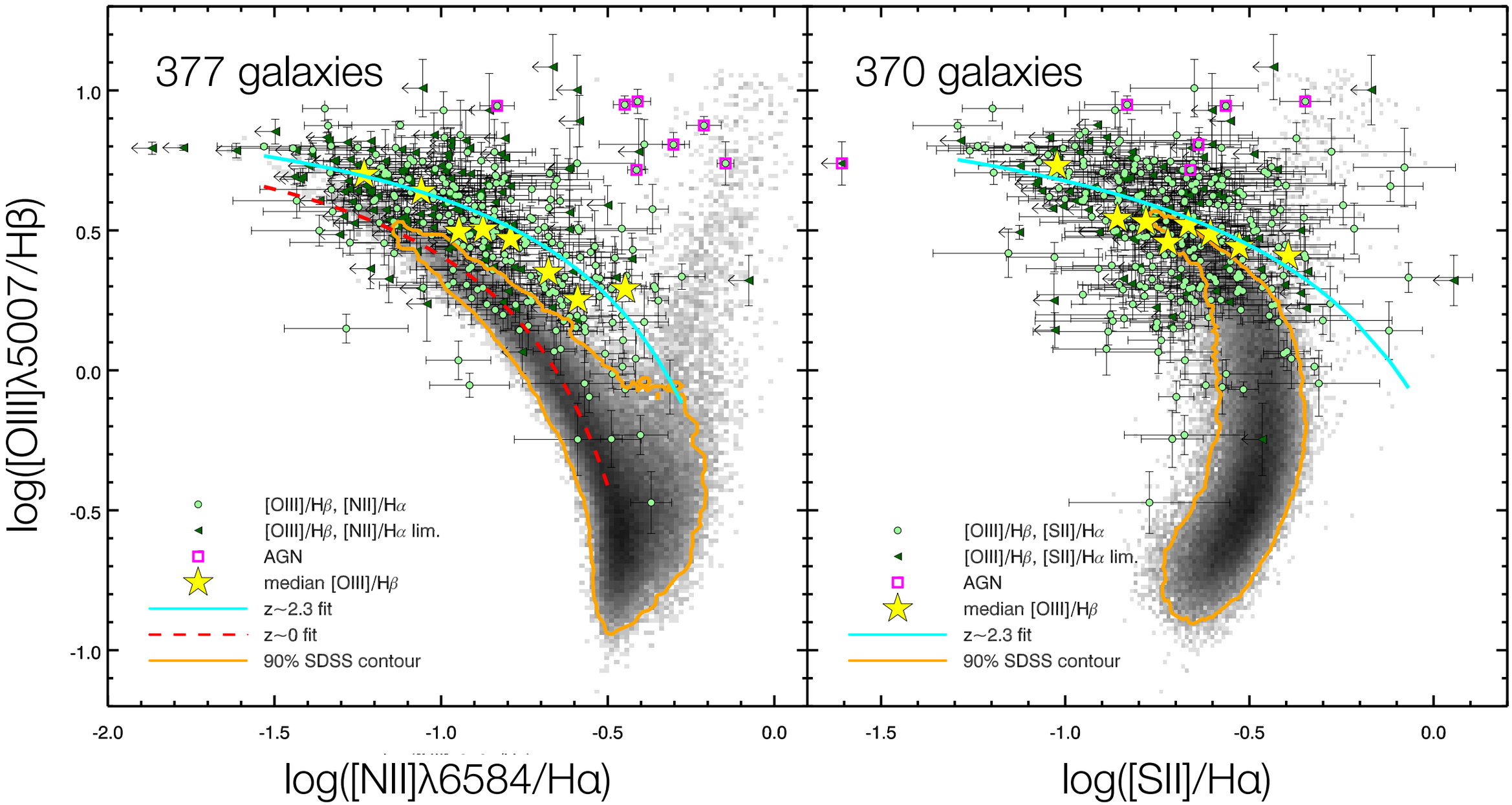

O32 vs. R23: powerful probes of ionization and excitation

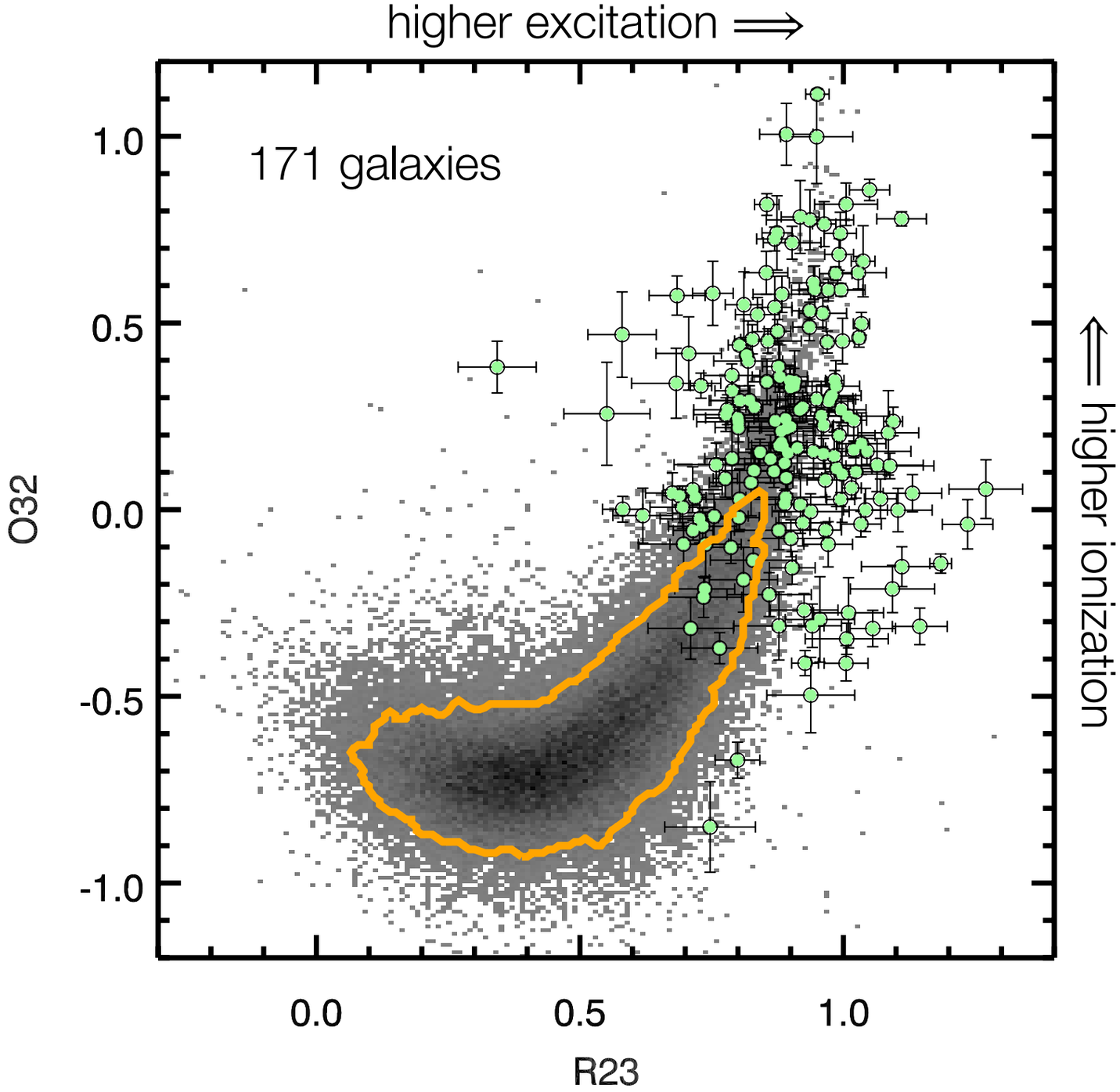

O32 = [OIII]/[OII]
traces ionization state

R23 = ([OIII]+[OII])/Hβ
used to estimate oxygen abundance

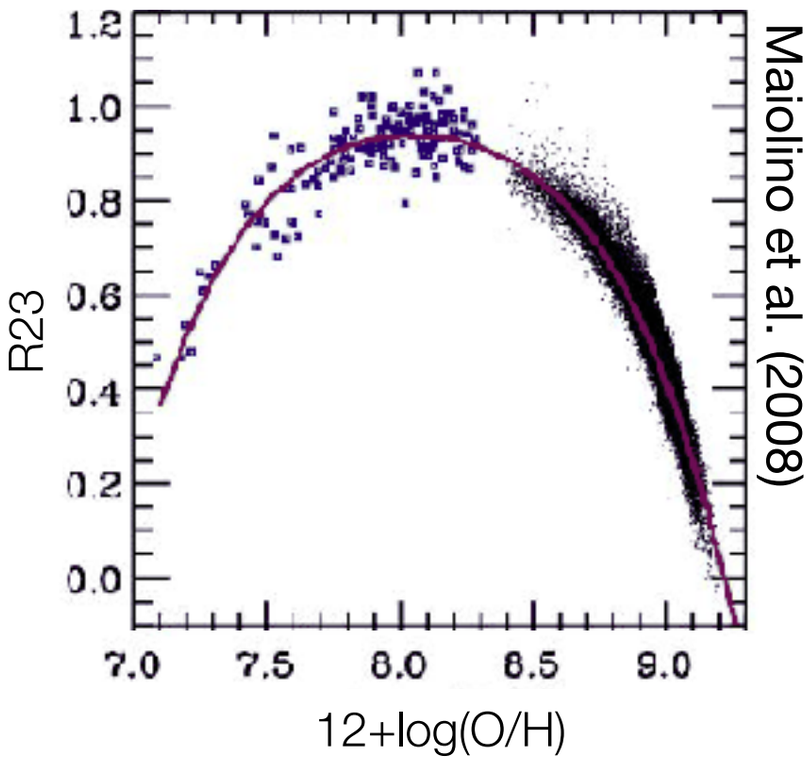

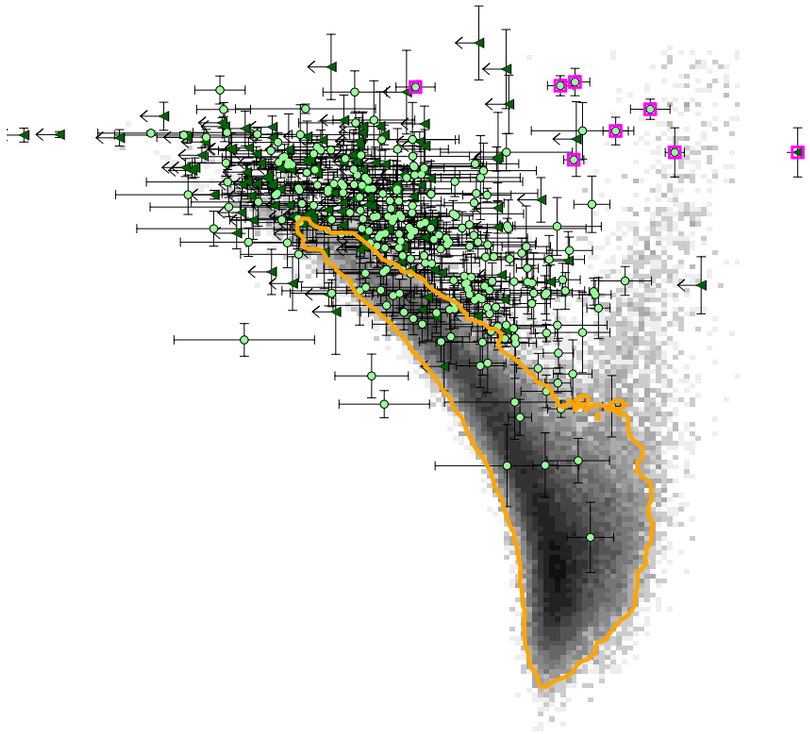

offset

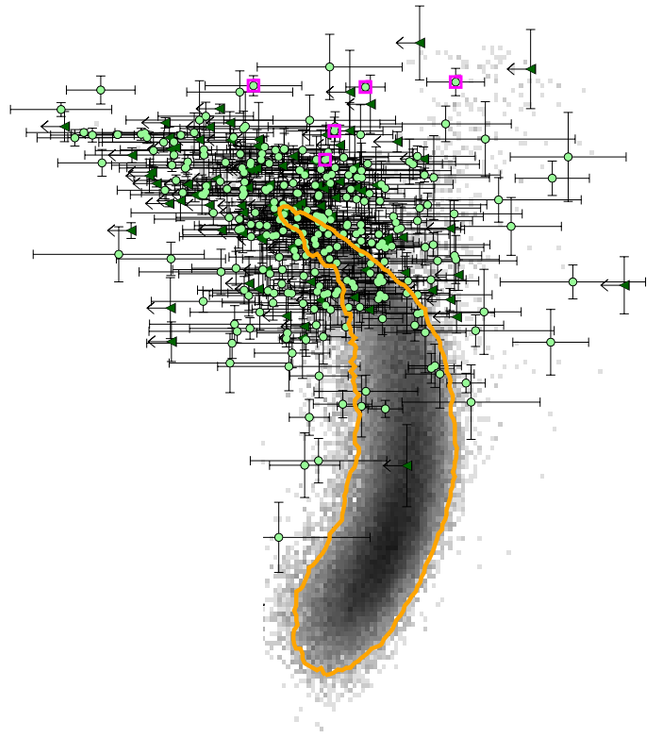

no offset

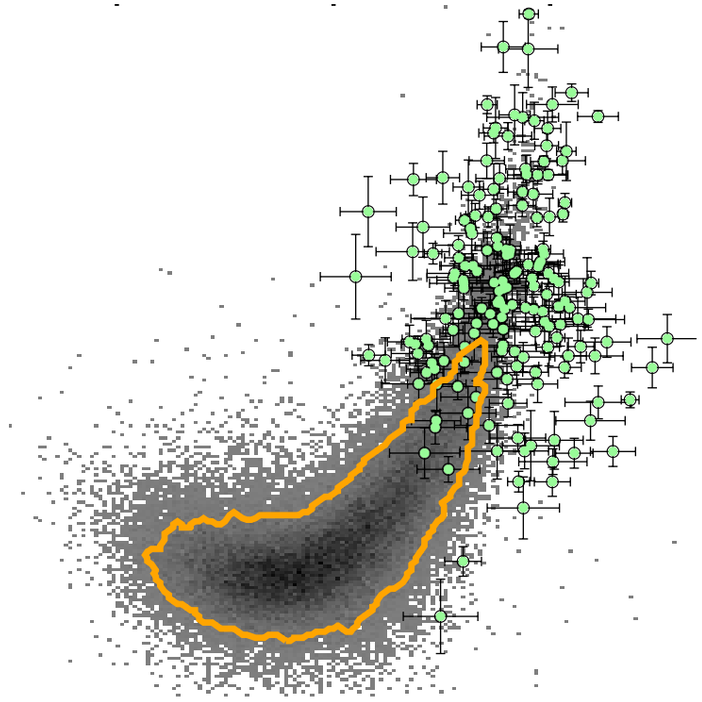

no offset

Offset from SDSS in the N2-BPT correlates with sSFR

Strom et al. (2016), arXiv:1608.02587

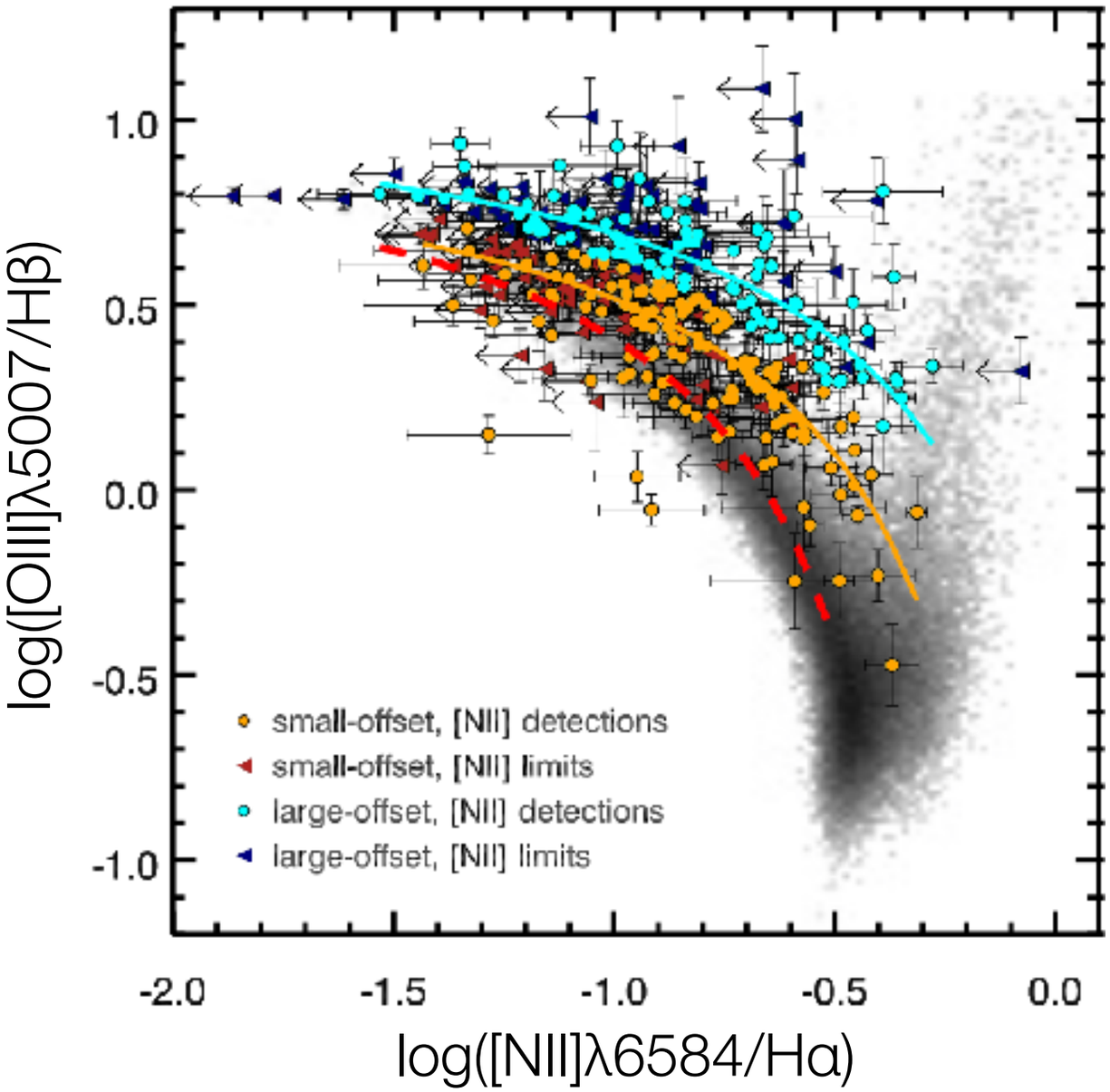

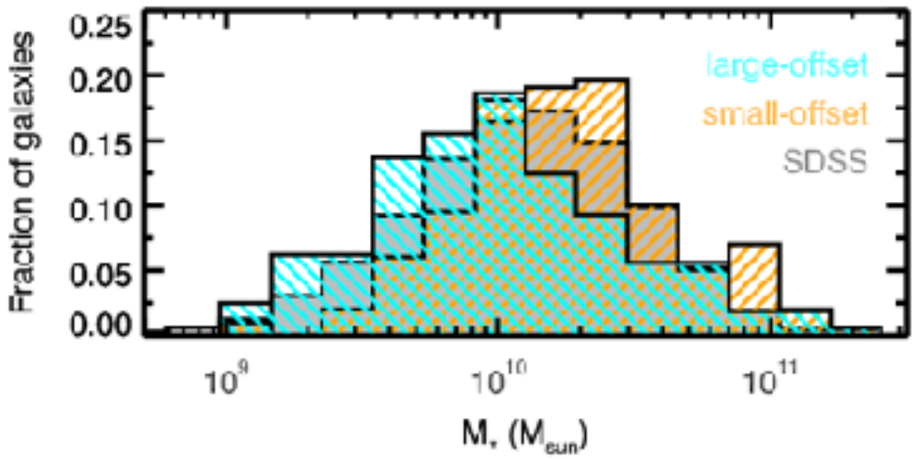

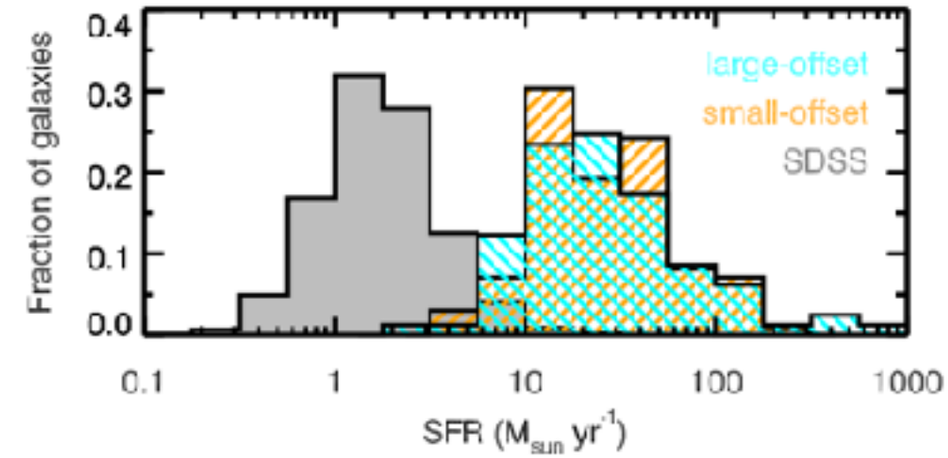

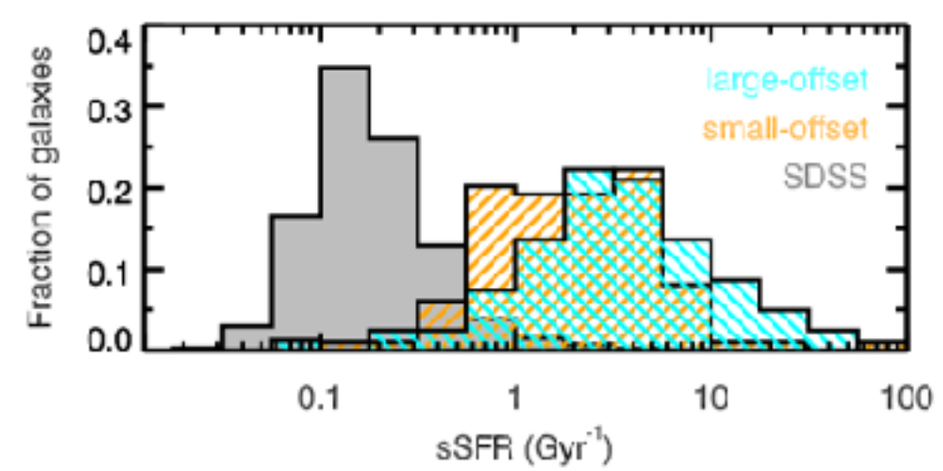

KBSS-MOSFIRE galaxies have similar densities

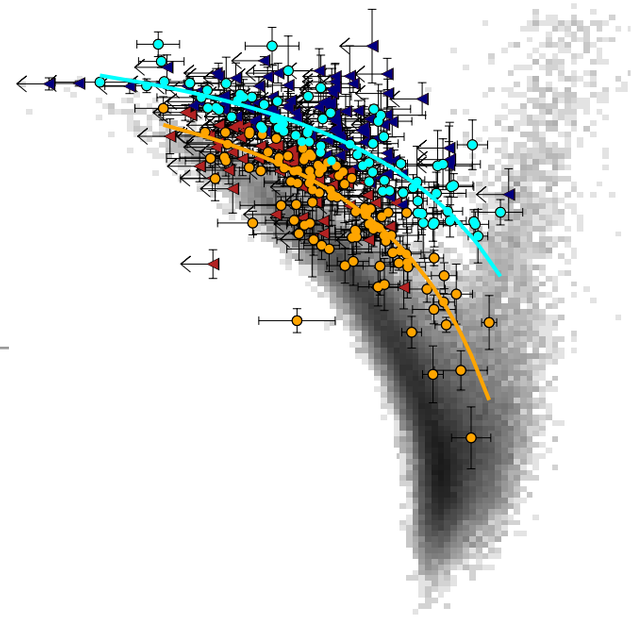

Strom et al. (2016), arXiv:1608.02587

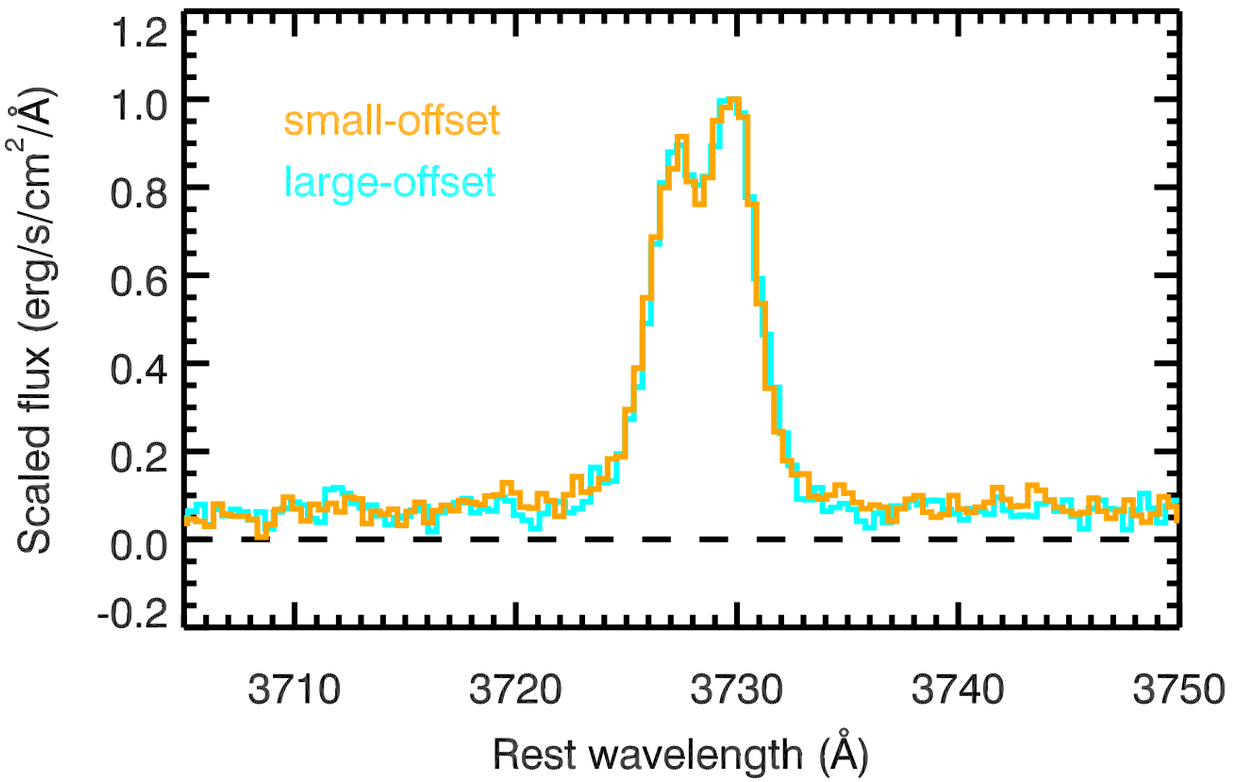

$$n_{e,\mathrm{small}} = 281^{+43}_{-39}\ \mathrm{cm}^{-3}$$

$$n_{e,\mathrm{large}} = 267^{+48}_{-43}\ \mathrm{cm}^{-3}$$

using diagnostic relation from Sanders et al. (2016)

Changes in excitation necessary to explain differences

Strom et al. (2016), arXiv:1608.02587

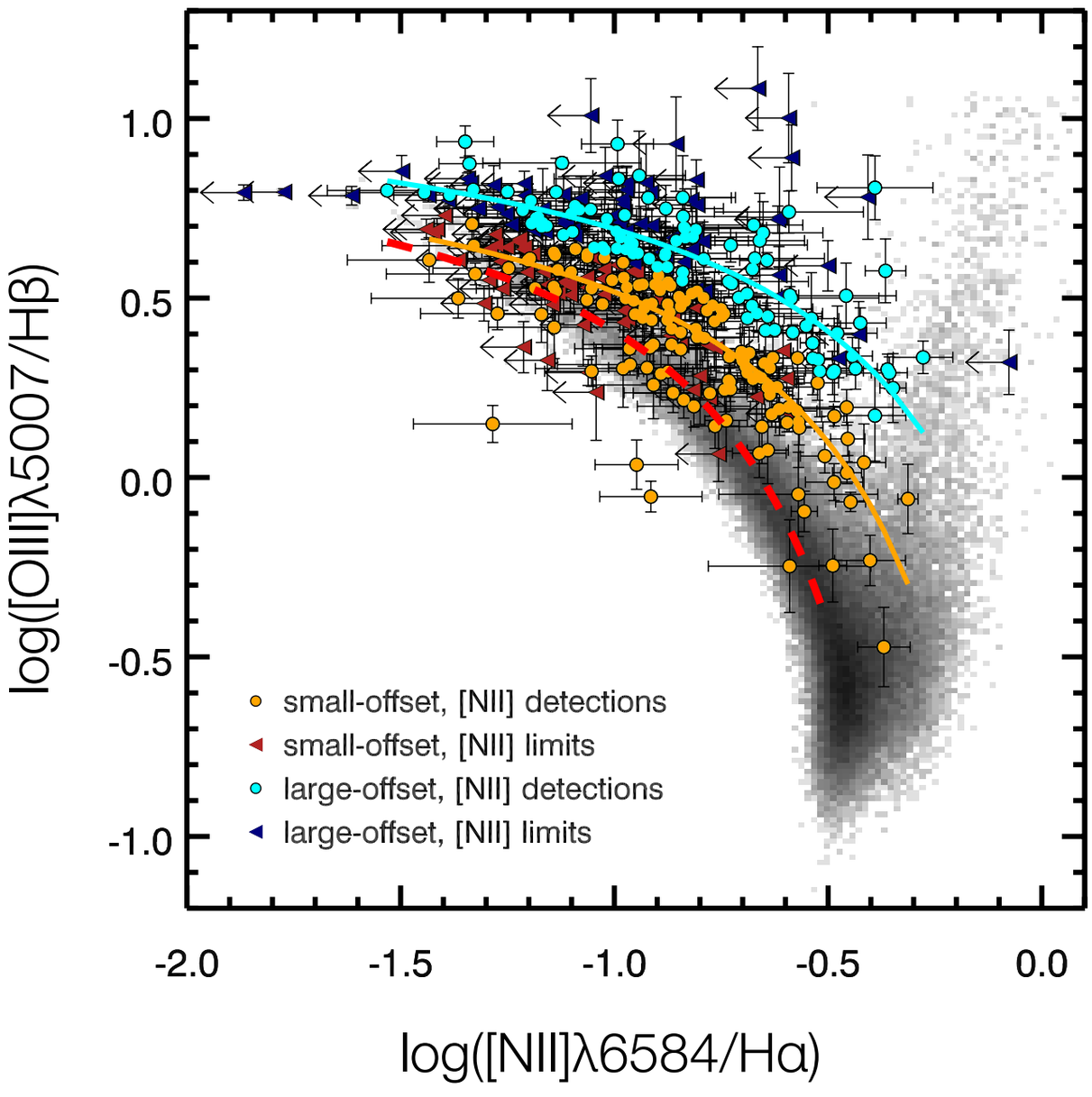

Changes in excitation necessary to explain differences

Strom et al. (2016), arXiv:1608.02587

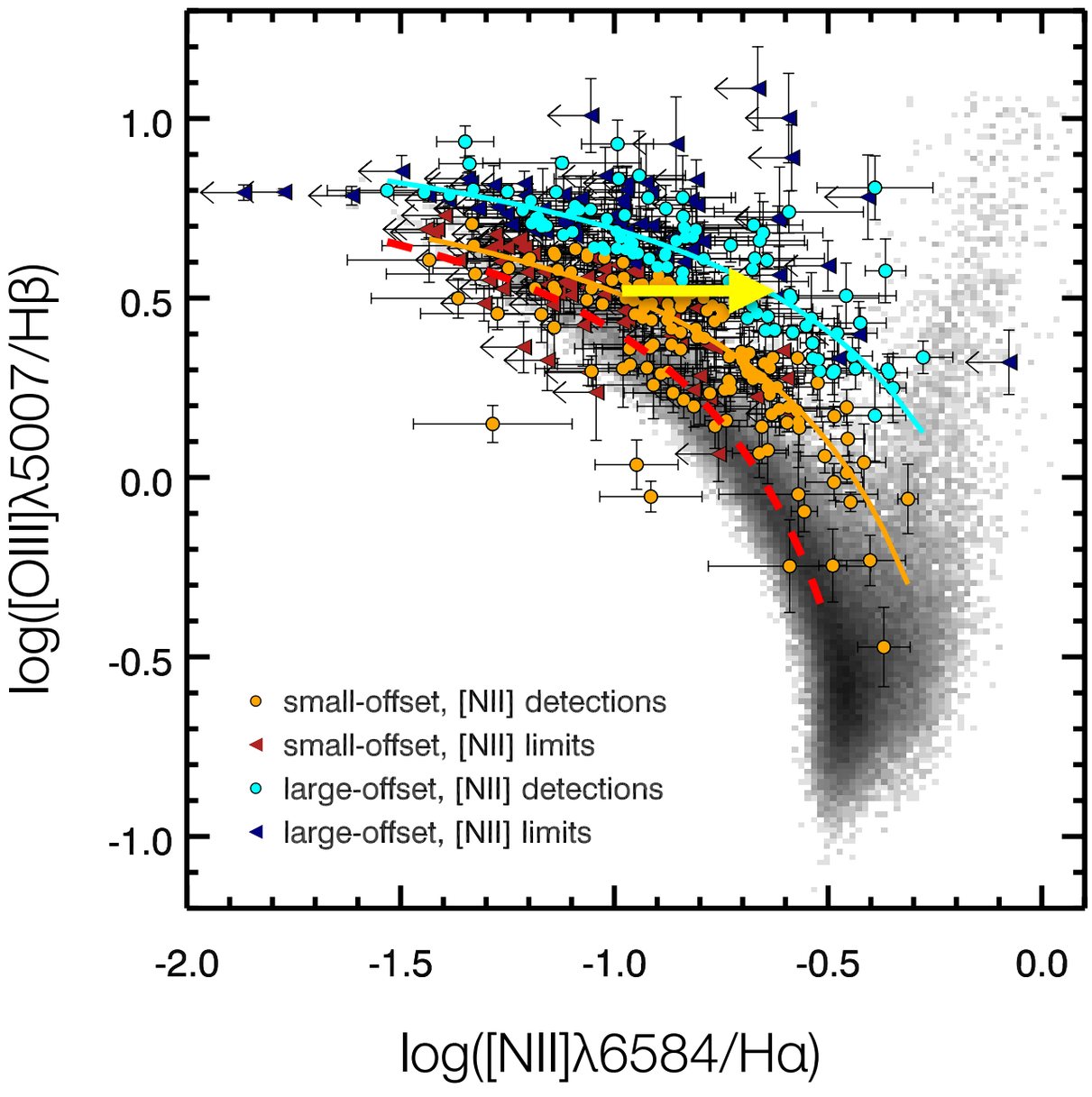

Changes in excitation necessary to explain differences

Strom et al. (2016), arXiv:1608.02587

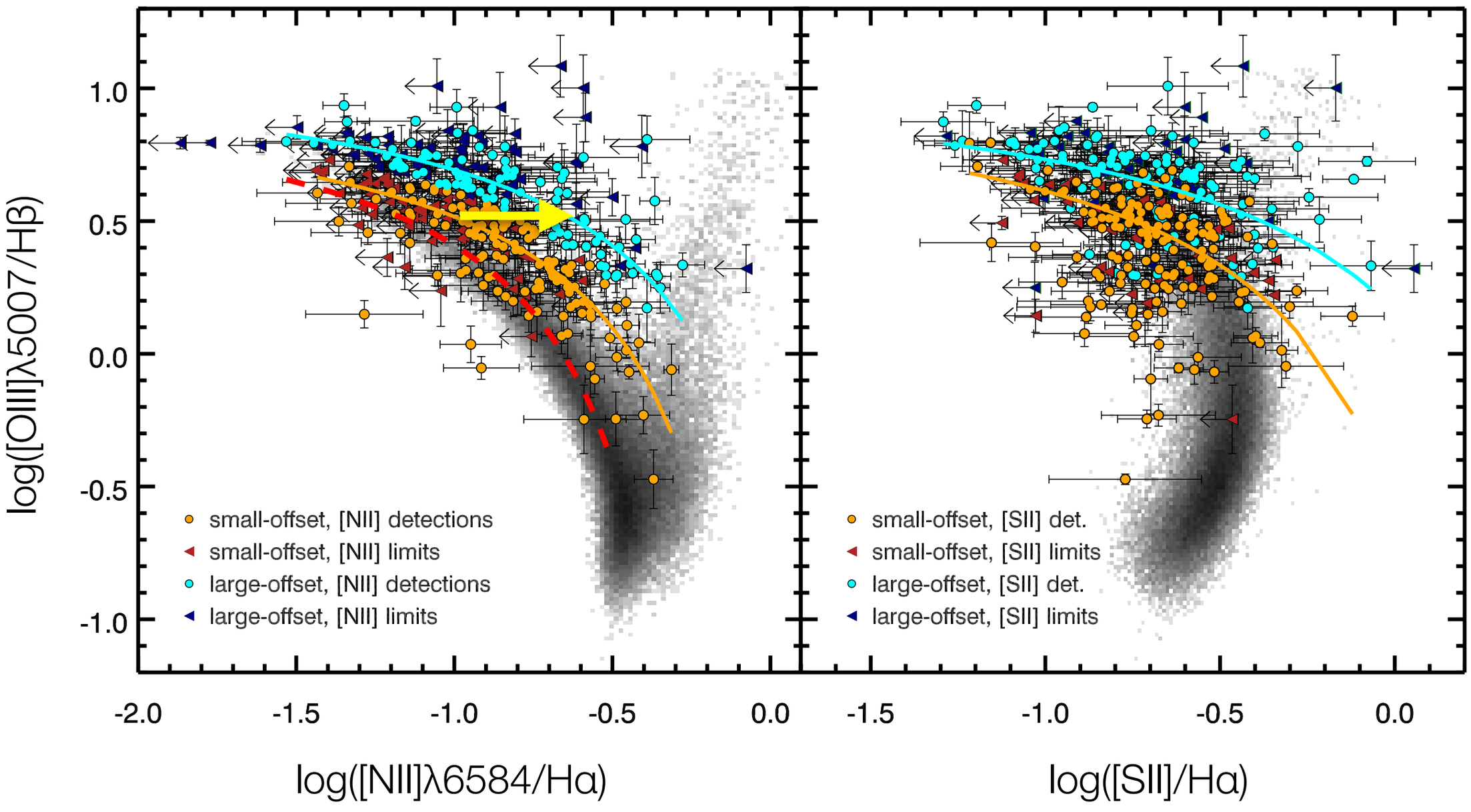

But do differences in nebular excitation explain everything?

SDSS "twins" selected to match KBSS-MOSFIRE in O32 and R23

Strom et al. (2016), arXiv:1608.02587

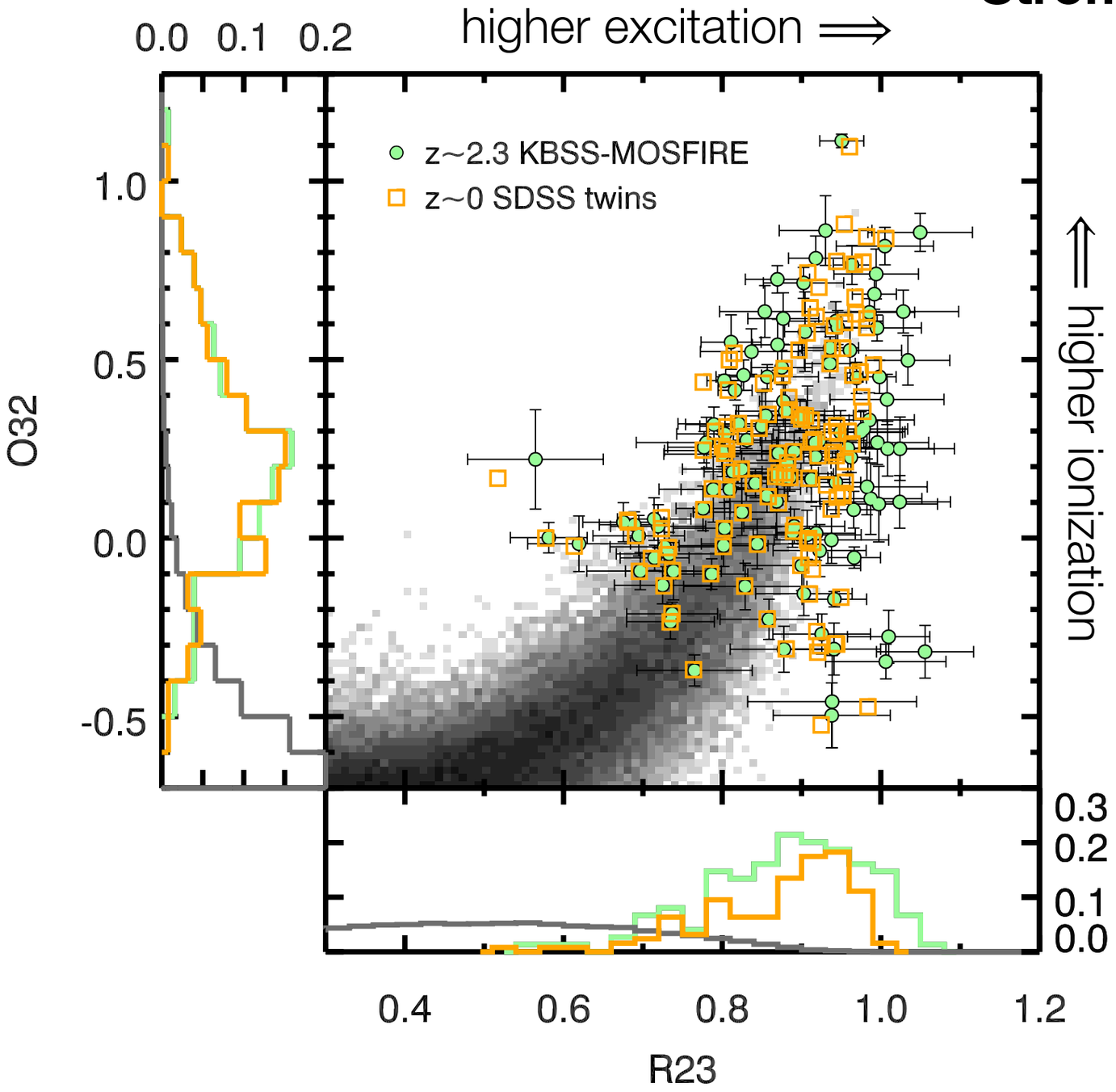

KBSS-MOSFIRE

SDSS twins

full SDSS sample

High-z galaxies still exhibit offset in N2 BPT

Strom et al. (2016), arXiv:1608.02587

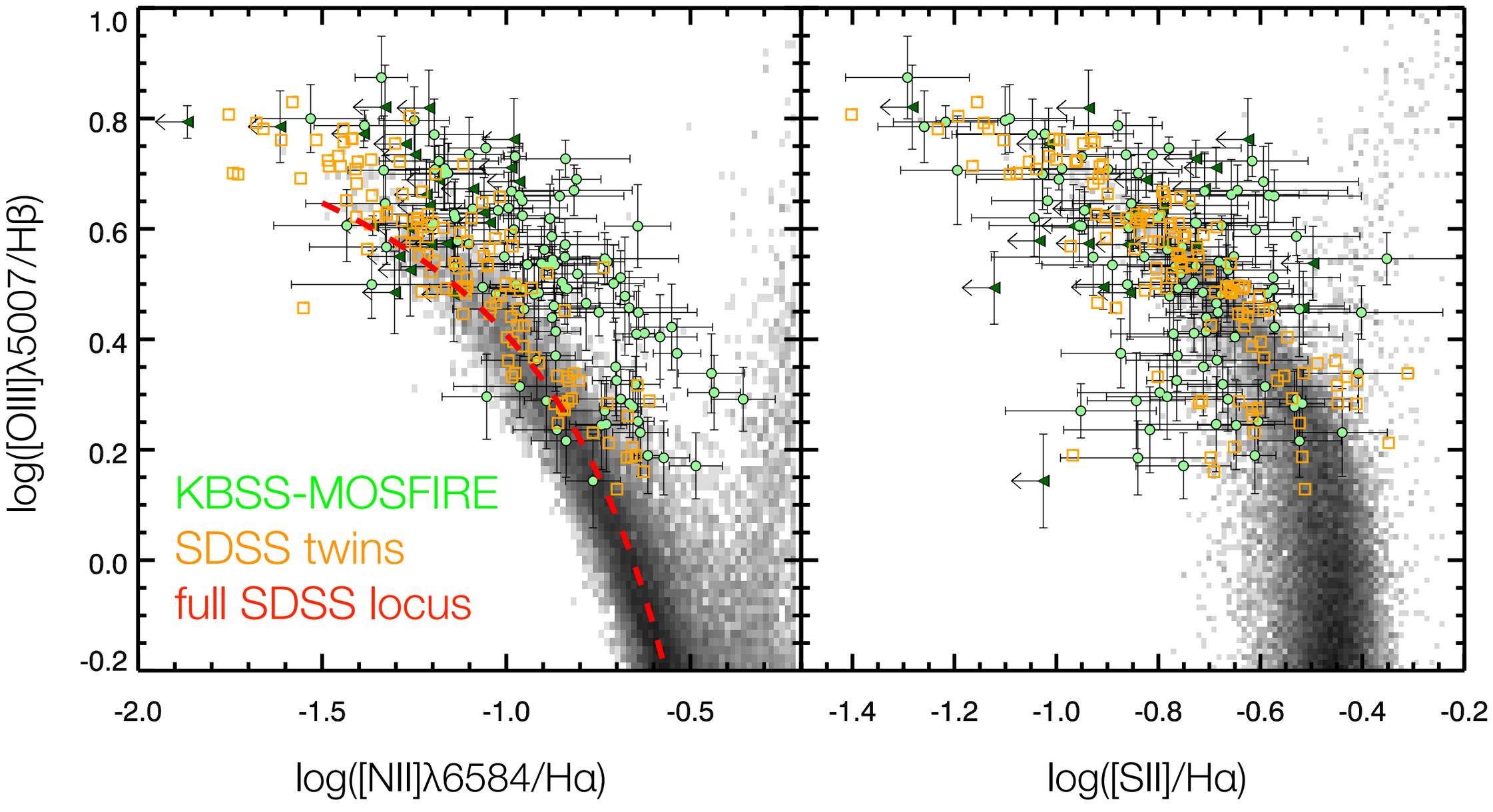

High-z galaxies still exhibit offset in N2 BPT

Strom et al. (2016), arXiv:1608.02587

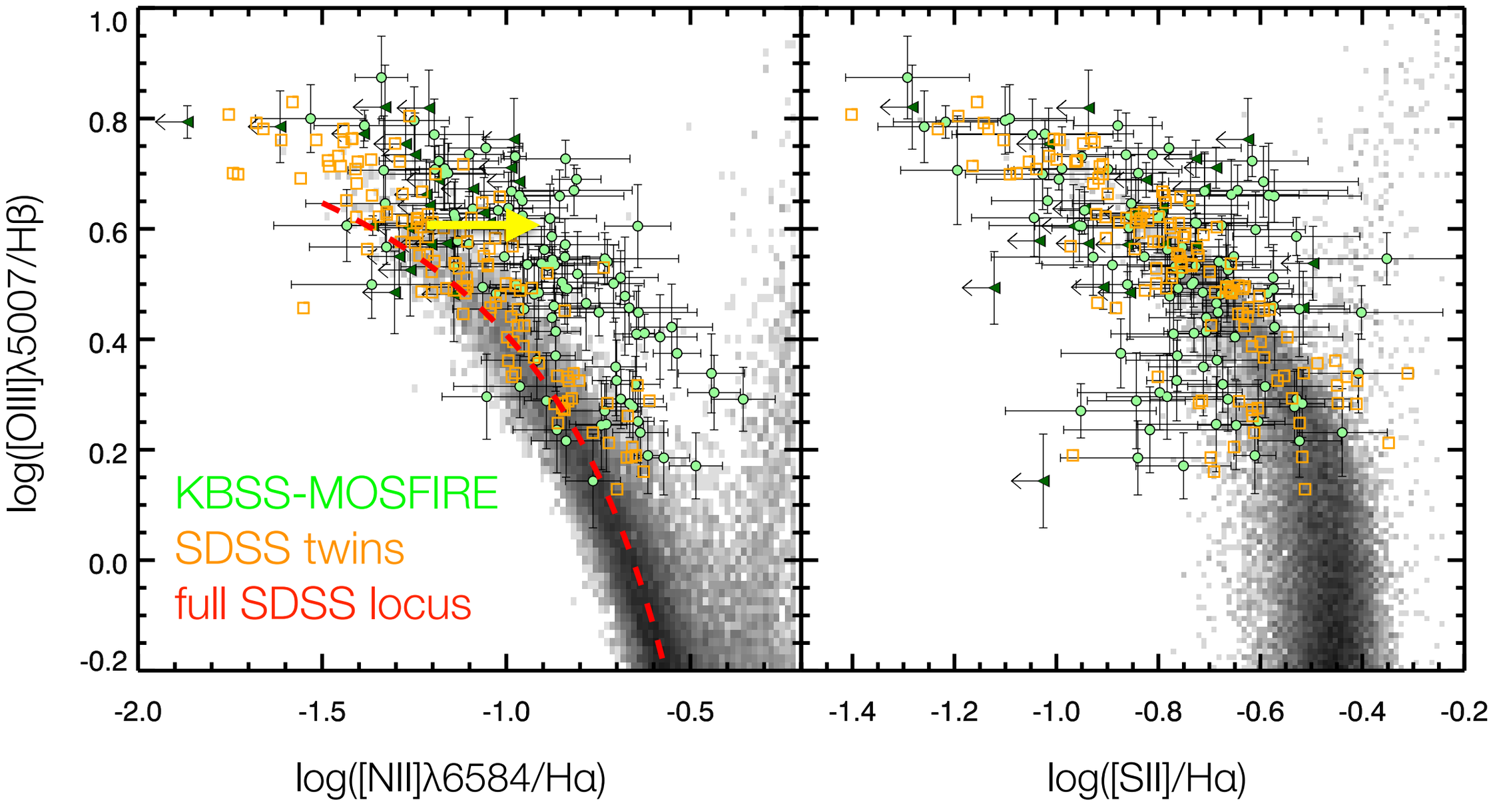

Offset consistent with a small increase in N/O

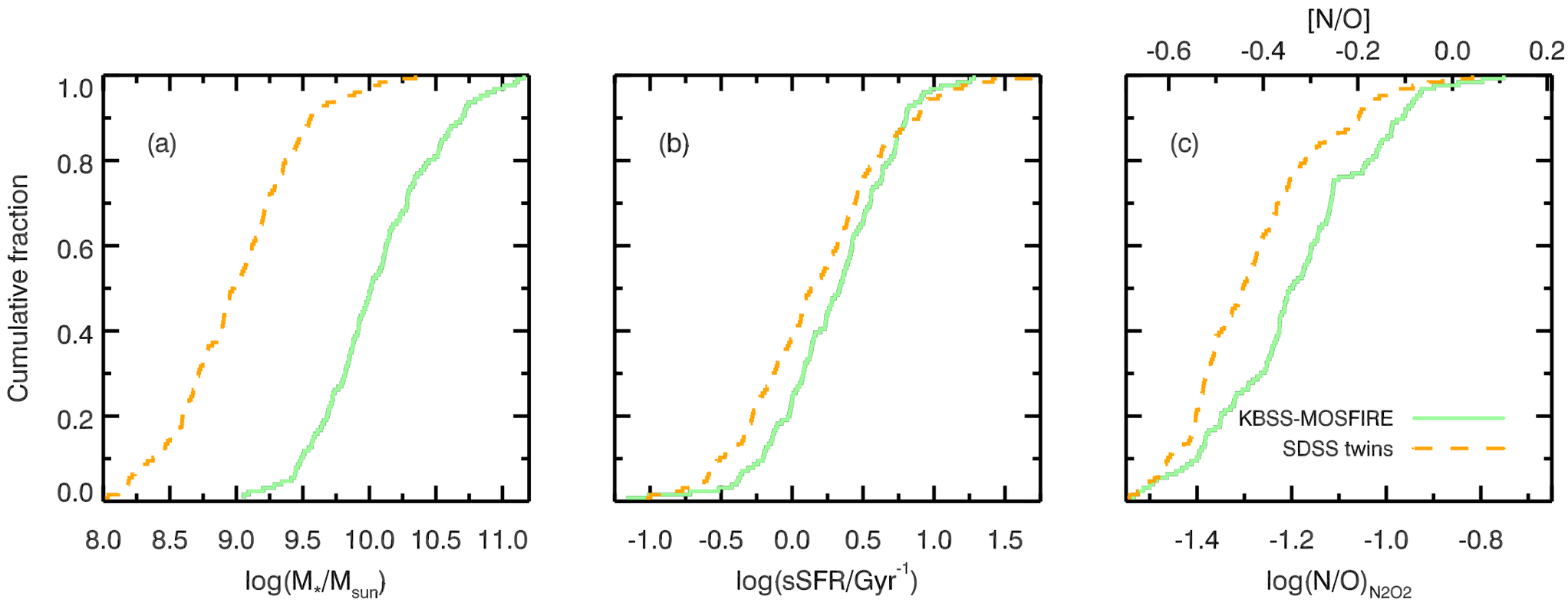

KBSS-MOSFIRE galaxies…

are 10 times more massive than SDSS twins

have higher sSFRs than SDSS twins

have higher N/O ratios than SDSS twins, but not enough to explain offset!

What is different about z~2-3 galaxies?

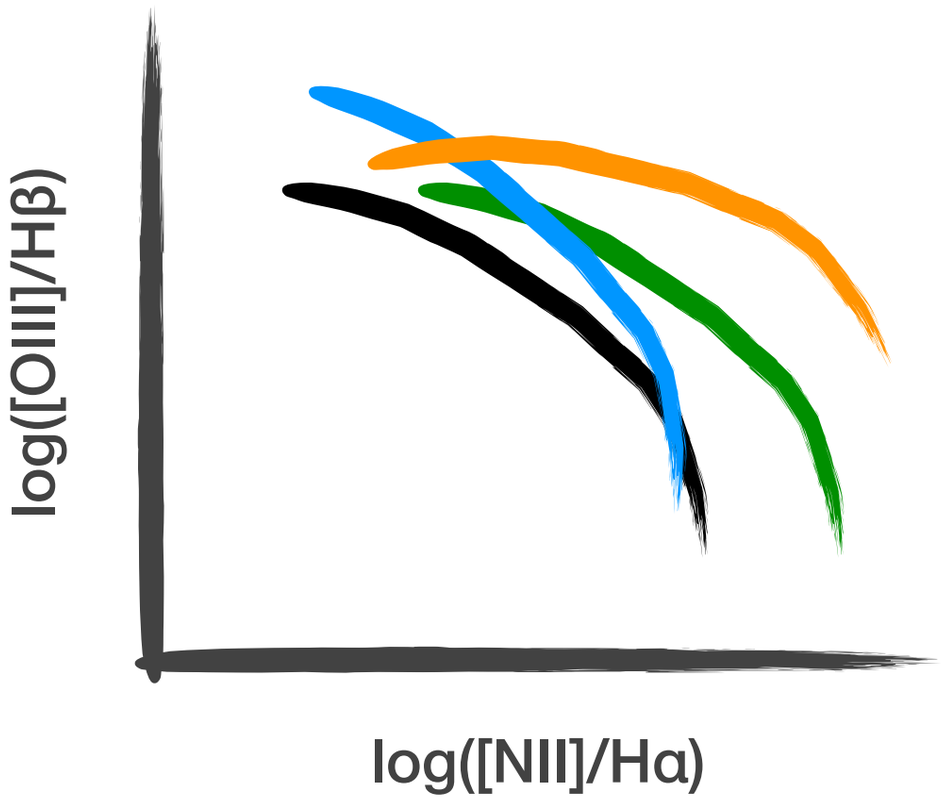

enhanced N/O at fixed O/H

difference in N/O for KBSS galaxies and SDSS twins <60% of offset

more ionizing photons

will increase O32, but cannot explain high [OIII]/Hβ and R23 at same time

harder ionizing radiation

can explain offset in [OIII]/Hβ and large values of R23 at fixed O32

What is different about z~2-3 galaxies?

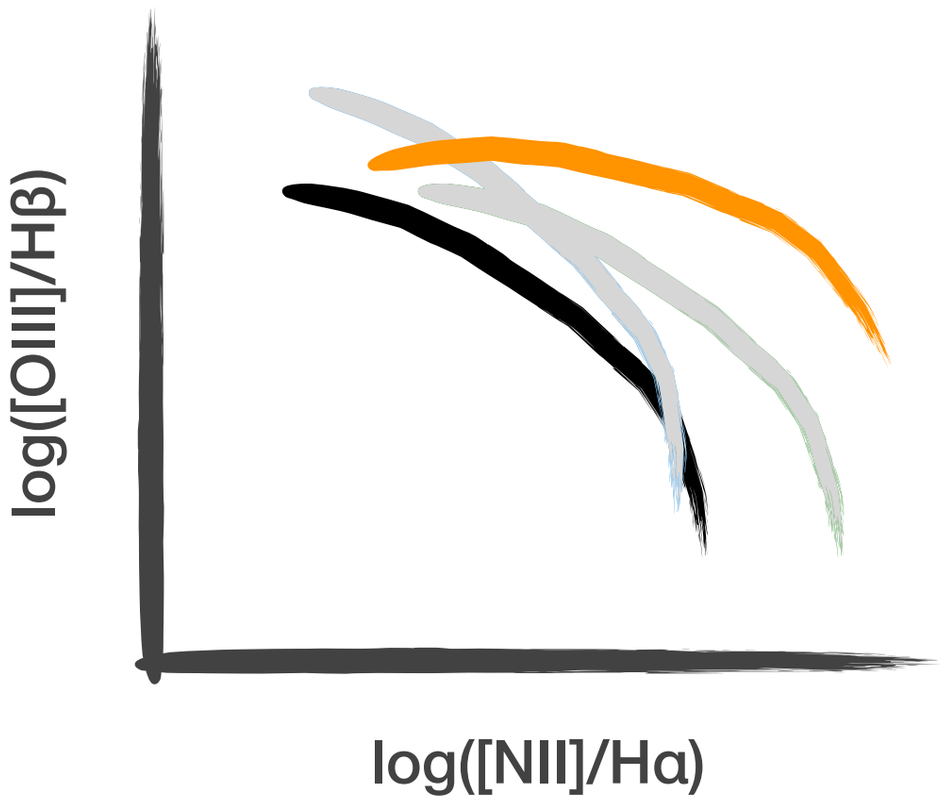

enhanced N/O at fixed O/H

difference in N/O for KBSS galaxies and SDSS twins <60% of offset

more ionizing photons

will increase O32, but cannot explain high [OIII]/Hβ and R23 at same time

harder ionizing radiation

can explain offset in [OIII]/Hβ and large values of R23 at fixed O32

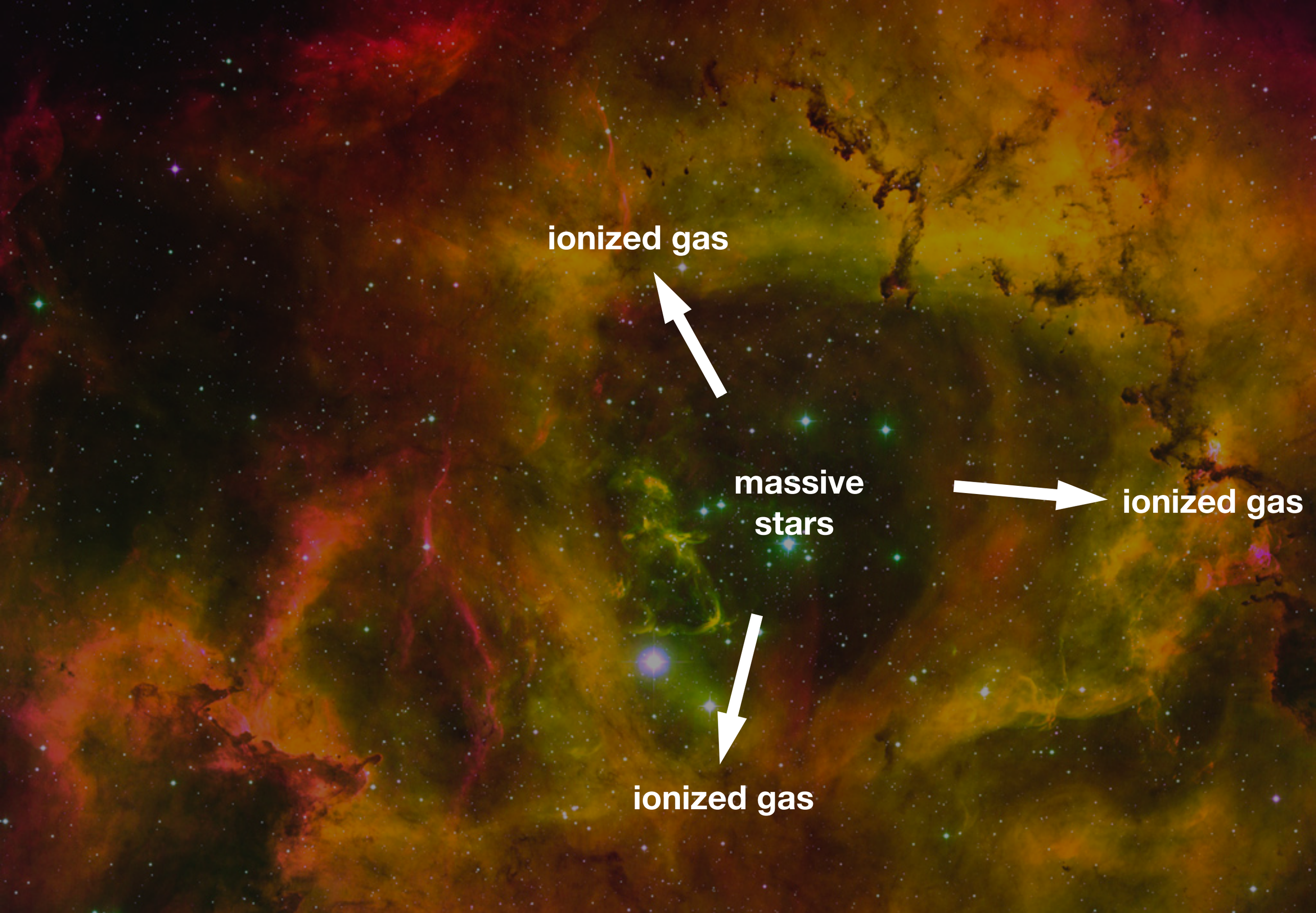
ionized gas
massive stars
ionized gas
ionized gas

Far-UV continuum of z~2-3 star-forming galaxies

Steidel, **Strom**, et al. (2016)

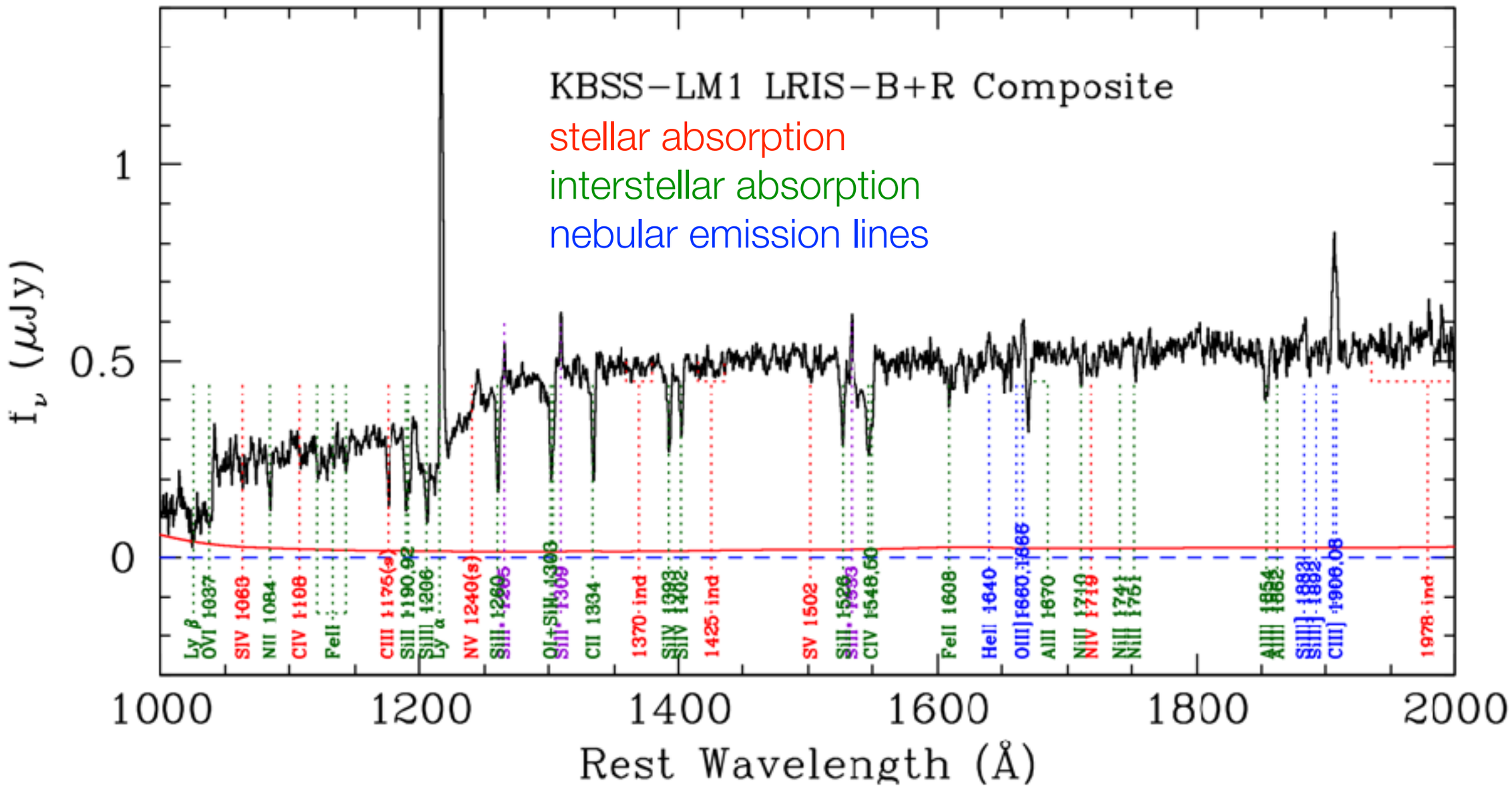

Signatures of massive stars in z~2-3 galaxies

Steidel, **Strom**, et al. (2016)

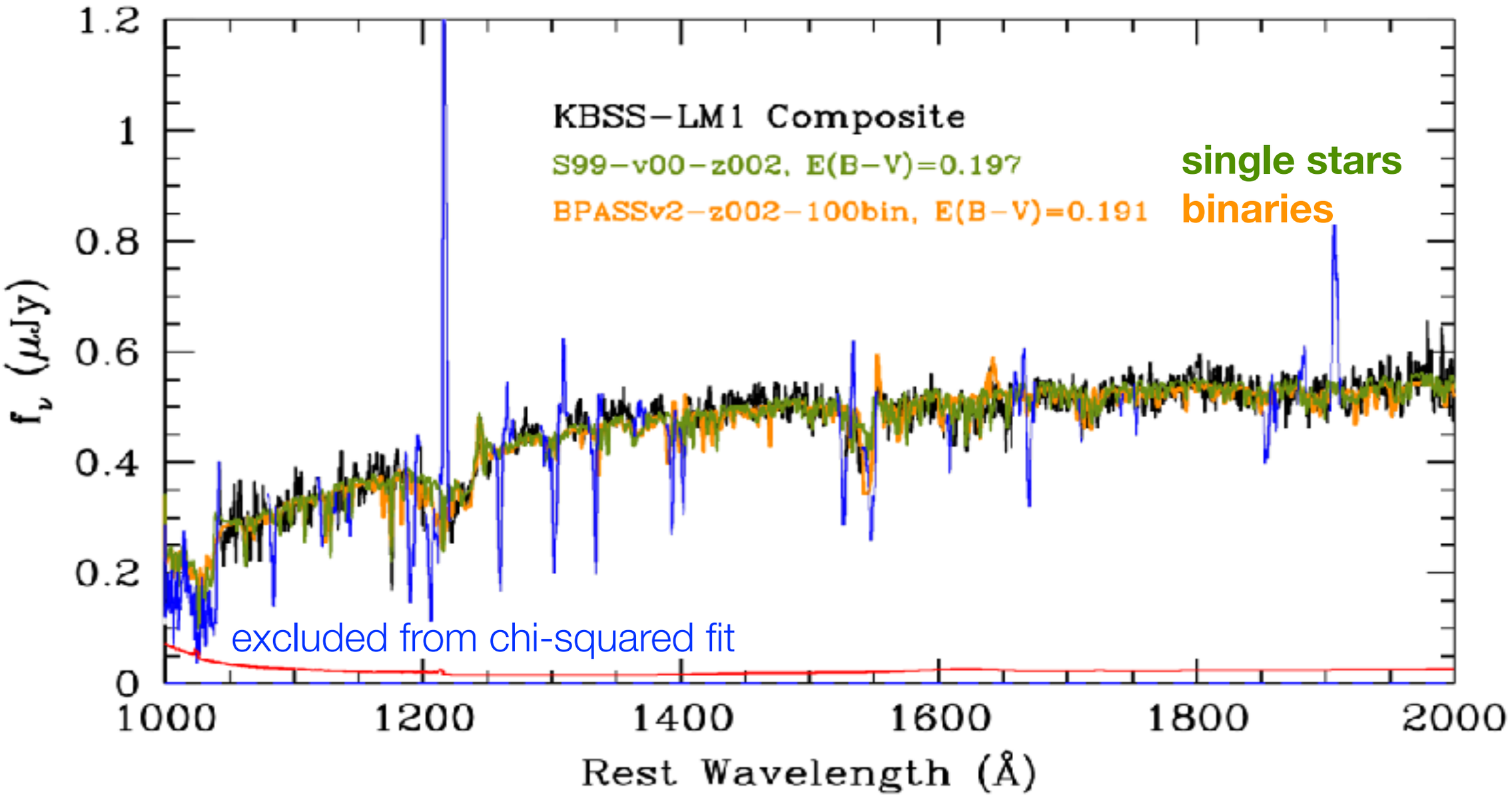

The non-ionizing UV continuum indicates Fe-poor stellar populations

Signatures of massive stars in z~2-3 galaxies

Steidel, **Strom**, et al. (2016)

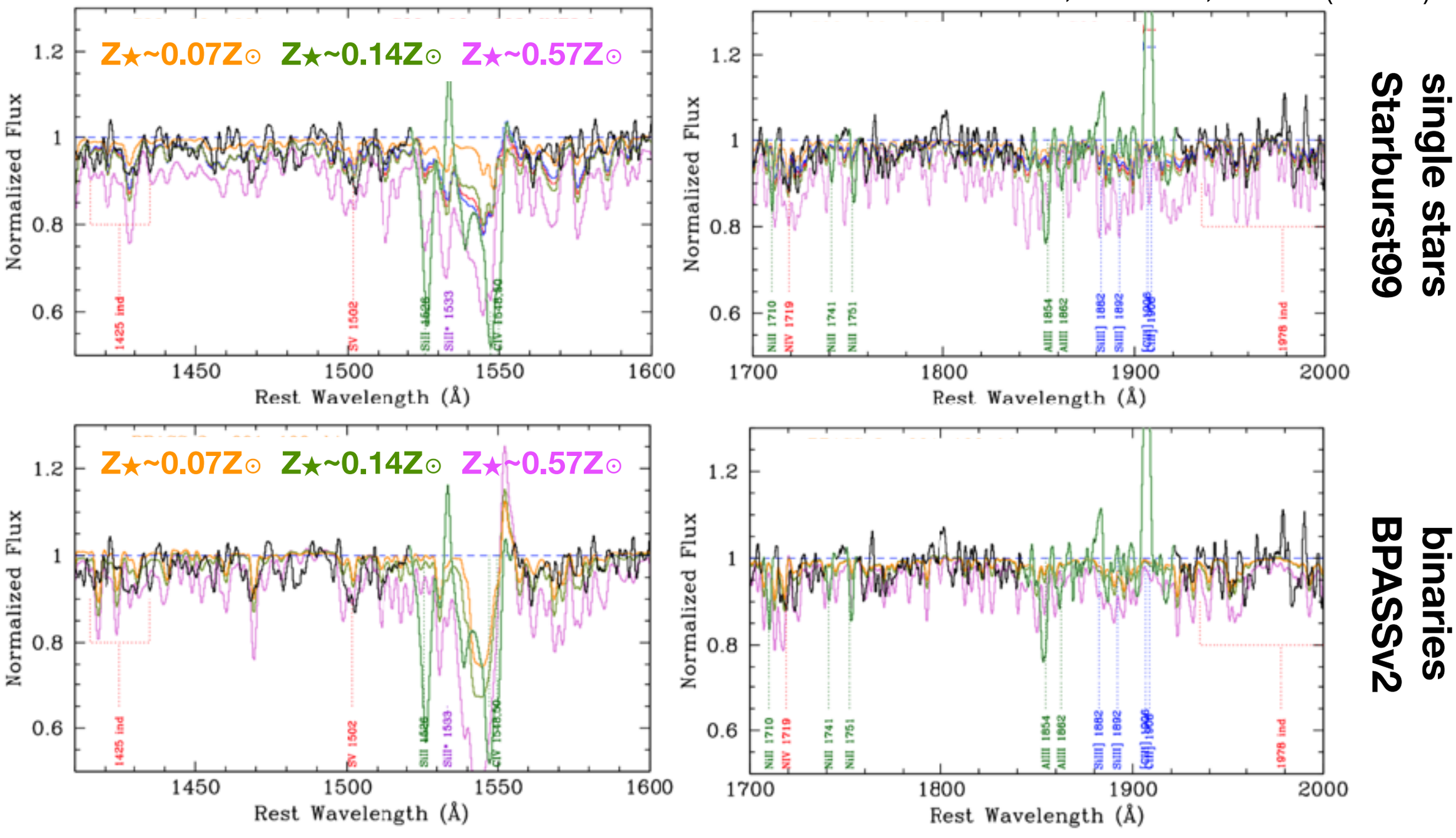

single stars
Starburst99

binaries
BPASSv2

To binary or not to binary

Sana et al. (2012): 50% of massive stars in 30 Dor show evidence of interaction with another star

Effects of binary evolution include

1. Mass transfer between close companions
2. Extended main sequence lifetimes
3. Tendency for stars to become hotter as they evolve

Changes EUV output of stellar population without changes to IMF

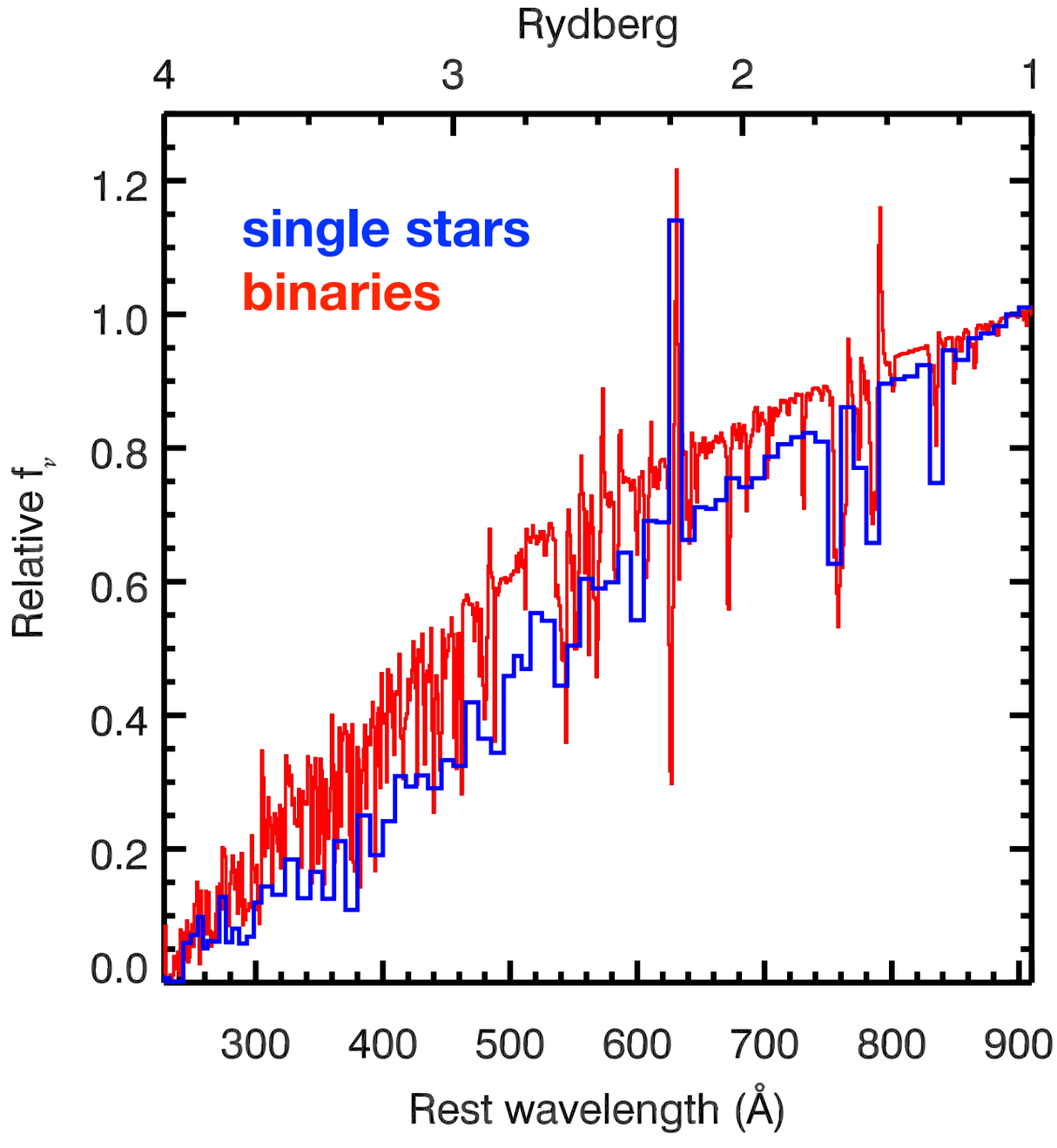

Evidence for binary stars: high R23 at fixed O32

Steidel, **Strom**, et al. (2016)

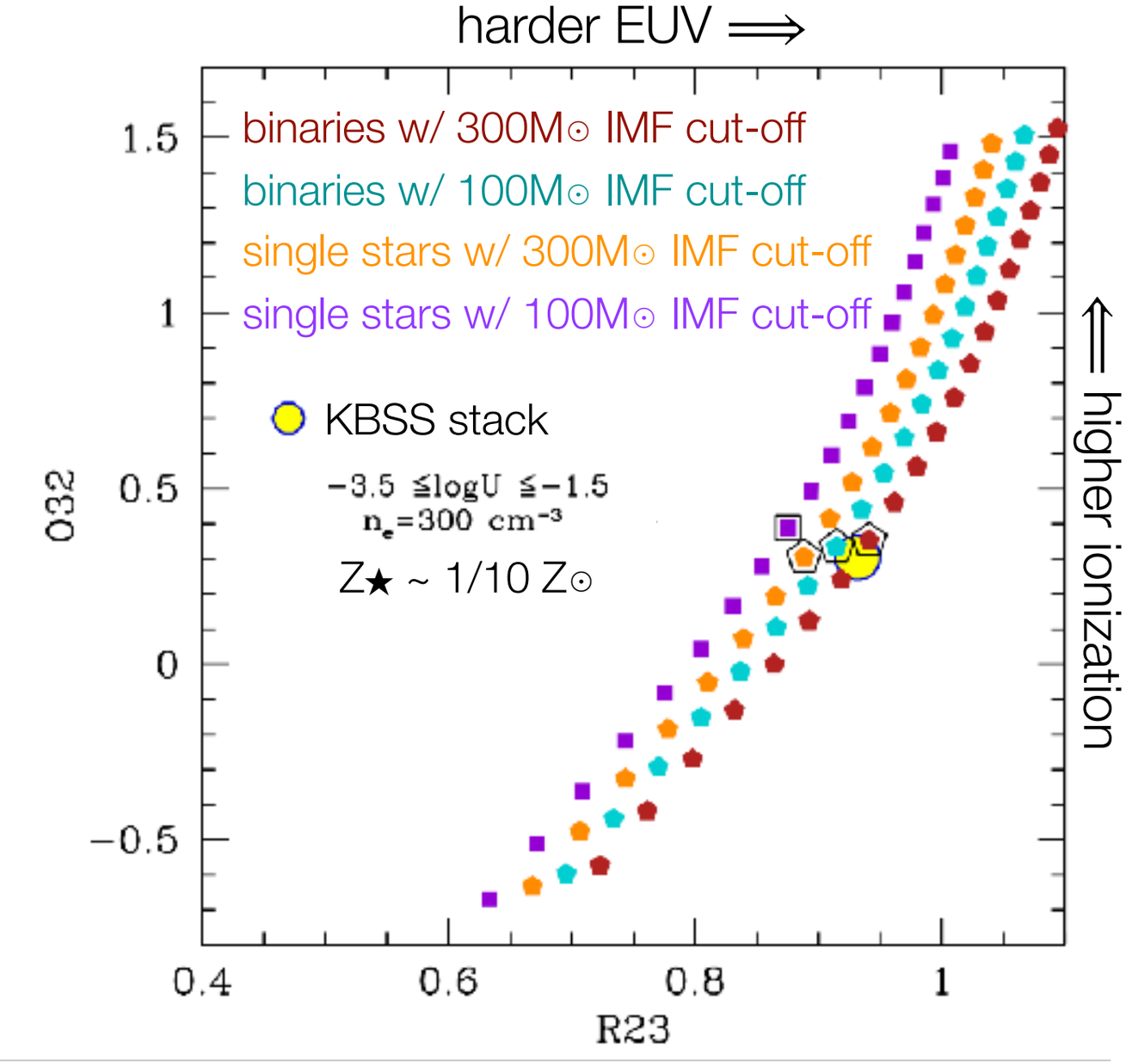

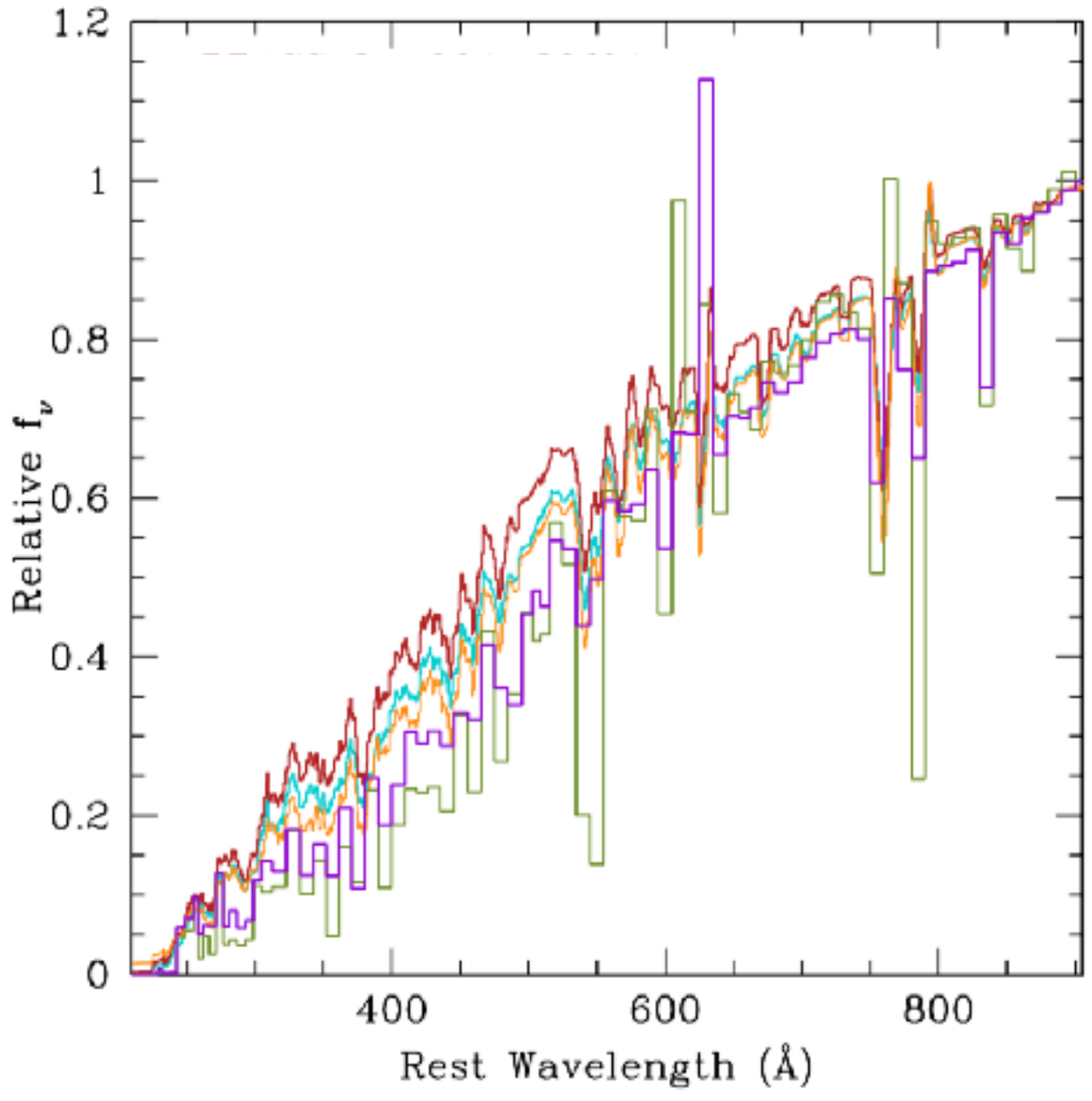

Evidence for binary stars: stellar HeII **λ***1640*

Steidel, **Strom**, et al. (2016)

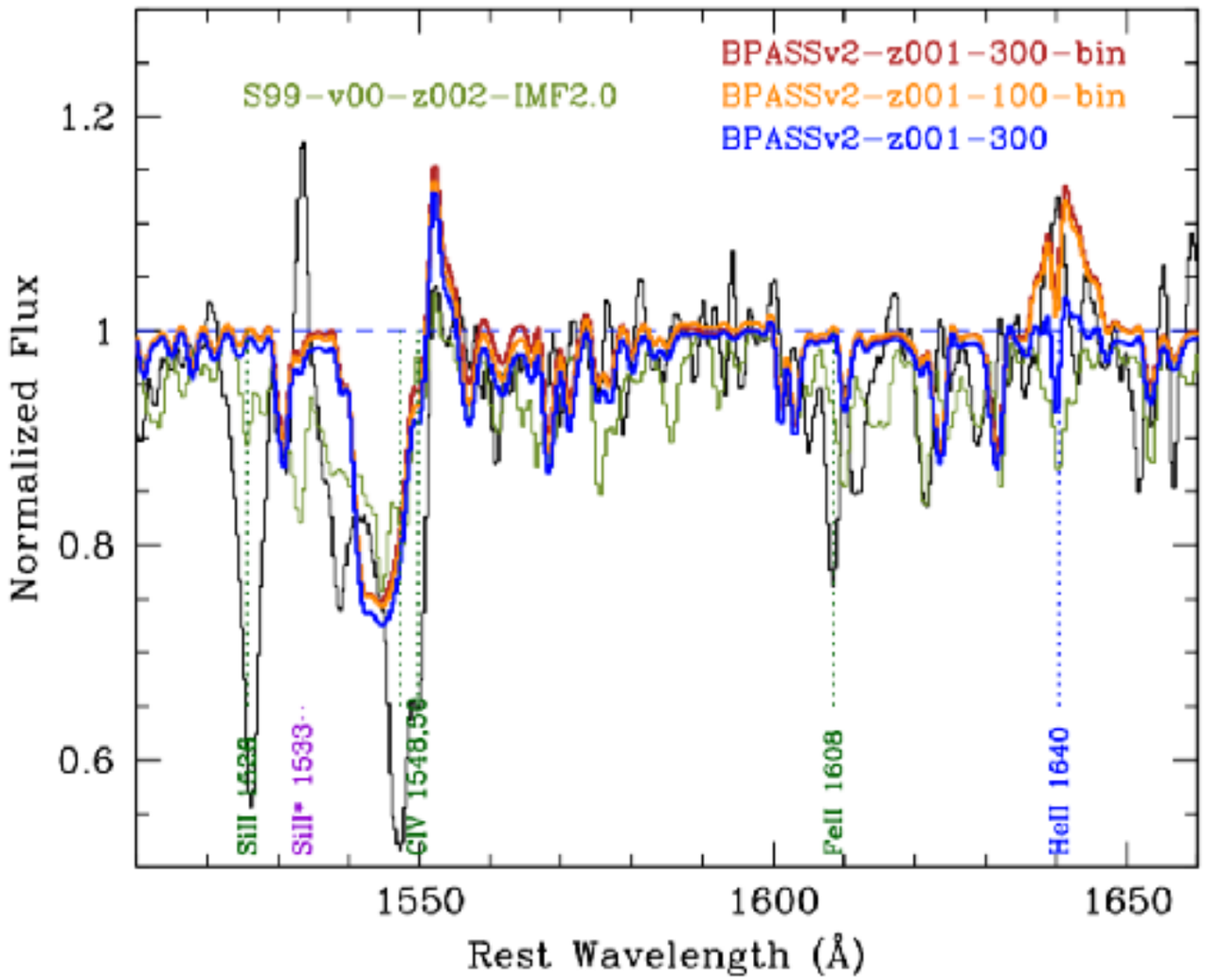

higher ionization ⟹

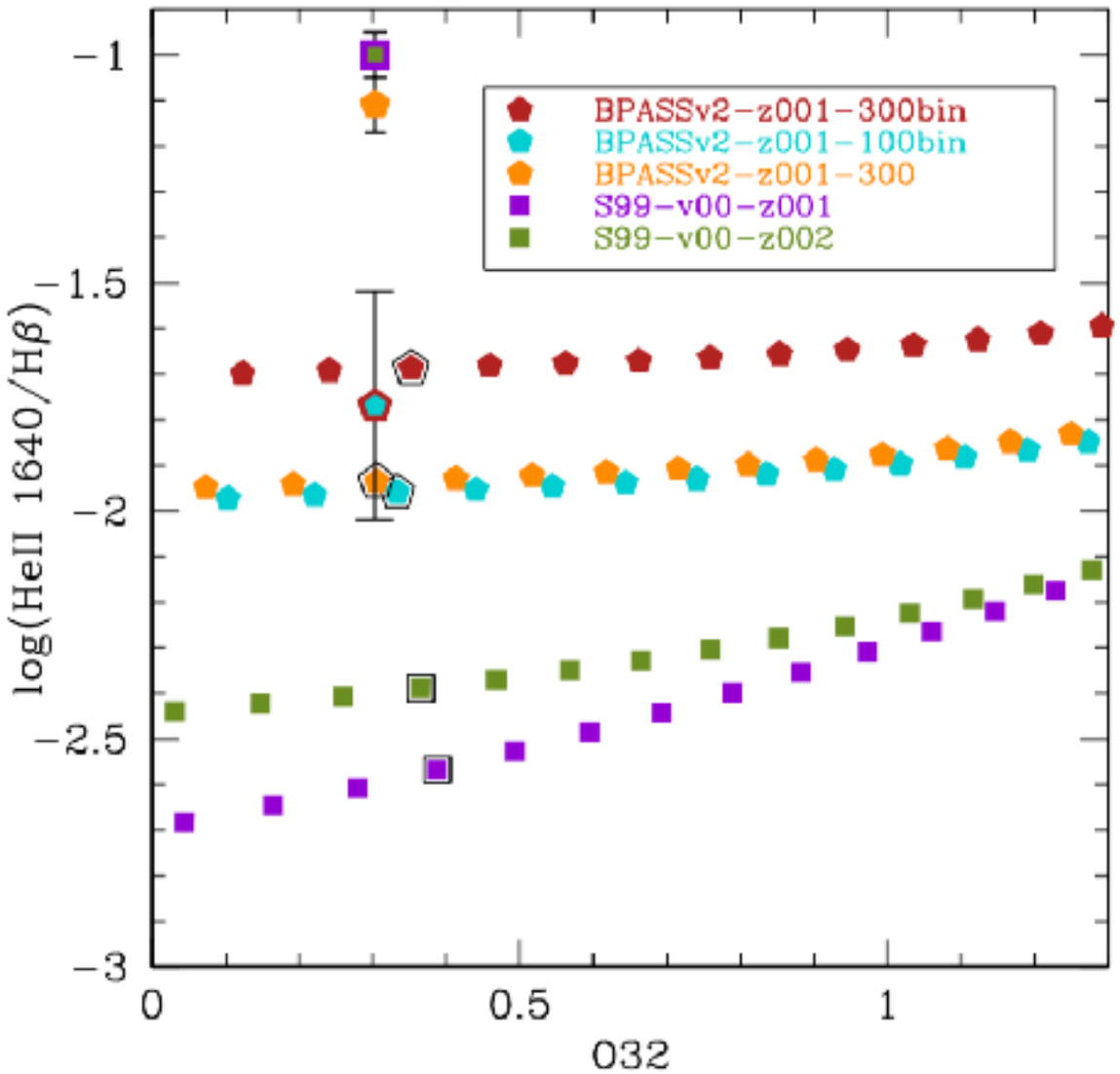

Photoionization models connect observations of stars and nebulae

line ratios
f(U, Z_{neb})

=

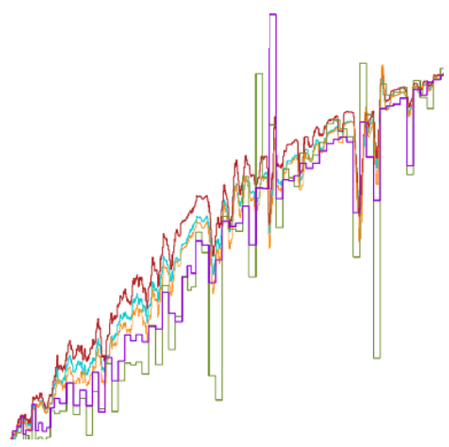

shape of EUV
Fe-poor binary stars

+

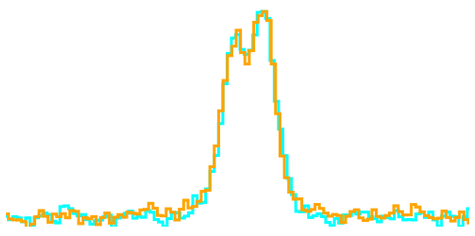

electron density
n_e = 300 cm^{-3}

+

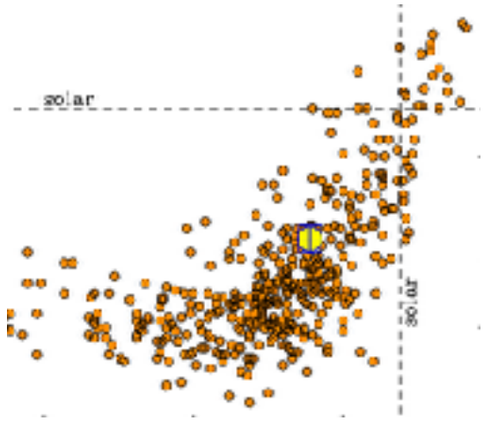

abundance ratios
same N/O vs. O/H

Photoionization models connect observations of stars and nebulae

line ratios
f(U, Z_{neb})

=

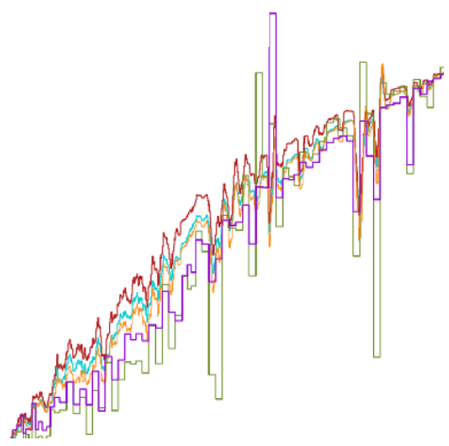

shape of EUV
Fe-poor binary stars

+

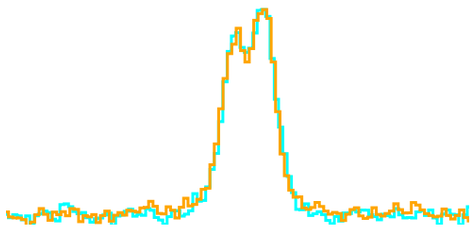

electron density
n_e = 300 cm^{-3}

+

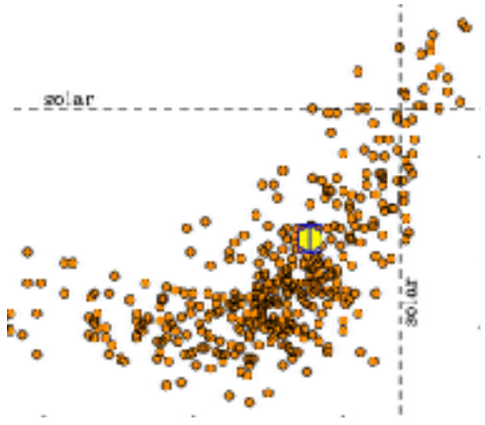

abundance ratios
same N/O vs. O/H

$Z_\star$ traces Fe abundance

Z_{neb} traces O abundance

Different $Z_\star$ and Z_{neb} imply O/Fe different from solar, but **not** gas and stars with different O or Fe

O32-R23 diagram sensitive to changes in ionizing radiation

Strom et al. (2016), arXiv:1608.02587

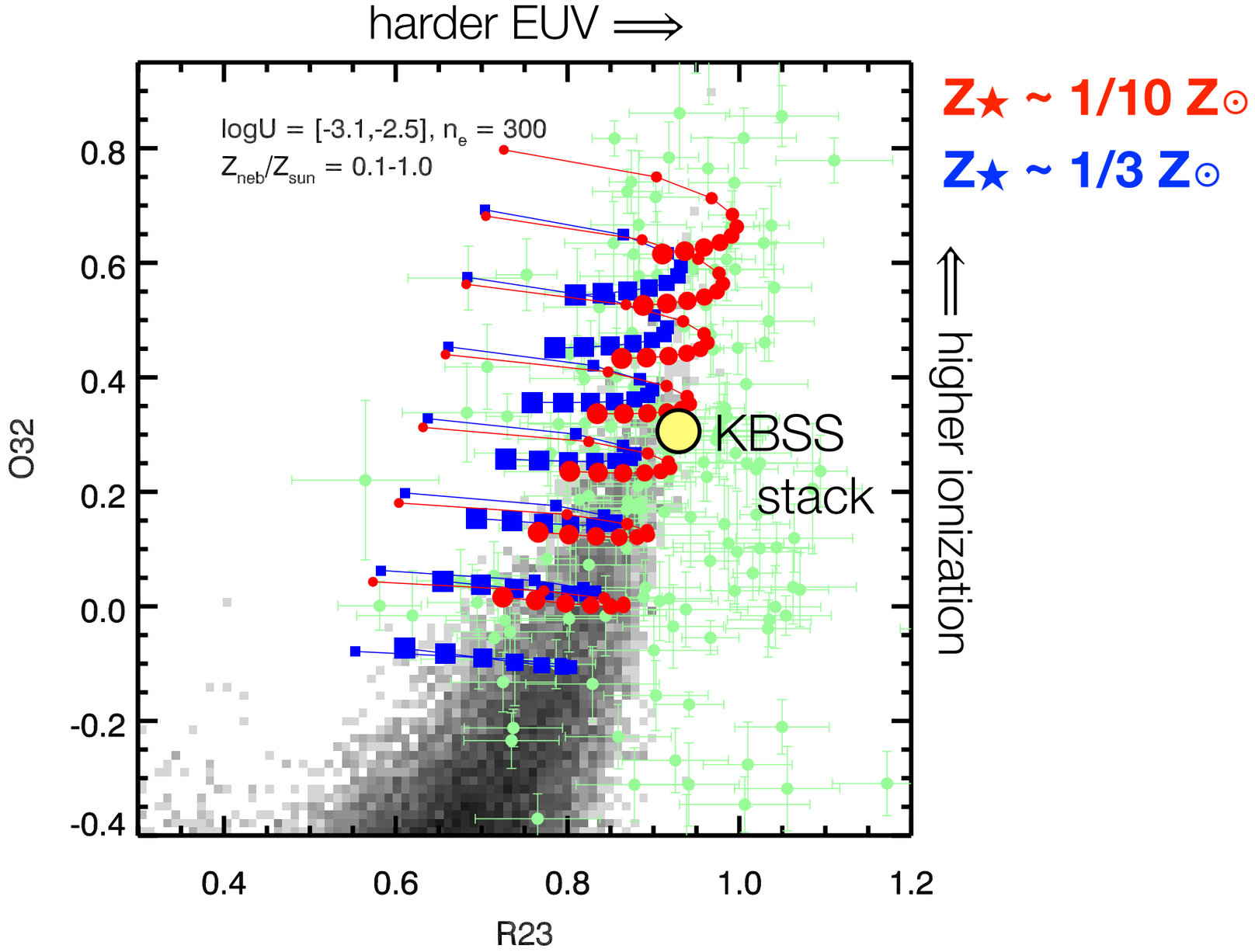

Z★ ~ 1/10 Z⊙

Z★ ~ 1/3 Z⊙

Can't reproduce high-*z* galaxy observations only by increasing U or lowering Z_{neb}

O32-R23 diagram sensitive to changes in ionizing radiation

Strom et al. (2016), arXiv:1608.02587

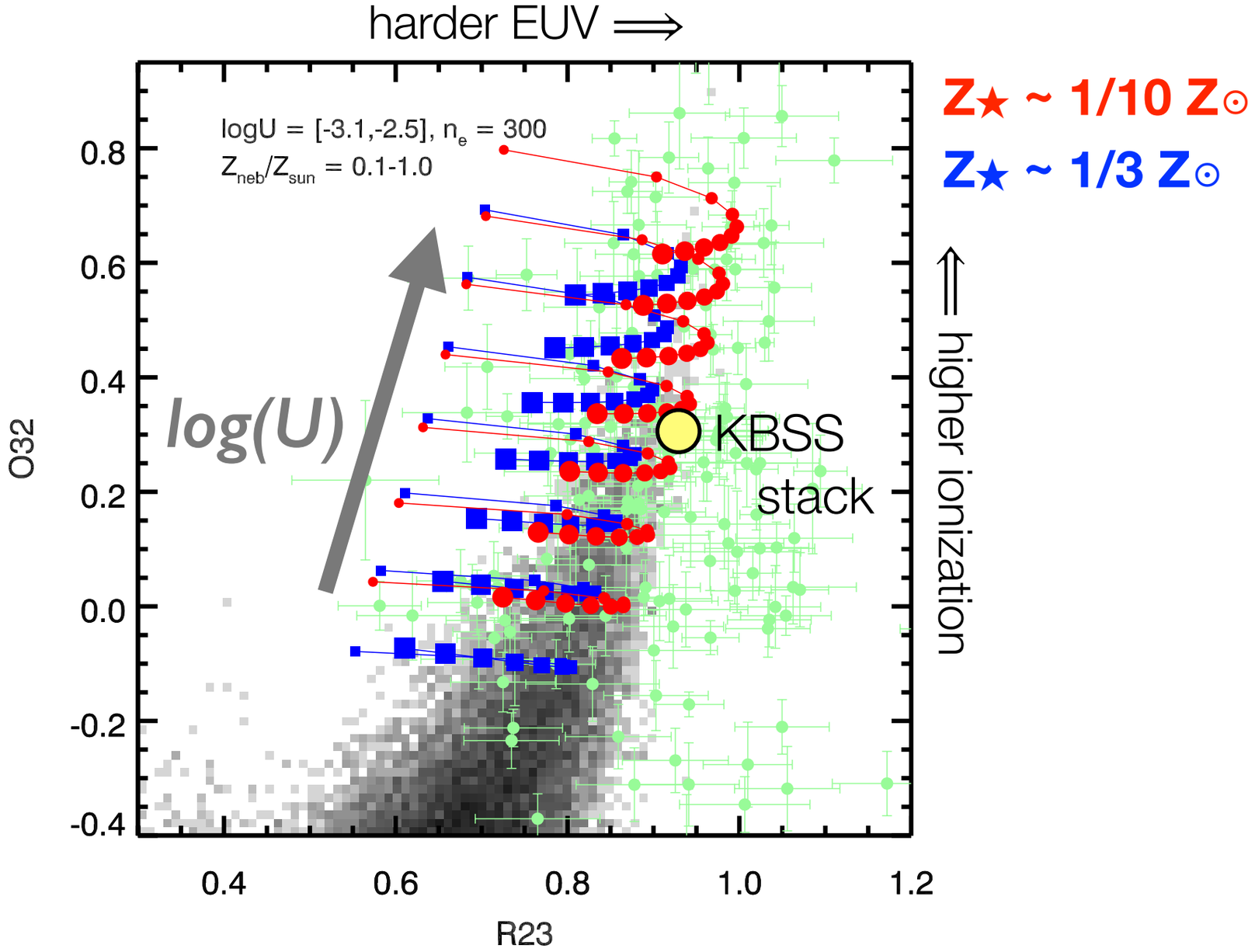

Z★ ~ 1/10 Z⊙

Z★ ~ 1/3 Z⊙

Can't reproduce high-*z* galaxy observations only by increasing U or lowering Z_{neb}

O32-R23 diagram sensitive to changes in ionizing radiation

Strom et al. (2016), arXiv:1608.02587

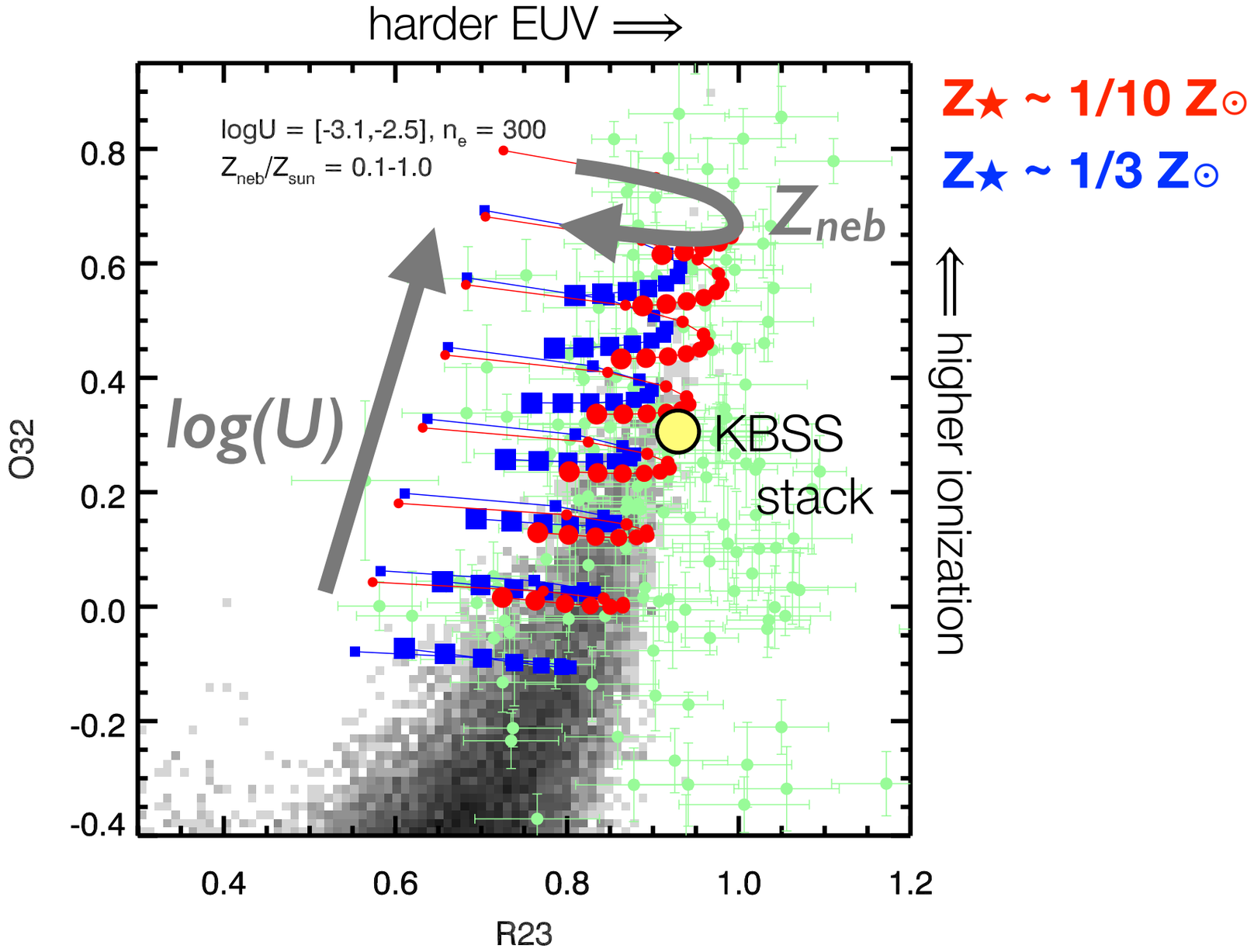

Z★ ~ 1/10 Z⊙

Z★ ~ 1/3 Z⊙

Can't reproduce high-*z* galaxy observations only by increasing U or lowering Z_{neb}

O32-R23 diagram sensitive to changes in ionizing radiation

Strom et al. (2016), arXiv:1608.02587

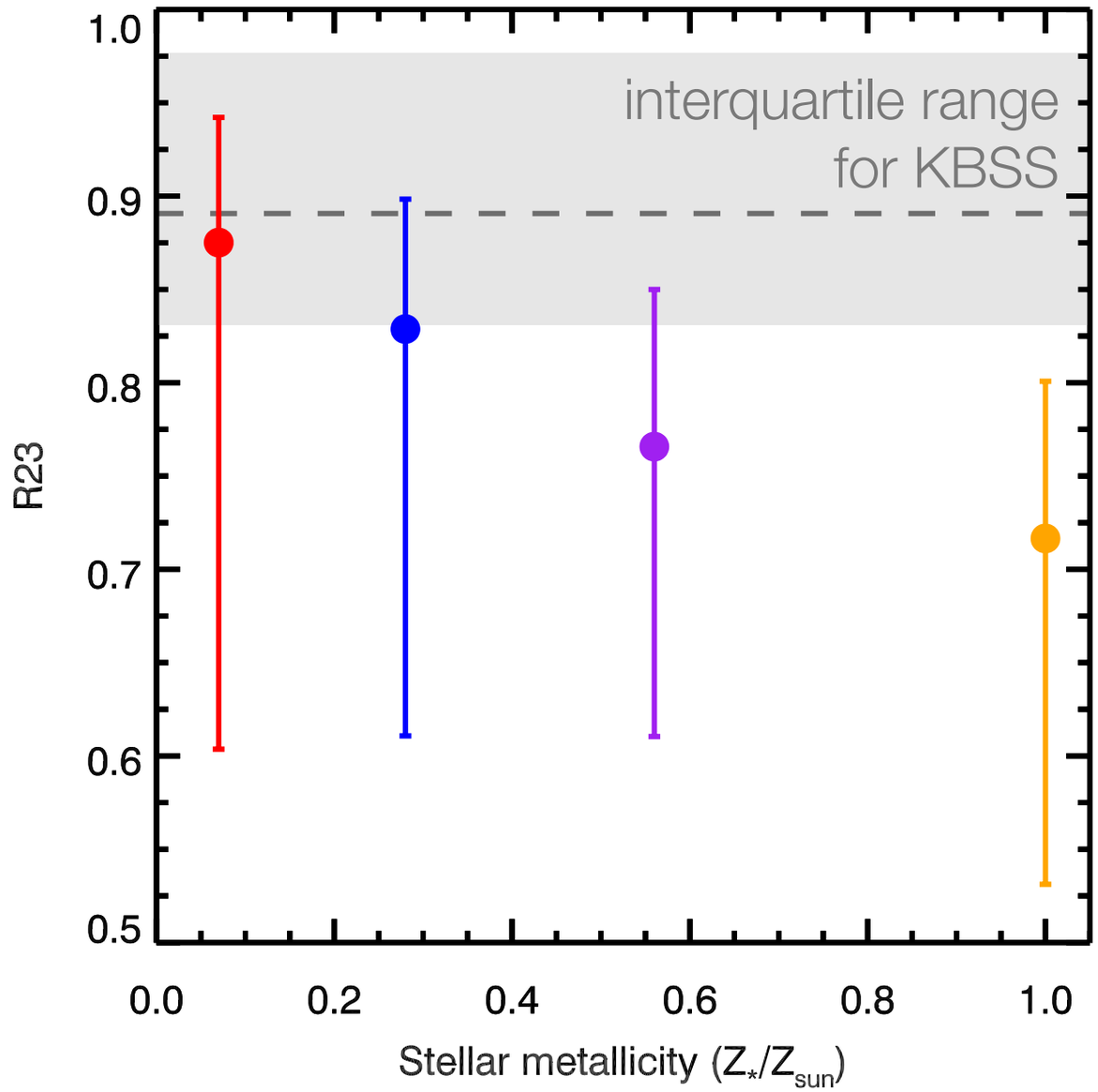

$Z_\star/Z_\odot > 0.5$ inconsistent with the majority of KBSS-MOSFIRE galaxies

Same models can reproduce locus in the N2-BPT

Strom et al. (2016), arXiv:1608.02587

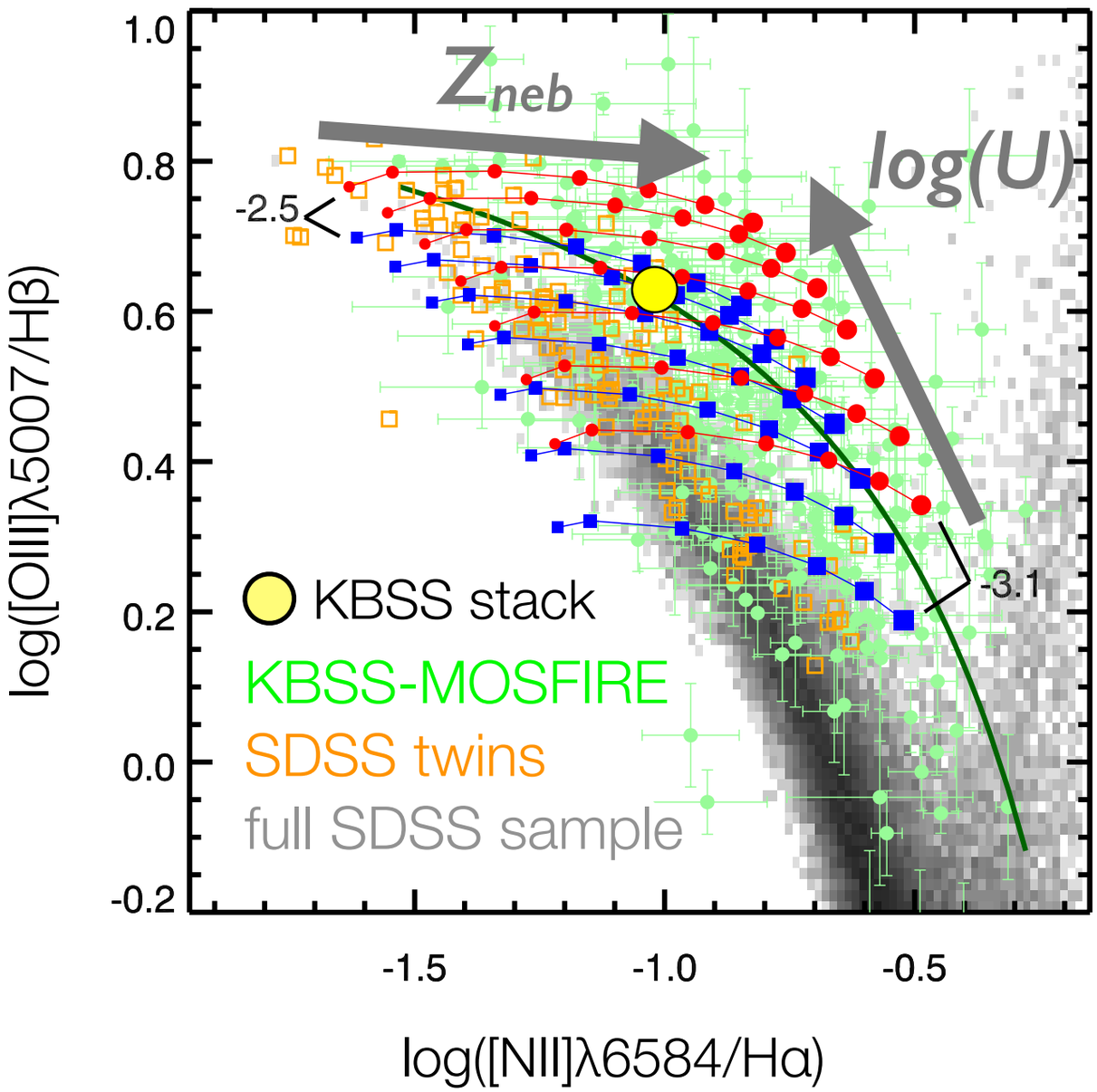

Z★ ~ 1/10 Z⊙

Z★ ~ 1/3 Z⊙

KBSS-MOSFIRE galaxies require higher Z_{neb} than twins

$Z_{neb}/Z★$ crudely traces O/Fe

High-z galaxies have O/Fe similar to bulge+thick disk stars

Steidel, **Strom**, et al. (2016)

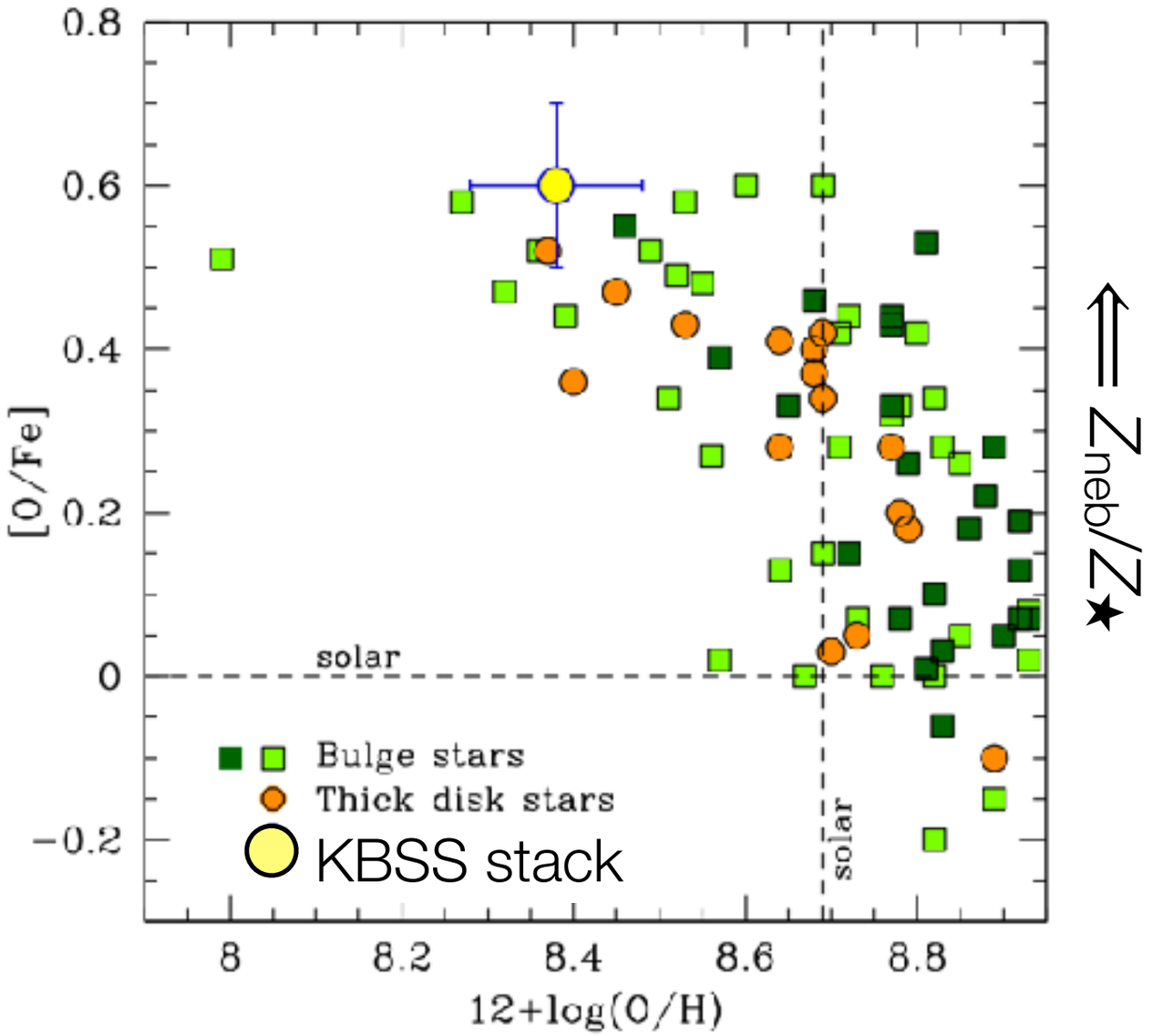

KBSS stack:
O/Fe ~ 4-5(O/Fe)⊙

consistent with predictions from Nomoto et al. (2006) for low-Z★ Type II SNe

O/Fe is related to age and star-formation history

Strom et al. (2016), arXiv:1608.02587

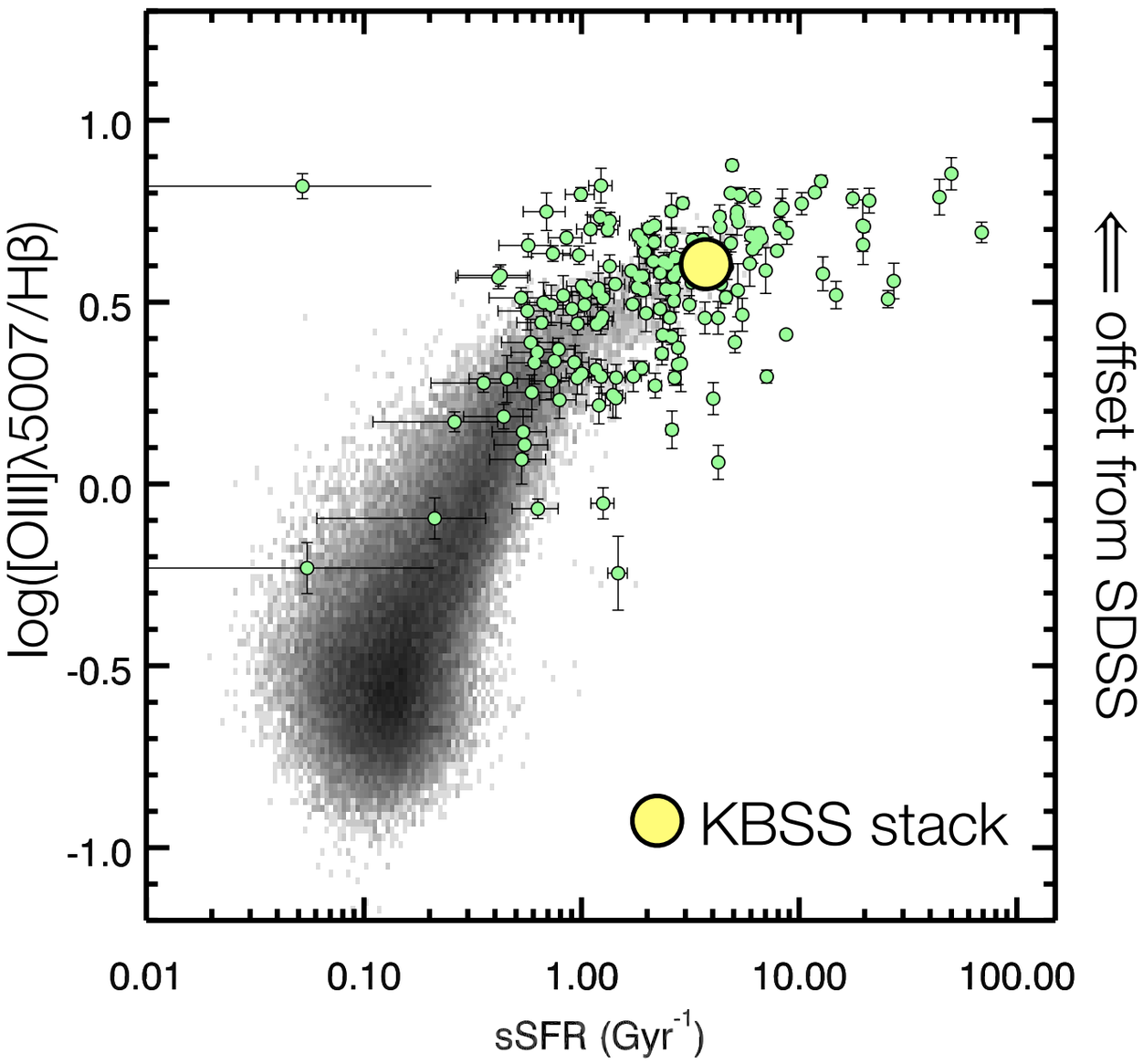

most O coming
from **Type II SNe**

most Fe coming
from **Type Ia SNe**

O/Fe ~ SFR(now)/SFR(past)

Can we apply the paradigm developed for understanding present-day galaxies to galaxies ~2-3 Gyr after the Big Bang?

Can we apply the paradigm developed for understanding present-day galaxies to galaxies ~2-3 Gyr after the Big Bang?

Not really.

Impact of star formation history on metallicity diagnostics

Strom et al. (in prep.)

Recent star formation will result in higher excitation (i.e., O3 and R23) at fixed O/H

Strong-line calibrations rely on the underlying correlation between

1. shape of the ionizing radiation (related to stellar Fe abundance)
2. gas-phase C, N, and O

Local metallicity calibrations will be inconsistent for high-z galaxies, especially at high 12+log(O/H)

Must carefully choose local “analogs”!

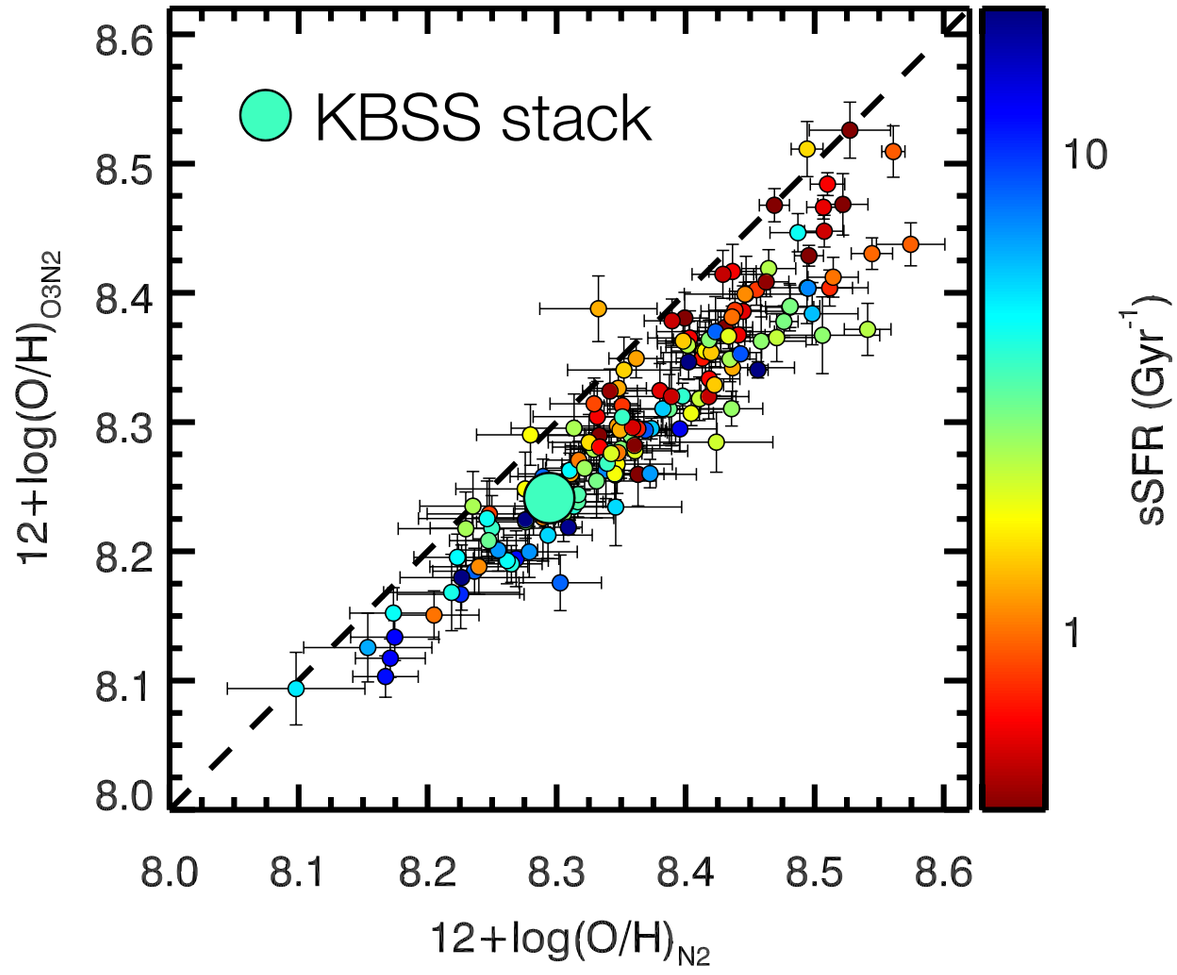

Measuring O/H, N/O and U for individual galaxies

Strom et al. (in prep.)

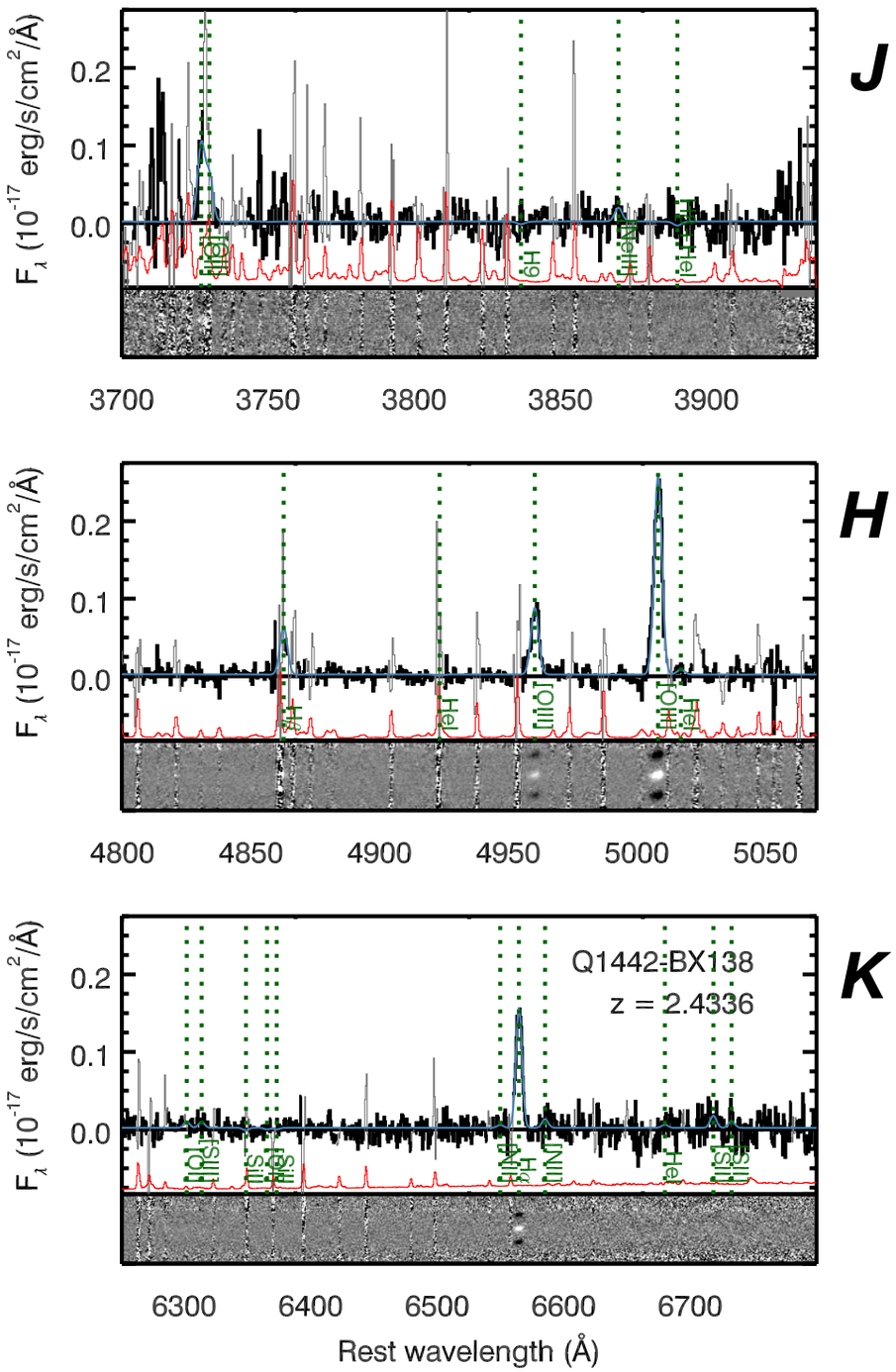

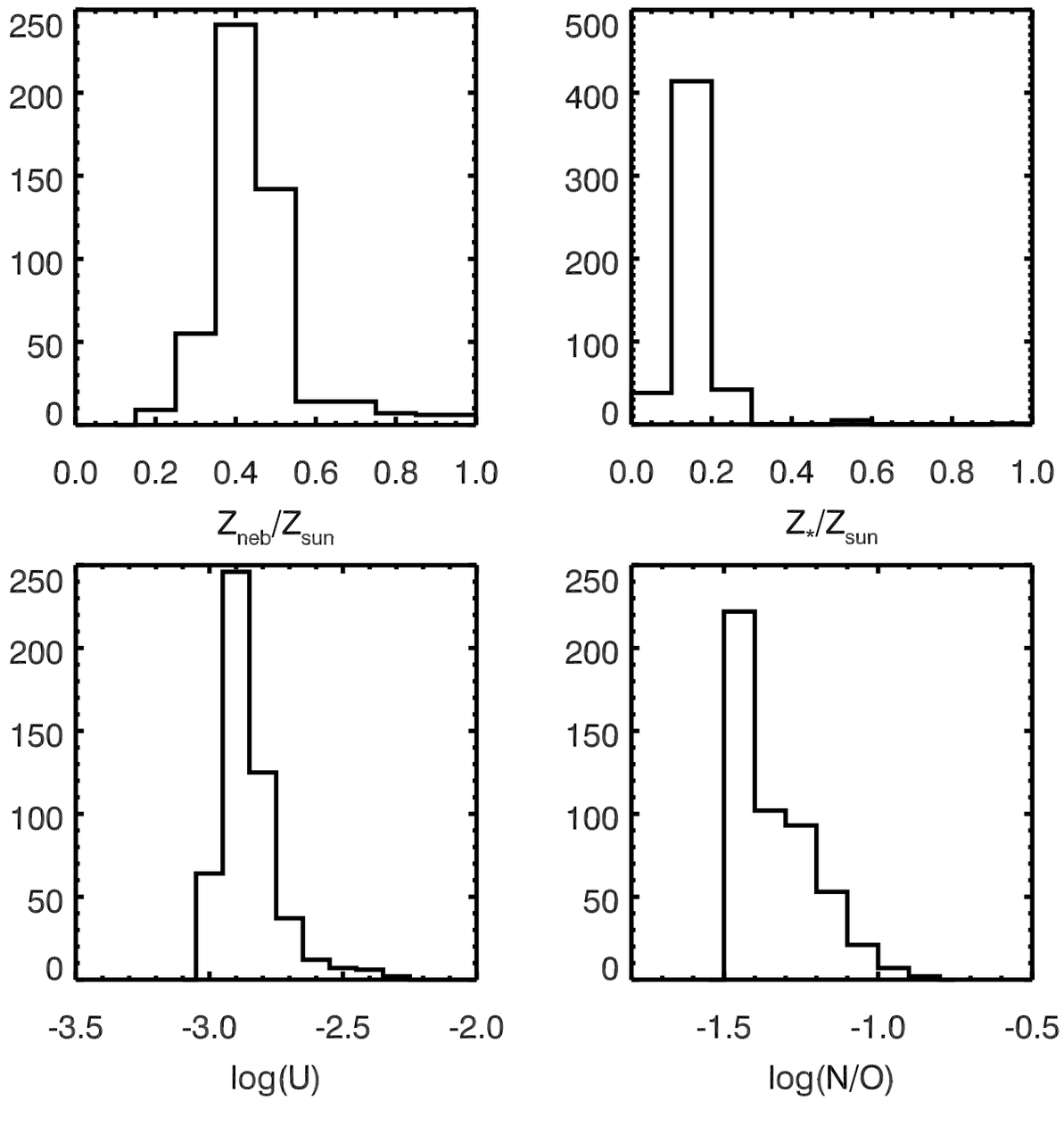

Precision in determining parameters depends on location in parameter space

Strom et al. (in prep.)

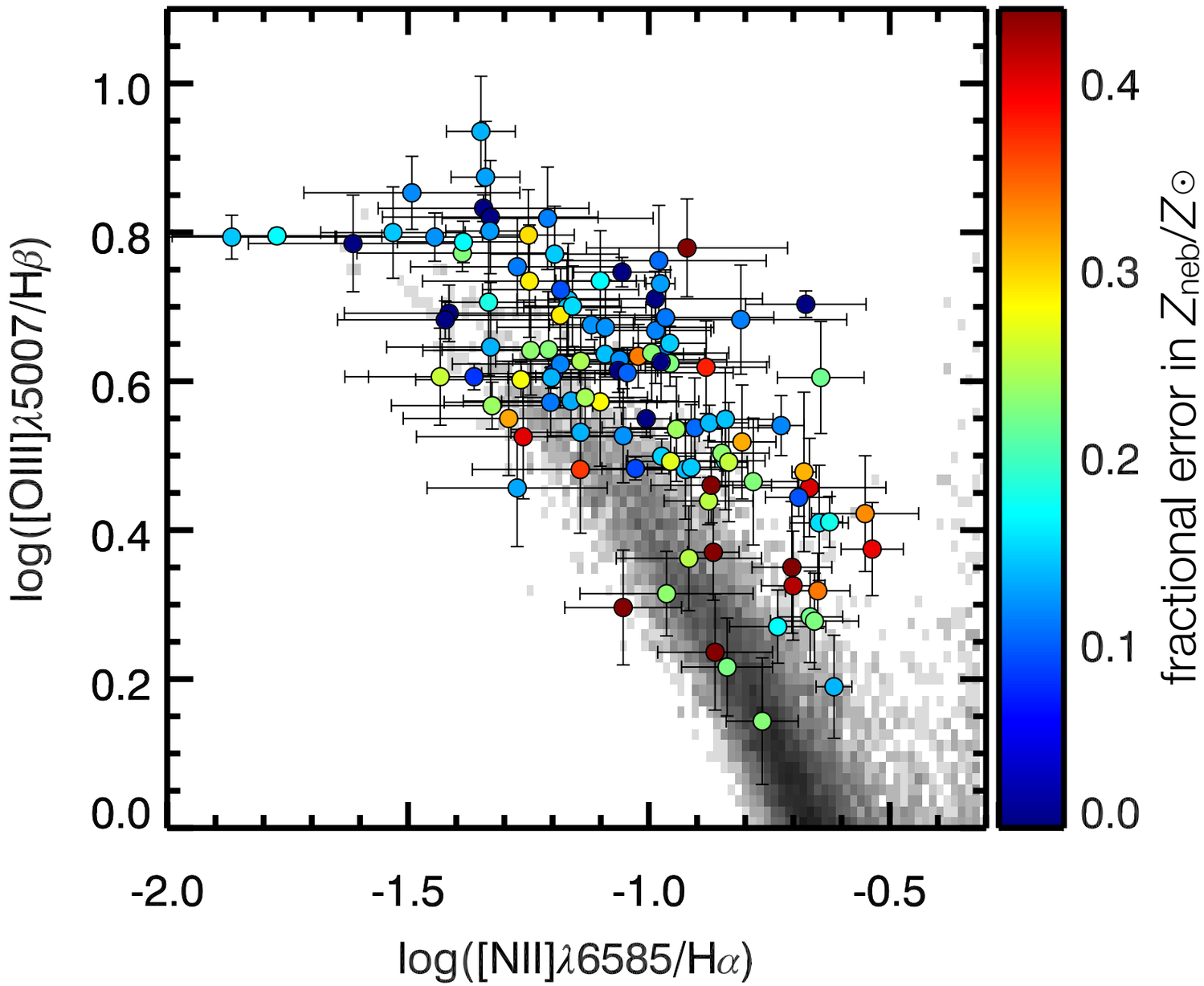

With KBSS, we can study the ***population*** *of z~2-3 galaxies*

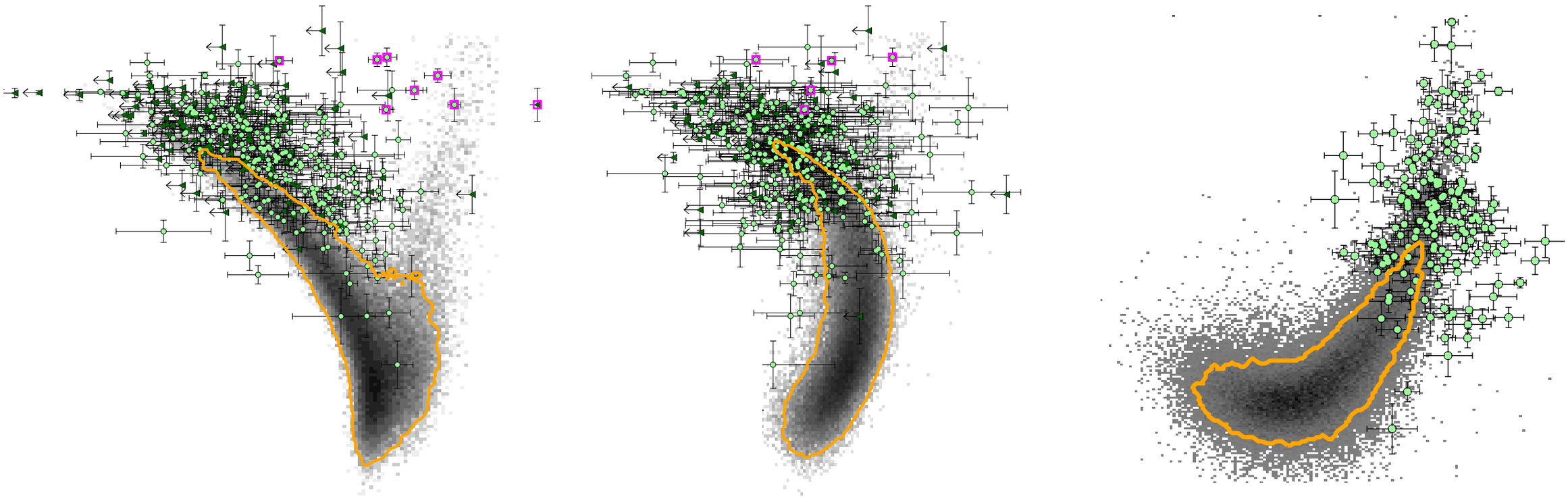

Commonly measured emission line ratios in *z*~2-3 galaxies are more sensitive to the shape of stars' ionizing spectra than to the details of the gas chemistry

Self-consistent models require both very hard ionizing spectra (produced by massive Fe-poor binaries) and moderate gas-phase O/H, indicating high O/Fe

High O/Fe ratios occur when ISM chemistry is dominated by CCSNe products, as is common in systems with high sSFR (>1 Gyr^{-1})